ENGINEERING LIBRARY

JUN 7 19[illegible]

NUCLEONICS

AN INTERNATIONAL JOURNAL
FOR TECHNIQUES AND APPLICATIONS OF NUCLEAR SCIENCE

May, 1948
(In two parts)

Part I

TRACKS OF [illegible] IN NUCLEAR EMULSIONS

ATOMIC [illegible] DEVELOPMENTS IN FRANCE

[illegible] HEINRICH

INTERACTION [illegible] RADIATION WITH MATTER

DOSAGE DETERM[illegible] WITH RADIOACTIVE ISOTOPES

CHART OF [illegible] OF RADIOACTIVE NUCLEI

ELECTRONI[illegible] FOR NUCLEAR PHYSICIST—IV

MA[illegible] DEFENSE DOCUMENTS

NUCLEONICS VOL. 2, NO. 5 (in two parts), MAY, 1948

An International Journal for Techniques and Applications of Nuclear Science

EDITORIAL BOARD

L. B. Borst
John R. Dunning
H. H. Goldsmith
Clark Goodman
F. C. Henriques, Jr.
W. F. Libby
L. D. Marinelli
I. Perlman
Edith H. Quimby
Winfield W. Salisbury
T. I. Taylor

With the cooperation of . . .

ITALY — E. AMALDI
GREAT BRITAIN — J. D. COCKCROFT
FRANCE — F. JOLIOT-CURIE
THE NETHERLANDS — C. J. BAKKER
DENMARK and SWEDEN — GEORGE HEVESY
SWITZERLAND — P. SCHERRER

CONTENTS—*(Part 1, pages 1–80; Part 2, pages 81–200)*

Tracks of Densely Ionizing Particles in Nuclear Emulsions . . 2
HERMAN YAGODA

The Neutrino 16
CHALMERS W. SHERWIN

Chart of Decay Periods of Radioactive Nuclei 25

Interaction of Isotopic Radiation with Matter—I 28
REX G. FLUHARTY

Manhattan District Declassified Documents 41

Dosage Determination with Radioactive Isotopes—II 44
L. D. MARINELLI, EDITH H. QUIMBY, and G. J. HINE

Electronics for the Nuclear Physicist—IV 50
W. C. ELMORE

Atomic Energy Developments in France 59

1947 SUMMARY OF NUCLEAR DATA 81-200

NUCLEONIC EVENTS . . 59 ABSTRACTS . . . . . 70 BOOKS 79

Walter M. DeCew . . . . Technical Editor

Jerome D. Luntz . . . . Assistant Editor
Ethel Pelzer . . . . . Assistant Editor

Robert Colborn . . . . Washington Editor
Gladys Montgomery . Washington Editor

Keith Henney . . . . . Consulting Editor
E. J. Tangermen . . . . General Manager

NUCLEONICS (with which is consolidated "Atomic Power" and "Atomic Engineering") May, 1948, Vol. 2, No. 5 (in two parts). Publication Office: 212 East York St., York, Pa. Editorial and Circulation Offices: 330 W. 42nd St., New York 18, N. Y. Published monthly by McGraw-Hill Publishing Company, Inc. Entered as second class matter December 17, 1947, in the Post Office at York, Pa., under the act of March 3, 1879.

Copyright 1948 by McGraw-Hill Publishing Company, Inc. All rights reserved. James H. McGraw, Jr., President; J. E. Gorrell, Secretary; Curtis W. McGraw, Treasurer. Price per copy $4.00; price each part $2.00. Allow at least two days for change of address. All communications about subscriptions should be addressed to J. E. Blackburn, Jr., Director of Circulation, 330 W. 42nd St., New York 18, N. Y. Subscription rates: United States and U. S. Possessions $16.00 a year. Canada and Latin America $20.00 a year. All other countries $25.00 a year. Return postage guaranteed. Member A.B.C.

NUCLEONICS . . . *Editorial*

An International Journal
for Techniques and Applications of Nuclear Science

Une Revue Internationale
de Techniques et Applications de Science Nucléaire

Eine Internationale Zeitschrift
für Technik und Anwendungen der Kernwissenschaft

The editors and publishers of NUCLEONICS announce the commencement of formal cooperation with distinguished leaders of nuclear research outside of the United States, with deep appreciation for the honor they have thus conferred upon our efforts. The responsibility for encouraging the proper representation of the findings of their national colleagues in NUCLEONICS has been generously assumed by Sir J. D. Cockcroft for Britain, Dr. F. Joliot-Curie for France, Dr. G. Hevesy for Denmark and Sweden, Dr. E. Amaldi for Italy, Dr. C. J. Bakker for the Netherlands, and Dr. P. Scherrer for Switzerland.

It is indeed fortunate and significant that this demonstration of the international character of nuclear science is possible during an unprecedented world crisis in human affairs. It reminds us that most of our knowledge and control of the properties of nature is continuously shared and advanced by experimenters in all civilized countries. Contributions to this journal from investigators in all parts of the world will make clear that by far the largest percentage of the findings of nuclear studies being carried on today is constructive and militarily meaningless.

All of us who have participated to some degree in the development of nuclear science and technology will recognize the great debt that we owe to the past contributions of P. Scherrer, C. J. Bakker, G. Hevesy, E. Amaldi, F. Joliot-Curie, and J. D. Cockcroft. Their cooperation with the editorial board of NUCLEONICS will now certainly contribute importantly to the earlier solution of scientific and engineering problems shared by all nuclear investigators using this journal as a medium for international communication with their colleagues.

—*W. M. D.*

Tracks of Densely Ionizing Particles in Nuclear Emulsions

A review of theory and application of photographic nuclear emulsions as a tool for precise radioactive measurements. Techniques for detection of mesons, protons, tritons, alpha particles, and fission fragments are described and illustrated

By HERMAN YAGODA

Laboratory of Physical Biology, National Institute of Health
Bethesda, Maryland

FOLLOWING BECQUEREL'S DISCOVERY of the activation of silver halide emulsions by radioactive radiations, photographic media were employed extensively in comparative activity measurements of minerals and their components. With the development of electrical counting instruments the photographic method lost its importance as an activity index. Nevertheless, a small number of investigators, including Blau at the University of Vienna and Zhdanov at the Russian State Radium Institute, persisted in their efforts to improve on the recording properties of silver halide emulsions. They clearly recognized the important potentialities of thick-layered emulsions as compact continuously recording media for the tracks of densely ionizing particles. Independently, they succeeded in preparing fine-grained emulsions in which the trajectories recorded by alpha particles and protons could be readily differentiated by the number of developed grains.

Space does not permit description of their pioneering efforts, nor of the early work of Wilkins at the University of Rochester and that of Taylor and Powell in England. An excellent summary of progress in emulsion technique is available in the 1942 review article by M. M. Shapiro (*1*).

Recent improvements in the preparation of concentrated, fine-grained emulsions provide the experimentalist with a versatile tool for precise radioactive measurements. These plates, based on the researches of Powell (*2*), Demers (*3*), and the Eastman and Ilford Research Laboratories have distinctly different characteristics from the plates employed in optical photography and are conveniently referred to as nuclear emulsions. The characteristics differentiating nuclear and optical emulsions are summarized in Table 1.

The nuclear emulsions exhibit low sensitivity to light, beta particles and gamma radiations. This permits their application in nuclear reactions for the detection of densely ionizing particles as the meson, proton, triton, alpha particle and the fragments arising from the fission of uranium. Optical-type emulsions which are readily activated by beta and gamma radiation are also blackened by densely ionizing particles. The optical plates, however, do not record microscopically resolvable tracks of the individual nuclear projectiles.

The nuclear and optical-type emulsions are also differentiated by their

TABLE 1

Differentiation of Nuclear and Optical Emulsions

Properties	*Optical Type*	*Nuclear Type*
AgBr: Gelatin, by weight	47:53	80:20
AgBr: Gelatin, by volume	15:85	45:55
Grain diameter	1 to 3.5 microns	0.1 to 0.6 microns
Grain separation	Interlocking	Isolated by gelatin
Emulsion thickness	2 to 3 microns	25 to 100 microns
Emulsion weight, mg per cm^2	1 to 4	5 to 20
Sensitivity to light	very high	poor or none
Sensitivity to H_2O_2 vapor	pseudophotographic effect	latent image eradication
Response to alpha particles	dense blackening	individual tracks
Response to beta particles	moderate blackening	faint fog
Response to gamma radiation	faint blackening	almost none

diametrically opposite response to pseudophotographic agents. Coarse-grained emulsions such as X-ray film and commercial ortho plates are rapidly fogged in the absence of light by exposure to minute quantities of hydrogen peroxide. As demonstrated by Churchill (*4*), even the traces of hydrogen peroxide generated in the reoxidation of freshly abraded metals, such as aluminum and cadmium, suffice for the activation of optical-type emulsions, and images of the abrasion marks are recorded on the developed plate after several days contact with the metals. In contrast, fine-grained emulsions, such as the Eastman "Fine-Grained Alpha" and NTA plates, and the Ilford Type C-2, commonly employed as recording media for the tracks of nuclear particles, are not fogged by prolonged exposure to high concentrations of hydrogen peroxide vapor (*5*).

Indeed, recent investigations (*6*) show that traces of hydrogen peroxide destroy the latent image of densely ionizing particles, and that this simple treatment suffices for the eradication of the accumulated background tracks in old plates, providing a clean slate for the registration of newly incident radiation. The role of hydrogen peroxide appears to be an important factor in the retention of the latent image, and has an important bearing in exposures of long duration to feeble radioactive sources.

The modern nuclear-type emulsions such as Eastman NTA and Ilford C-2, are composed of finely dispersed silver halides, essentially AgBr, in a medium of gelatin and residual water. Because of the high concentration of silver halide, nuclear particles expend a large proportion of their energy in the dispersed grains, and the developed tracks are very nearly continuous lines, despite the essential heterogeneous character of the recording medium.

The mechanism of track registration is shown schematically in Fig. 1. An incident particle or photon ($h\nu$) is captured by one of the component nuclei of the emulsion. On disintegration of the compound nucleus, several charged and uncharged fragments are ejected, of which, for simplicity, only three types will be considered. Each particle travels a distance in the emulsion, known as its range. This is dependent on its energy of ejection, its rate of energy expenditure and the stopping power of the emulsion.

The formation of a track and its

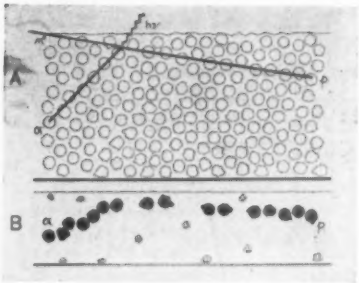

FIG. 1. Mechanism of track registration

A. Trajectories of a neutron (n), alpha particle (α) and a proton (p) in a thick layered fine-grain emulsion.

B. Tracks produced by the ionizing particles after development, fixation, washing and drying. The extraction of the nonactivated silver halide by fixation causes about a 50% depth shrinkage.

microscopic characteristics are defined essentially by its charge (e), mass (M) and energy (E) of the particle. The ionization produced along the trajectory is roughly proportional to e^2M/E. The doubly charged alpha particle and the singly charged proton cause ionization along their trajectories and form a latent image in the AgBr grains traversed. If the alpha particle and the proton are ejected with equal kinetic energies, their irrelative ionization will be about 16:1. The neutron having zero charge does not activate the emulsion. It may, however, record a track at some point distant from the initial event if it is captured by an atom in the emulsion.

Since the recording medium is heterogeneous, randomly oriented grains along the trajectory will be pierced by the particle along chords of variable length. When the charged particle passes through a major diameter, it is more apt to render the grain developable than when it crosses at or near grazing incidence. In emulsions of adequate sensitivity, nearly all grains are activated along the trajectories of slow alpha particles and heavy fission fragments. When the particle, as a fast proton, has but moderate ionizing power, only the more strongly activated grains are reduced to silver during the chemical development.

In exposures where the plate is developed *shortly* after the occurrence of the nuclear evaporation, the trajectories of the two ionizing particles under consideration, α and p, will be outlined by grains of silver, as shown in Fig. 1B. The initial and terminal silver grains are a measure of the range. The mean grain spacing, $\Delta = L/(n-1)$, where L is the track length in microns and n represents the number of developed grains, serves to differentiate particles of markedly different mass and charge. The nuclear emulsion is thus in many respects comparable to a *continuously* functioning cloud chamber in its ability to differentiate the trajectories of ionizing nuclear fragments.

Energy is also expended in traversing the gelatin separating the silver bromide grains. Under normal ambient conditions the gelatin retains about 10% water, and radiations, particularly alpha particles, decompose the water and generate hydrogen peroxide. On delayed development, the hydrogen peroxide has opportunity to diffuse into the surrounding grains and act on the latent image.* If the event described in Fig. 1 occurred during the early days of a prolonged cosmic-ray exposure, on development the proton track would not have been evident and the trajectory of the alpha particle would have been defined by a smaller number of grains.

The recording mechanism, as deduced from studies of factors controlling fading of the latent image (*6*, *7*), consists of two competitive processes. The formation of specks of metallic

* Hydrogen peroxide exerts a solvent action on colloidally dispersed silver. The rapid fading of the latent image of densely ionizing radiations is explicable on the basis of the solution of the silver specks by hydrogen peroxide.

TABLE 2

Track Characteristics in the Eastman NTA-emulsion

Particle	*Energy in Mev*	*Total Range in microns*	*Mean Grain Spacing in microns*	*Grain Density (grains per micron)*	
				Fast End	*Slow End*
RaF alpha particle	5.30	22.5	0.55	1.82	1.82
Proton	4.0	120	.72	1.22	1.64
Proton	7.5	348	.88	.79	1.65
Proton	11.2	684	1.20	.42	1.65
Meson of 200m_e	4.1	613	1.61	.36	1.13

silver in the silver bromide grains traversed by the densely ionizing particle and the generation of traces of hydrogen peroxide in the gelatin component. During photographic development, the silver specks serve as nuclei for the reduction of the entire grain to metallic silver.* The hydrogen peroxide tends to destroy the latent image and the exposure must be arranged so as to minimize diffusion of the hydrogen peroxide into the silver halide grains. These concepts help to explain the following observations on the fading of the latent image:

1) Track deterioration is much more pronounced in emulsions of high gelatin content.
2) Fading increases in exposures conducted in warm humid atmospheres.
3) Fading is inhibited by exposing at low temperatures in dry air.
4) The latent image is destroyed by incorporating traces of hydrogen peroxide in the atmosphere in which exposed plates are stored prior to development.

† This factor makes the microscopic detection of the track feasible. Measurements by Rutherford show that the radius of action of an alpha particle in zinc sulfide crystals is about 7×10^{-8} cm. In the emulsions under consideration the effective radius of action is limited by the grain size, measuring about 10^{-5} cm in radius. The photographic development increases the visibility of the initial trajectory by a factor of 10^4.

Differentiation of Ionizing Particles

In traversing the nuclear emulsion, a polonium alpha particle of 5.30 Mev records a track, about 23 microns long, composed of about 45 developed silver grains. With more densely ionizing radiation, as fission fragments, the tracks are practically continuous. The variation in grain density, n/L, or the mean grain spacing, $L/(n-1)$, along the tracks of protons and mesons, often permits their differentiation from the tracks produced by alpha particles or deuterons.

The grain density is dependent on the emulsion characteristics, the extent of fading, and the conditions of development.† Extensive data on grain characteristics of different nuclear particles have been accumulated by the British investigators using the Ilford C-2 emulsion. The characteristics of tracks recorded in the Eastman NTA plates is summarized in Table 2. The emulsion has a stopping power of about 1730 for alpha particles of 4.7 to 8.8 Mev kinetic energy. The difficulties of processing and observing thick-layered emulsions limits the practical emulsion thickness to about 100 microns. Long-ranged particles, there-

† It is not practical to describe laboratory procedures in the present review. Details on the preparation of thin sources, microscopy, and photographic processing are included in a manuscript in preparation (*8*).

fore, do not record their complete trajectories unless incident at small angles with the emulsion plane. More often, the tracks terminate in the glass or air interface and a direct estimate of the particle energy cannot be established from the recorded track length.

The tracks of certain particles, as fast protons, exhibit a marked variation in the grain density at the initial and terminal portions of the trajectory. When the origin of the track is defined, as in a nuclear evaporation, where all tracks originate from a common center, the grain density of the recorded portion, with the aid of calibration data as shown in Fig. 4, permits the extrapolation of the full track length.

Alpha-particle Tracks

The nuclear emulsion is a convenient tool for the study of radioactive systems containing alpha-particle-emitting isotopes. While these isotopes are limited to the members of the uranium, actinium, and thorium series (of chief interest in problems of geochemistry), the synthetic transuranium elements provide an additional group of new alpha emitters of both scientific and practical interest. The emulsion is poorly sensitive to beta particles, and the α tracks recorded by minor amounts of plutonium or actinouranium are readily detected in the presence of the beta-emitting fission products.

Alpha-particle activities can be measured by exposing thin weighed films of the sample or isolated carrier fractions in close proximity to the emulsion. Massive samples, such as the polished surface of rocks or minerals, can be placed in direct contact with the emulsion. By extending the exposure so that 10^7 tracks per cm^2 are recorded, a visual image of the radioactive segregates is produced. A second colinear brief exposure, producing a microscopically countable track population, permits a quantitative estimate of the activities of individual segregates. The reliability of these counting techniques has been investigated by Yagoda and Kaplan (*9*). Their preliminary results on the disintegration rate of uranium show good agreement with the accepted value.

In quantitative alpha-particle counting, each portion of emulsion serves as an independent measuring device. Since a separate plate is used for each sample, it is practical to incorporate the radioactive source in the emulsion. This is achieved either by immersing the plate in a solution of the sample or by allowing a measured volume to evaporate on its surface. This "loading technique," when applicable, offers many advantages. It provides a counting geometry of about 90%. The source is dispersed as ions in the emulsion, and the alpha particles record full energy tracks.

Recent studies of the loading technique by Broda (*10*, *11*) show that the mechanism of ion pickup is essentially one of adsorption. At constant temperature, plates loaded from solutions of increasing uranyl-ion concentration adsorb uranium, as indicated by autoregistration of the alpha tracks, following the well known Freundlich adsorption isotherm. When loading does not destroy sensitivity, small concentrations of nuclei of different atomic number can be incorporated in the emulsion. Thus, the incorporation of B^{10} or Li^6 permits the study of slow neutron fluxes.

By measuring the track lengths in uranium-loaded plates, Powell and collaborators (*2*) found that the groups of alpha particles emitted by UI and UII are readily resolved. Independent studies by Demers (*3*) show that for the alpha rays of ThC′ the standard deviation in range measurement is 2%. The straggling of the range is accentuated in emulsions owing to the large proportion of elements of high atomic

FIG. 2. Alpha-ray stars in a thorium-loaded emulsion. Darkfield illumination, magnification 620 ×

weight. In actinium-loaded emulsions, Gulliot and Perey (*12*) observed that the principal group of particles have a range of 3.46 air-cm. Measurements by Faraggi (*13*) on thorium-loaded emulsions yield a range of 2.43 ± 0.03 air-cm, bringing the range in better conformity with the pleochroic halo measurements for this element. The method has also been applied in the study of the short-ranged alpha particles emitted in the spontaneous decay of samarium. The measurements of Blau (*14*) and Cüer (*15*, *16*) indicate that, besides the principal body of 1.13 air-cm tracks, samarium or an allied rare earth also gives rise to more energetic alpha particles.

Another example of the diversified potentialities of the emulsion technique is illustrated by the work of Chang on the fine alpha-ray structure of polonium (*17*) and radium (*18*). The alpha particles, sorted out by a strong magnetic field, are focused onto a nuclear type emulsion. On development the principal body of monoenergetic alpha particles records a black line. Microscopic examination of adjoining areas of the plate reveals the presence and relative number of particles emitted with different initial velocities. Beams of ions of different mass can also be deposited on the emulsion, and track formation serves as an indicator for the radioactive isotopes. Wilkins and Dempster (*19*) were thus able to demonstrate that Sm^{148} is the isotope responsible for the short-ranged alpha particles emitted by the element.

Alpha Stars

When the emulsion is loaded with an alpha-emitting element whose decay products are short-lived and also disintegrate by alpha-particle emission, the event is recorded by two or more tracks originating from a common center, conveniently referred to as α stars. These α stars are particularly frequent when the plate is loaded from a dilute thorium solution, because isotopic RdTh and its successive disintegration products, ThX, Tn, ThA and ThC + ThC′, are short-lived and eject alpha particles. Typical alpha stars are illustrated in Fig. 2.

Radiochemically pure uranium, free from its disintegration products does not give rise to alpha stars during an exposure of 100 hours. Radium, like radiothorium, is a prolific star begetter, and quantities as little as 10^{-15} g Ra per mg of U can be detected in an emulsion loaded from a solution of the preparation. The Th stars and the Ra stars are readily differentiated by range measurements of the individual tracks. In a V-branch event, two or more tracks may terminate in the emulsion, and their full lengths provide a means for the identification of the parent element. When the ThC′ alpha track is fully recorded, the star can be identified by casual observation because its 49 micron length in the emulsion

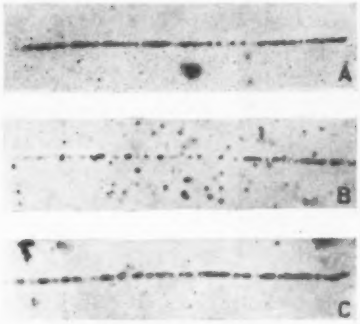

FIG. 3. Photomicrographs showing comparative grain density of alpha particle and proton tracks. Köhler illumination, 98 × oil-immersion objective, total magnification about 1000 ×

A. Complete trajectory of a ThC′ alpha particle, 8.8 Mev

B. Fast end of track produced by a 6.5-Mev proton

C. Slow end of the same proton track

distinguishes it from all other known spontaneous alpha-emitting elements.

Alpha-star formation is a characteristic of series disintegration. The technique was employed by the Canadian investigators (*20*) in establishing the presence of the $4n + 1$ series from the decay of U^{233}. The loading method should also prove applicable in similar studies on the alpha isotopes of americium and curium.

It is important to note that the gelatin employed in the manufacture of emulsions contains about 10^{-7} gm Th per gram. This gives rise to alpha

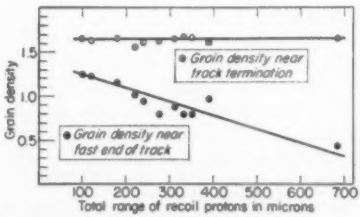

FIG. 4. Relationship between terminal grain density and range of proton tracks

stars at a rate of about 0.2 per cm^2 per day. In old plates the population of these terrestrial stars is appreciable, and because of partial fading of certain track structures they may be confused, at first glance, with cosmic-ray-induced nuclear evaporations. While VI-branched Th stars are possible, they are very rarely observed, even in emulsions loaded with thorium. Thus, the rare nuclear evaporations can be differentiated by a multiplicity greater than V and the presence of 1 or more tracks with a recorded length exceeding 50 microns. In cosmic-ray stars, proton tracks predominate; there is no possibility of confusion with the alpha stars in a properly exposed emulsion.

Proton Tracks

The modern nuclear-type emulsions record the tracks of protons with a mean grain spacing sufficiently characteristic to permit their ready differentiation from the tracks of alpha particles of comparable energy. For purposes of calibration, the emulsion is supported at right angles to a beryllium disk carrying a deposit of about 1 millicurie of polonium per cm^2. The fast neutrons originating from the $Be^9(\alpha,n)C^{12}$ reaction, on colliding with a hydrogen nucleus in the gelatin, cause its acceleration with the ultimate production of a proton track. These tracks have distinctive lengths and grain density and frequently exhibit scattering which permits their ready identification. A typical knock-on proton track is exhibited in Fig. 3. The variations of grain density as a function of full track length is represented in Fig. 4.

The registration of proton and deuteron tracks has played an important role in the study of the mechanisms of nuclear reactions. Plates are exposed in special scattering cameras, described by Wilkins (*21*) and Powell (*22*), so as to record the particles

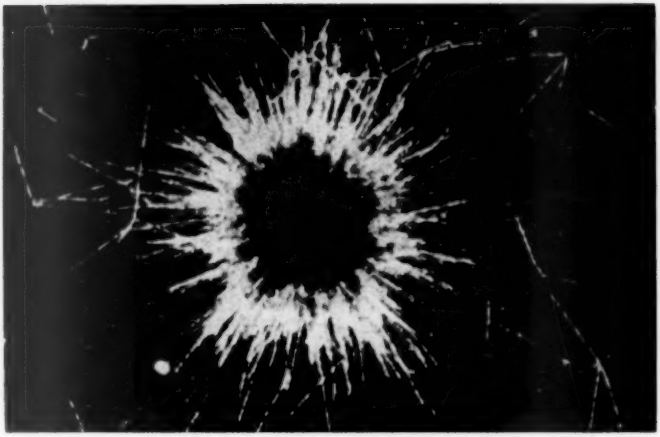

FIG. 5. Radiocolloid aggregate in a radium-loaded emulsion. Darkfield illumination, magnification 570 ×

The black core under darkfield illumination results from dense silver deposit at the point of origin of the tracks. The intermediary white halo represents the termination of the alpha particles originating from the decay of Ra, Rn and RaA. The external halo of individually resolvable tracks is composed of the tracks of the energetic RaC′ alpha particles.

Several alpha stars are recorded in the background. These originate from the series decay of individual radium atoms.

ejected from thin metallic foils under bombardment by cyclotron-accelerated particles. Details of these methods are described in the recent work of Powell and collaborators on proton (*23*, *24*) and deuteron (*25*) scattering by elements of low atomic weight. A modified scattering camera for studying the angular distribution of the alpha particles in the $Li^7(p,\alpha)\alpha$ reaction is described by Rubin (*26*, *27*).

Tracks of Fission Fragments

The massive fragments ejected in the neutron-induced fission of uranium, thorium and plutonium are very densely ionizing and produce distinctive tracks in emulsions of low sensitivity. By special processing the sensitivity can be reduced sufficiently so that protons and alpha particles do not record tracks, and only the trajectories of the fission fragments are delineated. Special plates of this character have been described by Borst and Floyd (*28*), and independently by Perfilov (*29*), Demers (*30*), and Richards and Speck (*31*). It is noteworthy that uranyl ions tend to desensitize nuclear-type emulsions. By augmenting their concentration in the emulsion, as shown in the work of Green and Livesey (*32*), the alpha tracks originating from the spontaneous decay of the uranium are weakened sufficiently so that the more robust tracks of the fission fragments can be differentiated.

The emulsion technique has revealed that the fission process is accompanied by the emission of light charged particles. Demers (*30*) and Wollan (*33*) have demonstrated the ejection of long range fragments with a mass comparable to the alpha particle. Very short

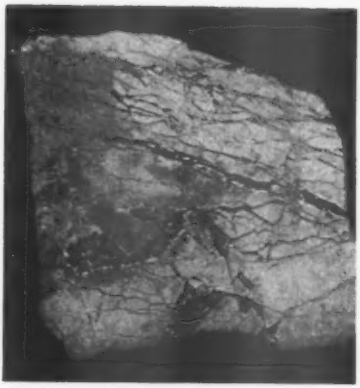

FIG. 6. Alpha-ray pattern of pitchblende from Belgium Congo. Positive print, no magnification. Variations in photographic density correspond to differences in uranium content throughout the cross section of the mineral

FIG. 7. Alpha-ray pattern of an essentially unaltered crystal of thorianite. Macrograph, 10 ×. White areas correspond with position of nonradioactive inclusions in the crystal cross section

range particles of 0.87 air-cm accompanying the fission fragments have been reported by Green and Livesey (*34*). Tsien San-Tsiang and co-workers (*35*) have observed events in neutron-irradiated uranium-loaded emulsions indicative of tertiary (*36*) and quaternary fission processes (*37*). The method has also been applied in the estimation of the energy of thorium fission fragments (*38*).

Radiocolloid Registration

By loading the emulsion with extremely dilute solutions of short-lived radioactive ions, microscopic examination of the processed plate reveals, besides the anticipated background of single tracks, structural units comprised of numerous tracks radiating from a common center. These track orientations suggest the point aggregation of several million radioactive atoms. Chamie (*39*, *40*), who first observed the phenomenon photographically, designated these units of extraordinary activity as "radiocolloids." A radiocolloid aggregation in an emulsion loaded with radium is exhibited in Fig. 5.

The radiocolloid aggregates present in solutions of high dilution, exhibit a pronounced tendency for adsorption within capillary structures. They are often encountered in alpha-ray patterns of biological tissues carrying tracer doses of alpha-particle-emitting isotopes. Radiocolloid aggregates are also formed in alteration processes of primary uranium minerals (*41*), and are occasionally encountered in radium content analyses of rock samples.

Alpha-ray Emission Patterns

The emulsion integrates all incident alpha tracks and, when the total radiation exceeds about 10^7 α particles per cm^2, on development a visual image of about 0.2 photographic density is produced. Because of the small range of alpha particles in solids, the visual pattern is sharply delineated and a microscopic resolution of about 20 microns is readily attainable. An autoradiograph of a polished surface containing alpha-active segregates, made on nuclear-type emulsions, provides a unique tool for studying distribution and measuring activity of the radioactive components.

The application of these "alpha-ray patterns" has been described (*5*) in

the classification of uranium and thorium minerals. The photographic density is an approximate measure of the alpha-ray activity and, hence, of the uranium and thorium contents of the minerals. The pattern depicts clearly the variation in alpha-ray activity within mineral sections, and provides an index for their suitability as indicators for age determinations by Pb/U ratios. Typical alpha-ray patterns of altered and unaltered radioactive minerals are described in Figs. 6 and 7.

Accurate activity measurements of individual minute segregates can be made by a dual-exposure technique. The first exposure is prolonged sufficiently (2–10 days) for the production of a visually discernible image. This is followed by a brief exposure of about 15–60 minutes on an adjacent portion of the same plate. On development the first exposure depicts the segregates, and the track population in the second exposure is suitable for activity measurements. The track count per segregate can often be translated in terms of the composition of the parent element giving rise to the activity by formulae based on the geometry of infinitely thick solids. The potentialities of this method in the study of the distribution of radioactive components in rocks has been considered in a mathematical treatment by Joliot-Curie (*42*). Preliminary experiments (*8*) show that, by prolonged exposures, activities comparable to 10^{-10} gm of Ra can be measured accurately, and smaller quantities are readily detected when the active components exhibit segregation.

Analogous methods are directly applicable in the study of localization of alpha-emitting elements in biological tissues, metals, alloys and synthetic crystals grown in the presence of traces of radioactive elements. With biological materials a thin section of the paraffin infiltrated material can be deposited in direct contact with the pre-moistened emulsion. The tissue adheres to the gelatin, and can be stained successfully after photographic processing. When examined microscopically, each alpha particle track can be traced back to the cell in which the alpha disintegration occurred. This technique developed by Endicott (*43*) is applicable to the precise localization of even long-lived elements such as thorium, and promises to become an important tool in histochemistry.

An alternative technique, applicable in the study of individual grains of finely divided materials, such as placer sands and soils, is to sprinkle the powder on a water-moistened emulsion. On drying, the granules become embedded in the gelatin and, when of an insoluble nature, persist in position during the stages of photographic processing. Microscopic examination, after a suitable period of exposure, reveals the individual incorporated sources. Radioactive grains are readily differentiated from inert ones by the radial alpha-ray tracks directed from them. A typical microscopic field is reproduced in Fig. 8. This method has been employed in the study of the radioactivity of soil minerals by Tyler and Marais (*4*). By growing bacteria in a culture medium containing radium

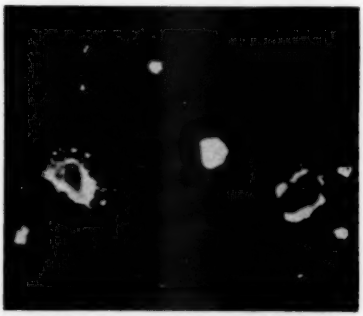

FIG. 8. Comparison of radioactive and nonradioactive mineral fragments. Darkfield illumination, magnification 310 ×

or other alpha-decaying tracer isotopes, the enhanced activity of the microorganisms can be demonstrated by depositing a suspension on a nuclear-type emulsion (*45*). The method should prove of interest in studying selective adsorption effects from culture media with admixed radioactive ions.

Cosmic Radiation

One of the principal advantages of the emulsion technique of radioactive measurements resides in the continuous recording properties of the medium. Rare radioactive events, necessitating the taking of thousands of individual cloud-chamber photographs can, therefore, be integrated in one prolonged exposure of a nuclear emulsion. This is particularly advantageous in the measurement of low neutron fluxes, and in the rare instances where components of the cosmic radiation cause nuclear evaporations with the production of densely ionizing particles.

The collision of fast neutrons with hydrogen atoms in the emulsion results in the formation of a proton track. When the energy of the neutron is high, the length of the proton tracks may exceed several millimeters in the emulsion. Owing to the limited thickness of the emulsion, only small portions of the proton trajectory are usually recorded. This does not permit an accurate evaluation of the energy of the incident neutron. In boron-loaded emulsions fast neutrons can interact with B^{10} nuclei as follows:

$$B^{10} + n^1 \rightarrow He^4 + He^4 + H^3$$

This event is recorded in the emulsion by a III-branched star composed of two alpha-particle tracks and a triton. The range of these particles is small; hence, there is a fair probability that all three tracks will be fully recorded within the emulsion layer. This technique has been studied by Lattes and Occhialini (*46*) for the estimation of the energy and momenta of fast neutrons in the cosmic radiation. In boron-loaded Ilford plates exposed to 13.4 Mev neutrons, microscopic examination revealed many III-particle disintegrations. Grain counts showed that two of the tracks were produced by α particles of 7.4 and 1.4 Mev, and the third by a triton of 5-Mev energy. It is thus seen that the total recorded energy of 13.8 ± 0.5 Mev is in close agreement with the known energy of the incident neutrons. In similar plates exposed at 2800 meters elevation, Lattes and Occhialini observed III-branched stars whose track lengths corresponded to neutron energies of 50 Mev.

Slow neutrons can be recorded photographically by loading the plates with boron or lithium. The incidence of the nonionizing neutrons is made manifest by the tracks of particles emitted in the following reactions:

$$(a) \quad B^{10} + n^1 \rightarrow He^4 + Li^7$$

$$(b) \quad Li^6 + n^1 \rightarrow He^4 + H^3$$

The total track lengths are comparatively short in reaction (*a*), the trajectories of both particles totaling about 7 microns. While the cross section of reaction (*b*) is smaller than in (*a*), it is favored by the distinctive grain spacing and greater range which totals 40 microns. Slow neutrons also interact with the nitrogen of the gelatin, $N^{14}(n,p)C^{14}$, and record protons of about 6-microns range.

Neutron fluxes can also be measured with the aid of uranium-loaded plates, the number of fission tracks serving as an index of slow-neutron abundance. Plates of this character have been exposed at high altitudes to cosmic-ray neutrons by Lark-Horovitz (*47*), and more recently by Froman, Rosen, and Rossi (*48*). Using foils of U^{235} weighing 1 mg/cm^2, in direct contact with fission plates, they observed a cosmic-ray neutron flux of 20 per cm^2 per min at an elevation of 10 km. When the exposures were conducted under paraffin, the number of recorded fission

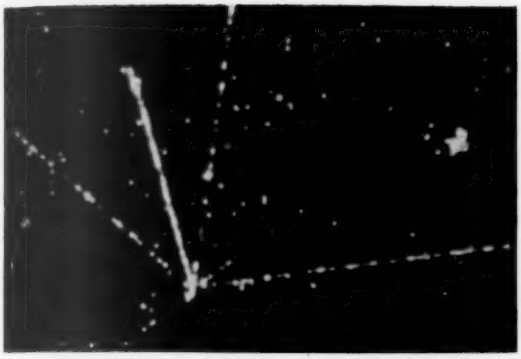

FIG. 9. Nuclear evaporation recorded in an emulsion exposed near sea level. Dark-field illumination, magnification 860 ×

This event is represented by one alpha particle and five proton tracks, as determined by grain counts at 1250 × magnification. The cosmic ray star probably represents a $_7N^{14} \rightarrow {}_2He^4 + 5_1H^1 + {}_0n^1$ disintegration.

tracks indicated a slow neutron flux of 130 per cm² per min.

Perhaps the most important application of the emulsion technique resides in the recording of the trajectories of the fragments resulting from nuclear evaporations. These cosmic-ray stars were first observed by Blau and Wambacher (*49*) in plates exposed on Mt. Hafelekar at 2300-meters elevation. The phenomenon was confirmed in studies by Zhdanov (*50*), Shopper (*51*), Bose and Choudhuri (*52*).

The multiplicity, relative number, and recorded lengths of the ionizing particles are variable. The number of proton tracks usually exceeds the number of alpha trajectories. By assuming the ejection of a number of neutrons equal to the recorded number of proton tracks, it is possible to evaluate the mass and charge of the target nucleus. In the evaporations observed most frequently, the recorded trajectories indicate the evaporation of C^{12} or N^{14} nuclei, but stars with as many as 22 and 25 branches have been reported by Roy (*53*) and Zhdanov (*54*), respectively.

An example of an N^{14} evaporation observed in an emulsion exposed near sea level is reproduced in Fig. 9. The sum of the binding energy and the kinetic energy of the fragments is explicable by the assumption of the entry and annihilation of a particle of 300 electron masses (*55*).

An important contribution to meson theory has been made in the observation by Perkins (*56*, *57*) and also Lattes, Occhialini and Powell (*58*) of the emission of light and heavy mesons during nuclear evaporation processes. The tracks of these particles have characteristic grain spacing that permits their differentiation from each other and also from heavier particles of the same charge, such as the proton.

A dual event, probably composed of two meson tracks, is described in Fig. 10. Perkins (*59*) has observed that the ratio of long single tracks to cosmic-ray stars is about 20 and that the ratio is nearly independent of the altitude and the atomic number of surrounding metallic filters. The use of background eradicated emulsions should prove serviceable in securing further data at different altitudes and geomagnetic latitudes, free from ambiguities intro-

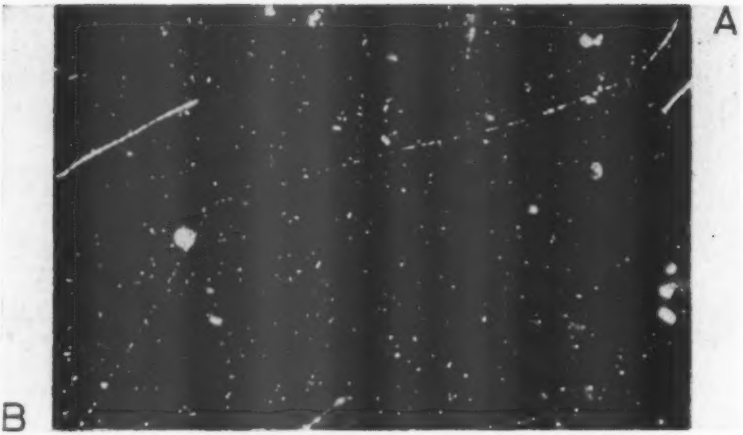

FIG. 10. Dual event of cosmic ray origin.
Darkfield illumination, magnification 570 ×

Track A is 127 microns long, and has a mean grain spacing of 1.05 microns. The grain densities at the initial and terminal points are not compatible with those of a proton of equal length. The track probably represents the trajectory of a meson. Track B terminates in the glass backing. The identity of the particle cannot be established with certainty from the recorded portion measuring 162 microns. Mean grain spacing of 2.05 microns is indicative of either a high-energy proton or meson. Surrounding short tracks were recorded by α particles from an experimental exposure.

duced by the age of the plates and variable fading of the latent image.

The nuclear-type emulsions are also of importance in studying disintegration of nuclei by incident particles accelerated to high velocities in cyclotrons. Gardner and Peterson (*60*) have observed numerous instances of multi-branched stars in emulsions exposed briefly to alpha particles and deuterons accelerated in the 184-inch Berkeley cyclotron. Studies of this character may lead to the detection of ejected meson particles, since the energy of the incident projectiles approaches those of cosmic ray components.*

The historian reviewing scientific developments between the time of Rutherford's transmutation of nitrogen and the present is likely to describe the period as one of elaborate instrumentation. Among the cyclotrons, linear accelerators, and mammoth atomic piles, the miniature nuclear emulsion is somewhat of an anachronism. Indeed, it is an incongruous item reminiscent of alchemy, prepared by mixing lunar caustic with an extract of cow's hide, in a room in which the light of the sun never enters. To complete the analogy, the adept examining the plate after its prolonged exposure on a mountain top may observe cosmic-ray stars.

---

* *Note added in proof:* The artificial creation of mesons has recently been accomplished by E. Gardner and C. M. G. Lattes [NUCLEONICS Vol. 2, No. 4, 71; *Science* **107**, 270 (1948)]. Alpha particles accelerated to 380 Mev by the 184-inch Berkeley cyclotron were passed through thin targets of several elements differing in atomic number. The charged disintegration products were deflected by a magnetic field and roughly focused on the edge of nuclear-type emulsions. Microscopic examination of the plates revealed about 50 meson tracks along an edge, as identified by grain spacing and scatter along the trajectory. Some of the meson tracks were observed to terminate in an evaporation star, similar to ones observed, on rare occasions, in plates exposed to cosmic radiation at high altitudes. The mean mass of the meson particles is estimated at 313 ± 16 m_e.

BIBLIOGRAPHY

1. M. M. Shapiro, *Revs. Mod. Phys.* **13,** 58–71 (1941)
2. C. F. Powell, G. P. S. Occhialini, D. L. Livesey, *J. Sci. Instr.* **23,** 102–106 (1946)
3. P. Demers, *Can. J. Research* **25A,** 223–51 (1947)
4. J. R. Churchill, *Trans. Electrochem. Soc.* **76,** 341–357 (1939)
5. H. Yagoda, *Am. Mineral.* **31,** 87–124 (1946)
6. H. Yagoda, N. Kaplan, *Phys. Rev.* **73,** 634 (1948)
7. H. Yagoda, N. Kaplan, *Phys. Rev.* **71,** 910 (1947)
8. H. Yagoda, "Radioactive Measurements with Nuclear Emulsions" (John Wiley & Sons, Inc., New York) in preparation
9. H. Yagoda, N. Kaplan, *Phys. Rev.* **72,** 356 (1947)
10. E. Broda, *Nature* **160,** 231 (1947)
11. E. Broda, *J. Sci. Instr.* **24,** 136–138 (1947)
12. M. Guillot, M. Perey, *Compt. rend.* **225,** 330 (1947)
13. H. Faraggi, *J. phys. radium* **7,** 353 (1947)
14. M. Blau, *Arch. Math. Naturwidenskab* **B42,** No. 4 (1939)
15. P. Cüer, C. M. G. Lattes, *Nature* **158,** 197 (1946)
16. C. M. G. Lattes, E. G. Samuel, P. Cüer, *Anais acad. brasil. cienc.* **19,** 1–28 (1947)
17. W. Y. Chang, *Phys. Rev.* **69,** 60–77 (1946)
18. W. Y. Chang, *Phys. Rev.* **70,** 632–639 (1946)
19. T. R. Wilkins, A. J. Dempster, *Phys. Rev.* **54,** 315 (1938)
20. A. C. English, T. E. Cranshaw, P. Demers, J. A. Harvey, E. P. Hincks, J. V. Jelley, A. N. May, *Phys. Rev.* **72,** 253 (1947)
21. T. R. Wilkins, *J. Applied Phys.* **11,** 35 (1940)
22. C. F. Powell, F. C. Champion, *Proc. Roy. Soc.* **183A,** 64 (1944)
23. A. N. May, C. F. Powell, *Proc. Roy. Soc.* **190A,** 170–180 (1947)
24. H. Heitler, A. N. May, C. F. Powell, *Proc. Roy. Soc.* **190A,** 180–195 (1947)
25. K. M. Guggenheimer, H. Heitler, C. F. Powell, *Proc. Roy. Soc.* **190A,** 196 (1947)
26. S. Rubin, W. A. Fowler, C. C. Lauritsen, *Phys. Rev.* **71,** 212 (1947)
27. S. Rubin, *Phys. Rev.* **72,** 1176 (1947)
28. L. B. Borst, J. J. Floyd, *Bull. Am. Phys. Soc.* **21,** No. 3 (1946)
29. N. A. Perfilov, *J. Phys. U. S. S. R.* **10,** 1–12 (1946)
30. P. Demers, *Phys. Rev.* **70,** 974 (1946)
31. H. T. Richards, L. Speck, *Phys. Rev.* **71,** 141 (1947)
32. L. L. Green, D. L. Livesey, *Nature* **158,** 272 (1946)
33. E. O. Wollan, C. D. Moak, R. B. Sawyer, *Phys. Rev.* **72,** 447–51 (1947)
34. L. L. Green, D. L. Livesey, *Nature* **159,** 332 (1947)
35. Tsien San-Tsiang, R. Chastel, Ho Zah-Wei, L. Vigneron, *Compt. rend.* **223,** 986 (1946)
36. Tsien San-Tsiang, Ho Zah-Wei, R. Chastel, L. Vigneron, *Phys. Rev.* **71,** 382 (1947)
37. Ho Zah-Wei, T. San Tsiang, L. Vigneron, R. Chastel, *Compt. rend.* **223,** 1119 (1946)
38. Tsien San-Tsiang, Ho Zah-Wei, H. Faraggi, *Compt. rend.* **224,** 1056 (1947)
39. C. Chamie, *Compt. rend.* **184,** 1243 (1927)
40. M. Halssinsky, "Les Radiocolloides" (Paris, 1934)
41. H. Yagoda, *Am. Mineral.* **31,** 462–470 (1946)
42. I. Joliot-Curie, *J. phys. radium* **7,** 313–319 (1946)
43. K. M. Endicott, H. Yagoda, *Proc. Soc. Exptl. Biol. Med.* **64,** 170 (1947)
44. S. A. Tyler, J. J. Marais, *J. Sediment. Petrol.* **11,** 145 (1941)
45. P. Demers, V. Fredette, *Phys. Rev.* **72,** 538 (1947)
46. C. M. G. Lattes, G. P. S. Occhialini, *Nature* **159,** 331 (1947)
47. K. Lark-Horovitz, W. A. Miller, *Phys. Rev.* **59,** 941 (1941)
48. D. Froman, L. Rosen, B. Rossi, *Bull. Am. Phys. Soc.* **22,** No. 3, 5 (1947)
49. M. Blau, H. Wambacher, *Sitzber. Akad. Wiss. Wien, Abt. IIa,* **146,** 259, 469, 623 (1937)
50. A. Zhdanov, *Nature* **143,** 682 (1939)
51. E. M. Schopper, E. Schopper, *Physik. Z.* **40,** 22–26 (1939)
52. D. M. Bose, B. Choudhuri, *Nature* **145,** 894 (1940); **148,** 259 (1941); **149,** 302 (1942)
53. R. R. Roy, *Nature* **160,** 498 (1947)
54. A. Zhdanov, N. A. Perfilov, M. Y. Deisenrod, *Phys. Rev.* **65,** 202 (1944)
55. H. Yagoda, Phys. Rev. **73,** 263 (1948)
56. D. H. Perkins, *Nature* **159,** 126 (1947)
57. D. H. Perkins, *Nature* **160,** 299 (1947)
58. C. M. G. Lattes, G. P. S. Occhialini, C. F. Powell, *Nature* **160,** 453, 486 (1947)
59. D. H. Perkins, *Nature* **160,** 707 (1947)
60. E. Gardner, V. Peterson, *Bull. Am. Phys. Soc.* **23,** No. 1, 7 (1948)

THE NEUTRINO

A review of the growth of experimental and theoretical evidence for the existence of the neutrino, including important recent experiments of the author. The philosophical reasoning behind the hypothesis of nuclear particles is also explained

By CHALMERS W. SHERWIN

Department of Physics, University of Illinois
Urbana, Illinois

THE NEUTRINO is a hypothetical particle which was invented mainly to save the principle of the conservation of energy, but it is also intended to conserve angular momentum (spin), and statistics, in the process of beta decay. Beta decay is considered to be an electron and neutrino leaving the parent nucleus. A proton (or a neutron) is transformed into a positive (or negative) electron and a neutrino (or antineutrino). There may be no observable difference between the neutrino and the antineutrino.

In the early 1930's, it was conclusively proved that roughly half of the energy known to be available in beta decay was disappearing in some indetectable manner. Pauli suggested that a neutral, lightweight particle could carry away this energy and still not be detected. In 1933, Fermi (*1*) included this particle in his beta-decay theory where its presence explains the distribution in the electron energies. The theory also has some success in calculating the half-lives of beta-active nuclei. A summary of the Fermi theory and its applications is given by Konopinski (*2*).

Probably the most remarkable characteristic of the free neutrino is a failure to react with matter in any detectable way. Nahmias (*3*) has shown experimentally that the neutrino must travel an average distance of *at least* 500,000 kilometers in ordinary air before producing a primary encounter. The probability of the inverse beta process (a neutrino enters the nucleus and an electron leaves the nucleus) can be calculated with the Fermi theory. The results predict that, on the average, a neutrino will go through the astronomical distance of 10^{16} kilometers of *solid matter* before this process occurs. The magnitude of this distance is illustrated by noting that it is 100,000,000 times the distance from the earth to the sun. Wollan (*4*) has recently looked for ionization produced by neutrinos near a pile which should be a very intense source. Again the results are negative. It thus appears that, once created, neutrinos are not detectable with present techniques.

Although the free neutrino has no presently measurable reaction with matter, there is reason to believe that, in the process of its creation, the neutrino should transfer a measurable impulse to the parent nucleus. Studying the neutrino by this method is analogous to studying a bullet fired from a rifle by measuring the direction and magnitude of the recoil of the rifle produced by the bullet. This paper will discuss experimental evidence regarding the energy and momentum of the nucleus produced by the beta-decay process.

It is an interesting philosophical ques-

tion whether the neutrino, if it can be detected only at its creation, will ever take on the degree of reality enjoyed, for example, by the neutron. From the operational viewpoint (*5*), all the particles of physics are devices or "constructs" that allow us to describe or "explain" a wide variety of experimental observations. A large collection of cloud-chamber photographs, meter readings, cathode-ray tube deflections, etc., are all accounted for by the neutron construct. In fact, one can almost regard the neutron as a sort of shorthand notation for this collection of observations. The neutron can never assume the "reality" of a telephone pole, for example, since it never contacts our senses in so direct a manner. When the number and *diversity* of observations quantitatively "explained" by the neutrino become large enough, it will probably take its place beside the other successful constructs. It may turn out that observations limited to the neutrino's birth, however numerous, will never completely make up for the lack of observations corresponding to its detection in the free state. For example, Peierls (*6*) recently remarked, "I need hardly say that we will never be quite satisfied about the neutrino unless we have succeeded in finding it not only emitted, but also absorbed."

Studying the recoil momentum of the parent nucleus offers a promising area of study, since momentum is a vector quantity capable of more complex combinations than is a scalar quantity like energy.

An ideal experiment would be to measure exactly the momentum of the electron and also the momentum of the parent nucleus. The vector sum would then be the negative of the neutrino momentum. The magnitude of this momentum could be compared to that calculated from the energy of the neutrino. This energy is just that part of the total available energy left over after the electron is given the energy required by its momentum. If the neutrino momenta calculated in these two ways are identical, then the neutrino satisfies both the principles of the conservation of energy and the conservation of momentum.

This experiment can be extended to measure the angular correlation between the electron and the neutrino. This is possible to do, since the measured momenta of the electron and recoil nucleus permit the reconstruction of the neutrino path in every case. The Fermi theory predicts different angular correlation functions (*7*) for the different formulations of the theory. This function is the probability that the neutrino will enter a solid angle element, $d\Omega$, making an angle θ with respect to the direction of the electron. One formulation of the theory predicts the function $\frac{1}{4\pi}(1 + \beta \cos \theta)$. Here, β is the ratio of the electron velocity to the velocity of light.

For this function, the most probable angle between the electron and the neutrino is about 60 deg. This means the neutrino goes most probably in the same hemisphere as the electron. This will be called a *forward* neutrino. If all elements of solid angle are equally likely, it will be called a *random* neutrino. Two formulations of the Fermi theory predict a neutrino which does not have a very strong dependence on angle and are similar therefore to the random neutrino. Finally, there are two forms of the Fermi theory which require $\frac{1}{4\pi}(1 - \beta \cos \theta)$ for the neutrino electron angular correlation function. This will be called a *backward* neutrino since it tends to go into the opposite hemisphere from the electron, the most probable angle between the neutrino and the electron being approximately 120 degrees.

All of the angular correlation functions listed above are supposed to hold only for the so-called "allowed" beta transitions. For a "forbidden" beta transition, Hamilton (7) has shown that the neutrino tends to go more in the general direction of the electron than it would if it were "allowed."

It may turn out that none of the angular correlation functions predicted by the Fermi theory will agree with experiment.

If the form of the angular correlation function could be measured experimentally, one would have a definite measurable characteristic attributable to the neutrino. This would aid in establishing its "reality." Also, definite proof that one of the functions predicted by the Fermi theory is in fact the observed function would be very useful in the further development of the theory. On the other hand, if the neutrino does not obey any of the theoretical functions, then the theory will have to be revised. It is clear, therefore, that the direction taken by the neutrino with respect to the electron is of considerable interest.

So far the rest mass of the neutrino has not been considered except to assume that it is very small. A recent summary of the evidence regarding the mass has been given by Frank (*8*). The method described by Frank in obtaining estimates of the neutrino mass is as follows: By studying data obtained by nuclear reactions outside of beta decay, the initial and final energy of the beta active nucleus is determined. The difference is the total available energy which must appear as kinetic energy of the electron, kinetic energy of the neutrino, and as the rest mass of the neutrino. At the extreme upper limit of the beta-particle spectrum, the neutrino kinetic energy is assumed to be zero. Thus, if the total available energy exceeds the maximum beta-particle energy, the excess energy should be accounted for by the neutrino rest mass. Frank concludes that the neutrino has a rest mass of less than one-tenth the electron mass, and that there is no evidence that the rest mass is different from zero.

The possibility of obtaining the neutrino rest mass by measuring the momentum it imparts to the nucleus will now be considered. If a neutrino has a kinetic energy E_ν and a rest mass m_ν, its momentum is given by the relativistic expression,

$$p_\nu = \sqrt{E_\nu(E_\nu + m_\nu c^2)}/c$$

When the rest mass is zero, this expression reduces to $p = E_\nu/c$. Now $m_\nu c^2$ corresponds to 50 kev if m_ν is 0.1 times the electron mass. Therefore only when the neutrino energy approaches 50 kev is there any hope that its rest mass will appreciably affect the magnitude of its momentum. Recent experiments (*9*) suggest that the rest mass may be the order of 5 kev or less. The kinetic energy imparted to even very light nuclei by these low-energy neutrinos is only of the order of one or two electron volts, an energy exceedingly difficult to measure. It thus appears that momentum measurements have little prospect of determining the rest mass (if any) of the neutrino.

An excellent survey of the neutrino problem is given by Bethe and Bacher (*10*) and Bethe (*11*). This paper will discuss only one aspect of the problem, namely, energy and momentum measurements on the beta-active nucleus. These measurements are difficult from the experimental standpoint, principally because the recoil nucleus has in most cases an energy of only about 100 ev or less. An atom or ion moving with this energy can have its energy and momentum altered greatly by even one collision with another atom. Also, since ordinary beta decay seems to involve three particles, detectors set up in some definite positions to detect the electron and the recoil atom will detect

only a small fraction of the total events. This makes the background of random counts a serious matter. Also it should be pointed out that unless the recoil atom is charged, or is itself radioactive, it cannot be detected.

Leipunski (*12*) in 1936 made a pioneer effort. He condensed radioactive CO_2 (C^{11}, $\beta+$) on a cold surface, and looked for the recoil of the boron atoms. He observed some pulses in his detection system which may have been due to genuine recoil ions, although this is not certain. Also he did not publish any data showing the upper limit, in electron volts, of the recoils. He very tentatively concluded that there were more high-momentum recoils than could be accounted for by the beta particles alone.

Crane and Halpern (*13*) in 1938 tried to observe the recoils from Cl^{38} in a cloud chamber but were unable to measure the recoil tracks well enough to draw any definite conclusions.

In 1941, Alvarez, Helmholtz and Wright (*14*) studied the recoil of the nucleus when Cd^{107} transforms, by *K*-capture, into Ag^{107}. In *K*-capture, a *K*-shell electron is captured by the nucleus since there is not enough energy available (namely, 1.02 Mev) to create a positive electron. During this process, a neutrino is assumed to be emitted, since, except for energy considerations, an electron entering the nucleus is equivalent to a positron leaving the nucleus. Fortunately, the Ag^{107} nucleus is in an excited state and is detectable by its radioactivity. If a neutrino leaves the nucleus, it should give about 8 ev energy to the nucleus by virtue of conservation of momentum. The Ag^{107} atoms were, in fact, kicked off the surface on which they were initially deposited by evaporation. Since they were not charged, no measure of their energy could be made. However, these experiments definitely lend weight to the neutrino hypothesis.

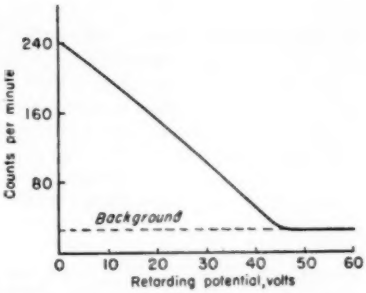

FIG. 1. Recoil ions from the *K*-capture of Be^7, as observed by Allen. The neutrino hypothesis predicts ions of 54 electron volts energy. Failure to observe ions of this energy could be ascribed to energy losses of the ions as they escape the surface on which they were originally mounted

Allen (*15*), in 1942, observed the recoil of the Li^7 ions produced by *K*-capture in Be^7. A thin source of beryllium, mounted on a platinum surface, was observed by an electron multiplier tube. Some interposing grids prevented the field of the multiplier from reaching the radioactive surface. After passing through the grids, the recoil particles, if they were positively charged, were accelerated. They struck the first dynode of the multiplier and produced secondary electrons which were then detected. Although Li^7 atoms produced are not initially charged, they become so when escaping from the high work function platinum surface. Allen applied a retarding field to the escaping ions to observe their maximum energy. Fig. 1 shows the results he obtained. Ions with energies up to about 45 to 47 ev were observed. Actually, if there were no surface effects or losses, the recoil ions should have been monoenergetic, with an energy of about 54 ev (assuming the neutrino has an energy of 0.85 Mev). There appears to be no explanation of these 45-ev recoils unless one assumes that a neutrino left the nucleus. A gamma ray known

to be present could only account for recoils up to 25 ev energy. The deviation of the observations from those predicted on the neutrino hypothesis can probably be ascribed to the effects of the surface on the escaping recoil ion.

In 1945 Jacobsen and O. Kofoed-Hansen (*16*) observed the recoil energy spectrum for Kr^{85}. A simplified drawing of their apparatus is shown in Fig. 2. The gas is at so low a pressure that the mean free path is long compared to the dimensions of the vessel. The recoiling Rb^{85} ion travels to the walls before there is any appreciable probability of collision. The Rb^{85} recoil ion is radioactive, and the deposit it makes on the wall (after going against the retarding electric field) can be measured. The fact that the radioactive source is a monatomic gas is a great advantage, since then the momentum or energy it is observed to have is due entirely to the electron (and neutrino). One difficulty with interpreting the data is correcting the observations for the effect of the retarding field on ions of differing direction. In fact, only the direction of these corrections is known, and not their magnitude.

Fig. 3 shows Jacobsen's observations along with the calculated (integrated) recoil energy distribution curves for Kr^{85}. It should be noted that the calculated curves cannot be directly compared with the experimental data. The corrections mentioned above require that the experimental curve be everywhere corrected upward on the graph. The "no neutrino" case is thus clearly in strong disagreement with the observations. Which of the other cases can be considered to be in general agreement with the data depends somewhat on the magnitude of the corrections necessary for the experimental curve. Basing his conclusions on the extreme high-energy part of the curve where the corrections must be smallest, Jacobsen very tentatively decided that

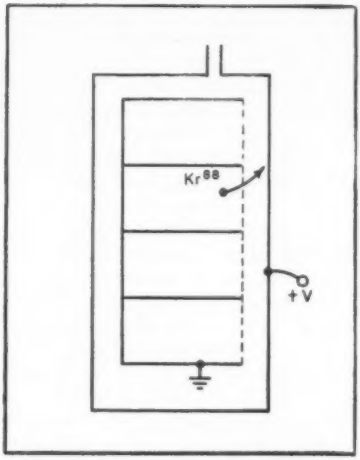

FIG. 2. Apparatus used by Jacobsen for measuring the energy of the recoil ions from the beta decay of Kr^{85}. The Rb^{85} ions pass through the grid, against the retarding potential, *V*, and deposit on the right-hand wall. The number of ions deposited can be readily measured, since Rb^{85} is radioactive

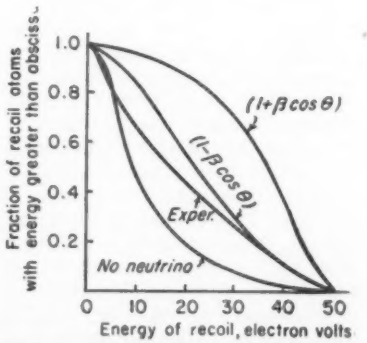

FIG. 3. Comparison of Jacobsen's experimental results on the energy of the recoil ions from Kr^{85} with the results predicted from the neutrino hypothesis. It is important to note that the experimental curve must be corrected upward at all points by an unspecified amount before it can be compared with the calculated curves. The disagreement between the experimental data and the "no neutrino" case is very clear

the $(1 + \beta \cos \theta)$ neutrino-electron correlation function is favored. This is a "forward" neutrino, going most probably into the same hemisphere as the electron.

In 1947 Fowler, Lauritsen *et al.* (*17*) made cloud-chamber measurements of the radioactive decay of Li^8. Here the Li^8 goes into Be^8 by the emission of an electron (and presumably a neutrino) and then immediately breaks up into two energetic alpha particles. The tracks of the two alpha particles and the electron can be simultaneously observed in only a few cases. However, there are many cases where the two alpha particles are both visible. Because of experimental limitations, only the projection of the tracks on one plane can be observed. Taking all the observations into account, the authors conclude that the average magnitude of the observable component of recoil momentum is about twice that due to the beta particle alone, and approximately equal to that due to an electron and a neutrino whose direction is random compared to the direction of the electron.

Thus with varying degrees of certainty all the experiments described above show that momentum is not conserved in beta decay if only the electron and the recoil nucleus are taken into consideration.

During the past year, the author (*18*) has made some experiments using very thin beta-active sources. With the availability of very high activity, separated, carrier-free radioactive materials from the Clinton Laboratories, the possibility of producing true monolayer sources of adequate activity (order of 10^4 per sec) is particularly promising. If the radioactive material is truly in the monolayer form and if the energy of the recoil ions is much larger than the surface binding energy, it is hoped that scattering of the recoil ions at the surface may not be serious. If this should prove to be the case, this type of experiment makes possible the accurate measurement of the direction of the recoil ion as well as the electron. The localized nature of this source (compared to, for instance, diffuse gas as a source) simplifies angle measurements.

The localized source also permits using the time-of-flight technique, so useful in neutron velocity studies for example, to be employed in the measurement of the momentum of individual recoil ions. The beta particle, traveling with substantially the speed of light gives indication of the time of formation of the recoil with negligible delay. The recoil ion is allowed to travel an exactly known distance in a field free space and then it is quickly accelerated and detected with an electron multiplier of the type described by Allen (*19*). Thus the time of flight and, therefore, the velocity of individual recoil ions, is measured. This method can be used to measure the mass of the recoil ion (assuming it to be singly charged).

If a grounded grid is placed directly in front of the monolayer source and the source placed at a negative potential, the time of flight is reduced due to the higher energy of the ion. The comparison of the time-of-flight measurements for different added ion energies permits a rather accurate measurement of the mass and also of any zero errors in the timing system.

The preparation of thin-layer sources is accomplished by evaporation in a vacuum. After its formation, the surface is kept in a good vacuum continuously to prevent too rapid contamination. Even so, in periods of time varying from 20 minutes to 2 hours, deterioration of the surface due to deposition from residual gases and vapors becomes noticeable.

Fig. 4 shows the experimental arrangement of the source S and the detecting equipment. The Geiger counter starts a sweep on the oscilloscope a very

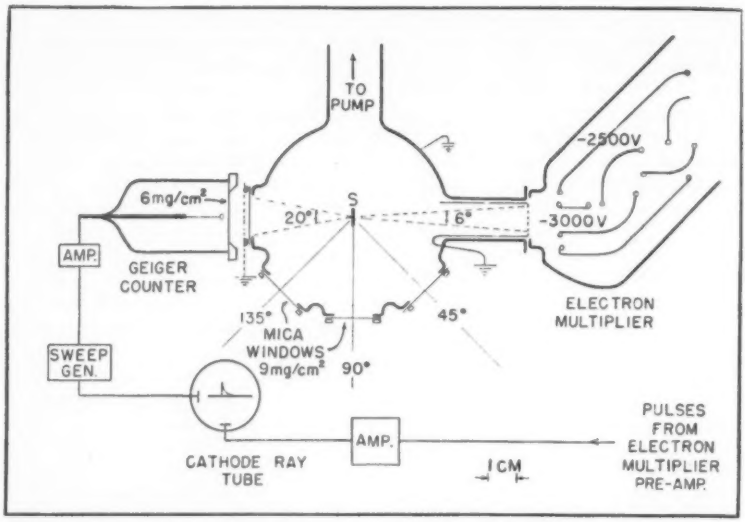

FIG. 4. Apparatus for measuring the time of flight of the recoil ions from the beta decay of P^{32}. A thin layer (probably a monolayer) of the radioactive material is mounted on S, facing the electron multiplier. The electron starts the sweep on the cathode-ray tube, and several microseconds later, the recoil ion arrives at the multiplier, causing a vertical deflection on the oscilloscope

short time after the particular beta disintegration that produced the electron occurred. Several microseconds later a pulse is observed some place on the cathode-ray tube sweep providing the recoil nucleus traveled in the right direction, and providing that it was charged. Time-of-flight spectra are observed with the Geiger counter at each of the four windows. In all cases tried thus far, the intensity of the recoils was low enough so that each recoil could be observed visually, and the time interval in which it occurred recorded. The simultaneous collection of time-of-flight data in many time intervals is essential since only this rapid process permits enough data to be collected before the source is contaminated.

Fig. 5 shows the observed recoil-momentum spectra for the beta decay of P^{32}. The most significant point about the figure is the great difference between the observations and the "no neutrino" case. If there were no neutrino, the electrons and the recoil nucleus would always go in exactly opposite directions and have the same momentum spectra. If there is no neutrino, *and* if there is no scattering of the recoils or electrons, there will be no recoils at angles other than 180 deg. The presence of recoil ions at other angles thus does not in itself give strong support to the neutrino hypothesis.

Before discussing the comparison of the observations with neutrino theory it may be well to list the basic assumptions used in calculating the recoil spectra expected from various forms of the neutrino hypothesis.

The following equations are assumed to hold for beta decay where the neutrino mass is small compared both to the electron mass and to the mass

equivalent of the neutrino kinetic energy. E_0 = total available energy; E_e and E_ν are the kinetic energy of the electron and neutrino respectively; $\mathbf{p}_r$, $\mathbf{p}_e$, and $\mathbf{p}_\nu$ are the momenta of the recoil nucleus, the electron and the neutrino, respectively.

$$E_0 = E_e + E_\nu \quad \text{(conservation of energy)}$$

$$\mathbf{p}_r = \mathbf{p}_e + \mathbf{p}_\nu \quad \text{(conservation of momentum)}$$

$$p_\nu = E_\nu/c$$

Here it is also assumed that the kinetic energy of the recoil is negligible.

Combining the above equations with the following expression for the electron kinetic energy,

$$E_e = c\sqrt{\mathbf{p}_e^2 + (m_e c)^2} - m_e c^2$$

one obtains the useful relation between the magnitude of the neutrino momentum and that of the electron momentum (m_e is the electron rest mass).

$$\frac{\mathbf{p}_\nu}{m_e c} = \left(\frac{E_0}{m_e c^2} + 1\right) - \sqrt{\left(\frac{\mathbf{p}_e}{m_e c}\right)^2 + 1}$$

where $m_e c$ is equivalent to 1,700 gauss centimeters, and $m_e c^2$ is equivalent to 0.51 Mev.

It remains only to take into account the angular correlation between the neutrino and the electron and, with the known solid angles (see Fig. 4), compute the number of recoils per beta particle that should be observed in each recoil momentum interval. This calculation is clumsy analytically, but can be done rather easily by a combination of graphical methods with numerical integration.

The calculated recoil-momentum spectra for two assumptions about the neutrino angular correlation are plotted in Fig. 5. In plotting these curves on Fig. 5, all the ordinates of the $(1 - \beta \cos \theta)$ curves were first divided by the factor 18.5, and the ordinates of the $(1 - \beta \cos \theta)^2$ curves by the factor 12.2. This normalizes the amplitudes of the calculated 180-deg. peaks with the observed amplitude. If one assumes

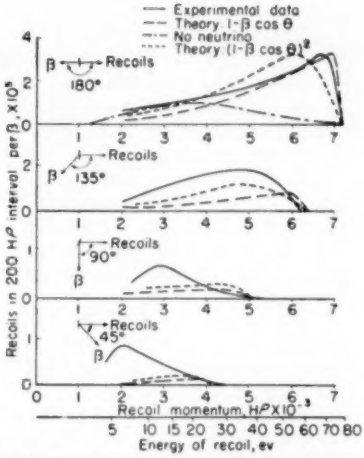

FIG. 5. The observed momentum spectra of the recoil ions from the beta decay of P^{32} compared with the neutrino hypothesis. For the $(1 - \beta \cos \theta)$ and the $(1 - \beta \cos \theta)^2$ neutrino-electron correlation functions, the most probable angle between electron and the neutrino is 120° and 135° respectively

the neutrino to be present, this discrepancy in absolute intensity can be explained by assuming that only about 6–8% of the recoil ions escape in the charged state.

In the high-momentum region, the observed and calculated curves are in fair agreement. The 180-deg curve favors the $(1 - \beta \cos \theta)$ function, and the 135-deg. curve favors the $(1 - \beta \cos \theta)^2$ function. "Random" and "forward" neutrinos each predict a very sharp high-momentum peak for the 180-deg. curve. These were never observed, even in the first few minutes after the formation of a fresh source.

The systematic disappearance of the high-momentum recoils as the angle between the beta particles and the recoils is decreased is called the "geometrical cut-off." The agreement between the predictions of the neutrino hypothesis and the observations regarding this cut-off effect is considered

to be a good argument in favor of the hypothesis.

Disappearance of the high-momentum recoils at angles other than 180 deg also indicates that scattering of the high-momentum recoils is confined to angles less than 45 deg.

The unexpected number of low-momentum recoils below about 20-ev energy is unexplained. Anomalous effects can be expected, however, when the recoil energy approaches the surface binding energy.

It should be mentioned here that some data (*20*) on yttrium-90 substantiate the conclusions based on the P^{32} data just described. The chemical nature of the Zr^{90} recoils coming from the beta decay of Y^{90} is very different from the S^{32} recoils from P^{32}. The velocity and kinetic energy are also quite different. Thus this Y^{90} data permit a rather good check on the dependability of the P^{32} measurements.

Y^{90}-recoil-momentum spectra differ from P^{32} spectra of Fig. 5 in the following points: (*a*) The Zr^{+90} recoils appear to lose about 6 ev energy in escaping from the surface. (*b*) There is no excessive intensity of the low-momentum recoils; in fact, they are too low in intensity. (This can be qualitatively explained by the presence of a 6-ev work function). (*c*) Nearly all the Zr^{90} recoils escape in the charged state. (*d*) No recoils, above background, were observed at 90 deg and 45 deg, which fact is consistent with the neutrino hypothesis and the statistical accuracy of the background measurement.

The Y^{90} data (corrected for a 6-ev energy loss) agree best with the $(1 - \beta \cos \theta)^2$ neutrino-electron angular correlation function. Thus, both P^{32} and Y^{90} data are "explained" by assuming a neutrino which most probably goes into the opposite hemisphere from the electron.

The weakness in the conclusions reached above is that *quantitative* measurements of the surface effects on the recoil ions have not been made. Until the surface effects can be exactly corrected for, the conclusion that a strongly "backward" neutrino "explains" these results must be tentative.

Considering the results of all the different investigators, it is increasingly evident that, without the neutrino, momentum is not conserved in beta decay. With the assumption of the existence of a neutrino, however, the requirements of both the conservation of energy and the conservation of momentum appear to be simultaneously satisfied. For sixteen years the neutrino has been slowly emerging from the mists of hypothesis. When, if ever, it will completely lose its wraith-like appearance and take on real substance, remains to be seen.

BIBLIOGRAPHY

1. E. Fermi, *Z. Physik* **88,** 161 (1934)
2. E. J. Konopinski, *Revs. Mod. Phys.* **15,** 209 (1943)
3. Nahemias, *Proc. Cambridge Phil. Soc.* **31,** 99 (1935)
4. E. O. Wollan, *Phys. Rev.* **72,** 445 (1947)
5. P. W. Bridgeman, "The Logic of Modern Physics" (Macmillan Co., New York, 1927)
6. R. E. Peierls, *Proc. Physical Soc. (London)* **59,** 415 (1947)
7. D. R. Hamilton, *Phys. Rev.* **71,** 456 (1947)
8. F. C. Frank, *Proc. Physical Soc. (London)* **59,** 408 (1947)
9. D. J. Hughes, C. Eggler, *Bull. Am. Phys. Soc.*, N. Y. Meeting, Jan., 1948
10. H. A. Bethe, R. F. Bacher, *Revs. Mod. Phys.* **8,** 186 (1936)
11. H. A. Bethe, "Elementary Nuclear Theory" (John Wiley & Sons, Inc., New York, 1947)
12. A. I. Leipunski, *Proc. Cambridge Phil. Soc.* **32,** 301 (1936)
13. H. R. Crane, J. Halpern, *Phys. Rev.* **53,** 789 (1938); **56,** 232 (1939)
14. L. W. Alvarez, A. C. Helmholtz, B. T. Wright, *Phys. Rev.* **60,** 160 (1941); also B. T. Wright, *Phys. Rev.* **71,** 839 (1947)
15. J. S. Allen, *Phys. Rev.* **61,** 689 (1942)
16. J. C. Jacobsen, O. Kofoed-Hansen, *Mat. Fys. Medd.* **23,** Nr. 12 (1945)
17. R. F. Christy, E. R. Cohn, W. A. Fowler, C. C. Lauritsen, T. Lauristen, *Phys. Rev.* **72,** 698 (1947)
18. C. W. Sherwin, *Phys. Rev.* **73,** 216 (1948)
19. J. S. Allen, *Rev. Sci. Instr.* **18,** 739 (1947)
20. C. W. Sherwin, *Phys. Rev.* (in press)

Chart of Decay Periods of Radioactive Nuclei

The chart on the following two pages is taken from "A Table of Radioactive Isotopes Arranged According to Half-lives," by J. W. Jones and H. M. Clark (issued by the Clinton National Laboratory, October, 1947). The material below, which is pertinent to the chart, is part of the introductory description of the table.

THE INCREASING use of neutron activation as a method of instrumental analysis, and the necessity for identification both of mixed cyclotron activities and impurities in pile-activated materials has created a need for a convenient method of identifying radioactive isotopes from their measured properties. The principal compilations of radioactive data which are available are arranged according to atomic number. If one knows the element and either the isotope or the half-life, it is a reasonably straightforward matter to locate the other properties or literature references to the isotope. However, where the element is not known, it is necessary to search through a major portion of these tables.

The information has been arranged according to half-life. Not only is the half-life usually the simplest property of a radioactive material to measure, but it also has the widest range values. The other nuclear properties which suggest themselves for classification are type of radiation, energy of radiation, and method of production. No one of these properties is as definitive as the half-life. In addition, it is common practice to identify an isotope by its half-life and element rather than by isotope number and element. The table should prove convenient for locating isotopes where certain limits of half-lives are necessary. All radioisotopes of established half-life have been included in the table except alpha emitters.

The distribution of radioactive isotopes according to decay period has been presented in chart form on the following two pages. The logarithms to the base ten of one over λ (the decay constant), $\log 1/\lambda$, is shown as one of two abscissas. Since λ is in sec^{-1}, $\log 1/\lambda$ is then log seconds. There are several reasons for the inclusion of this number. First, the use of some continuous system to arrange decay periods is desirable. The overlapping of reported half-lives of seconds into minutes, minutes into hours and so on, make it easy to overlook two adjacent activities because they are expressed in different units. The use of logarithm in seconds of either the half-life or the decay constant provides a continuous system of simple numbers for the entire system of radioactive isotopes. $1/\lambda$ instead of half-life was selected in order to provide an additional nuclear constant.

The (n,γ) and (n,n) produced isotopes are segregated below the heavy line. If an isotope is produced only by other processes it appears above the line. The isotopes are listed in columns with $\log 1/\lambda$ increasing from left to right in steps of 0.2. A scale of conventional time units is shown at the top of the graph.

It is interesting to note that the (n,γ) and (n,n) isotopes fall generally into 5 groups with almost equal periods —a time factor of approximately 40 from peak to peak. The overall (n,γ) distribution centers around $\log 1/\lambda$ equal to 5 or a half-life of 20 hours. There is also a period between $\log 1/\lambda$ equal to 4.4 and 4.6, near the center of the table, where no (n,γ) activities have been reported.

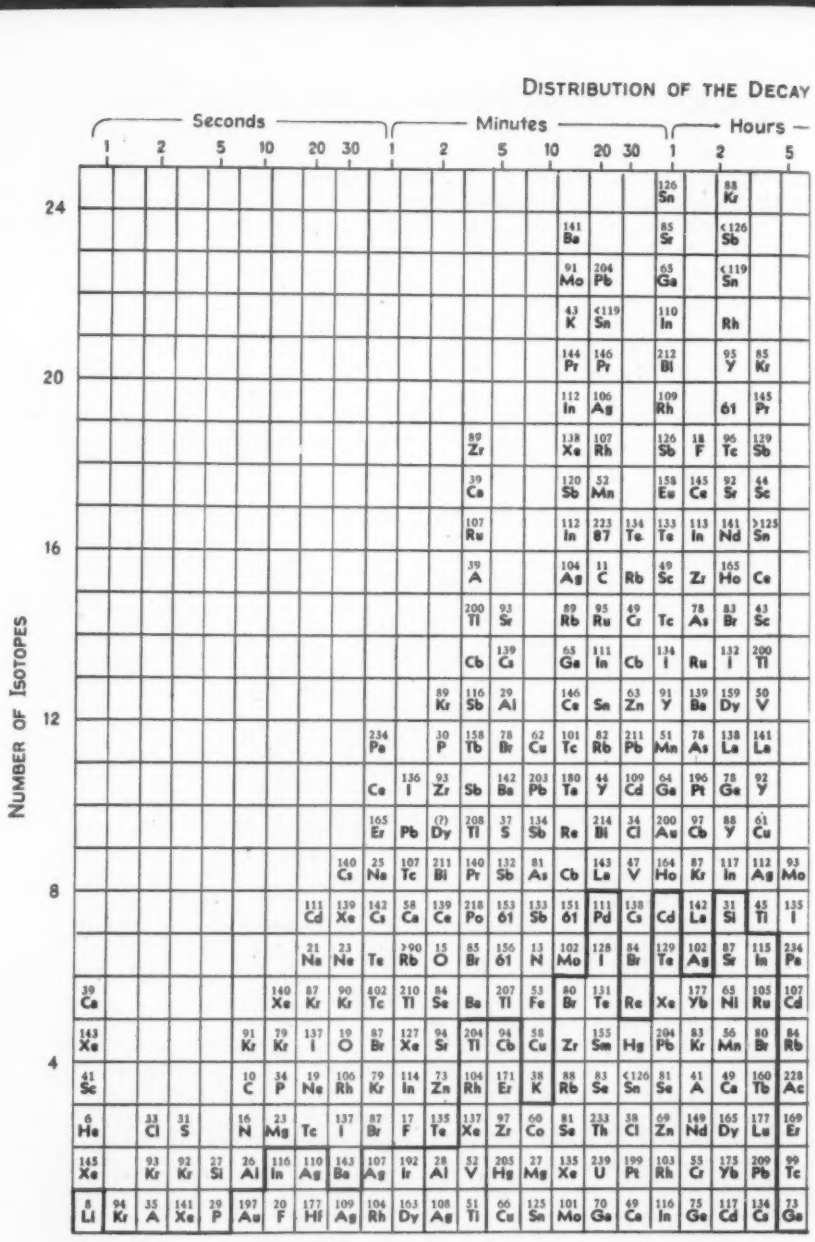
DISTRIBUTION OF THE DECAY
Seconds
Minutes
Hours
1 2 5 10 20 30 1 2 5 10 20 30 1 2 5
NUMBER OF ISOTOPES
24
20
16
12
8
4
0 1 2 3 4

PERIODS OF RADIOACTIVE NUCLEI

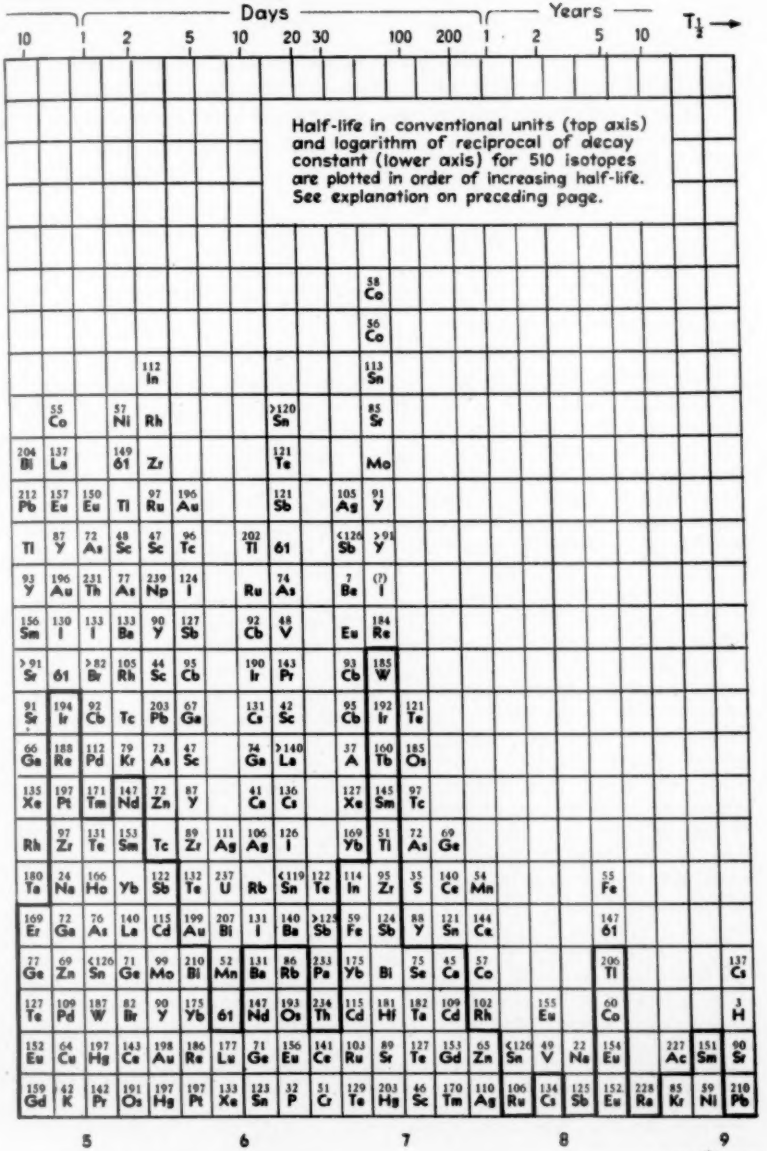

Interaction of Isotopic Radiation with Matter—I*

A review of the basic physics of radioactivity and the interaction of alpha, beta, and gamma rays with matter. Principles and methods for measurement of alpha and beta activities are explained in this first part. The discussion should serve as a background for tracer and therapeutic uses of radioisotopes

By REX G. FLUHARTY

Department of Physics and Laboratory for Nuclear Science and Engineering
Massachusetts Institute of Technology, Cambridge, Massachusetts

THE PURPOSE of this paper is to give a general physical description of the types of radiation encountered in radioactive isotopes and to review some of the practical considerations involved in their interaction with matter. For clarity and continuity of exposition, qualitative physical pictures are stressed, together with selected quantitative results.

The discussion will utilize two points of view: an examination of the individual effects of single radiations; and an examination of the overall effect of many radiations. In the case of single radiations, the result will be independent of the source of the radiation. For example, we can discuss the individual interactions of a high energy electron with matter without knowing whether or not it is a beta particle.† But in the case of many radiations, the result will depend upon the types of radiation present.

Segre Isotope Chart

A method of classification of radioactive isotopes is presented in the Segre isotope chart, a portion of which is shown in Fig. 1.

Radiations from a nucleus are the manifestations of the tendency in nature for a system to occupy its lowest energy state, and these radiations are the means by which the energy transitions are detected. A chemical analogy is the detection of molecular or bonding energy changes by means of the emission of light and heat. In chemical transitions, the nucleus of the atom remains unchanged, although variations occur in the electronic structure. (This is consistent with the fact that the energy involved in an individual chemical reaction is very small compared to the binding energy of the nucleus.‡) But in nuclear transitions, the very nature of the atom may be changed, for the radiations may involve a change in the charge on the nucleus. Hence nuclear energy transitions may change one element into another element.

Types of Radiation

Alpha particles consist of helium atoms stripped of their electrons. Each alpha particle has a double positive charge and a weight of four atomic mass units. The emitting nuclei are converted, during the process of emission

* This work was supported in part by the Office of Naval Research.

† A beta particle is a high energy electron which originated in the nucleus of an atom.

‡ Chemical energies vary from 0.1 to 10 ev, whereas nuclear energies observed in radioactive radiations vary from 0.1 to 10 Mev.

of alpha particles, into nuclei having correspondingly smaller charges and masses. Alpha particles are emitted almost exclusively by the heavier nuclei involved in the natural and transuranic radioactive decay series. They are observed to have energy values grouped between 2 and 9 Mev.

A negative beta particle is a negative electron emitted from a nucleus. After emission, the atomic number of the emitting nucleus is increased by one; the mass of the nucleus remains essentially unchanged, since an electron has a mass of only $1/1840$ of an atomic mass unit. The emission of a negative beta particle represents the transition of a neutron into a proton within the nucleus. Therefore it usually signifies an unstable nucleus with a greater excess of neutrons over protons than is normal for the atomic number of this nucleus.

Positive beta particles are positive electrons and represent the inverse process to that of negative beta particles. Thus it follows that the number of protons in the nucleus is in excess to the number normally accompanying the number of neutrons present. As a consequence a positive electron is emitted with a decrease of one in the atomic number of the emitting nucleus. The maximum energies of beta particles vary from 0.05 to 4 Mev.

Gamma rays represent energy emitted

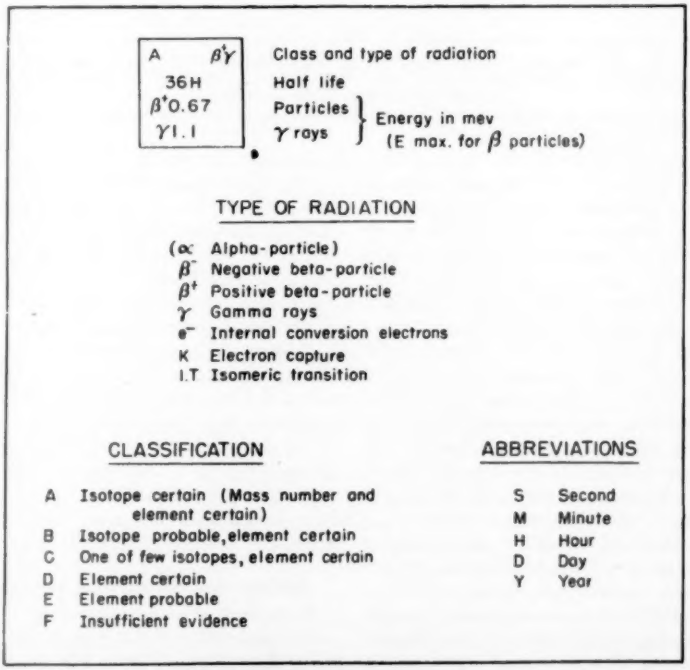

FIG. 1. A portion of the legend from a Segre isotope chart showing the types of radiation encountered in radioactive isotopes, and the type of information that is given about an isotope in the chart proper. The entries in parentheses have been added by the author

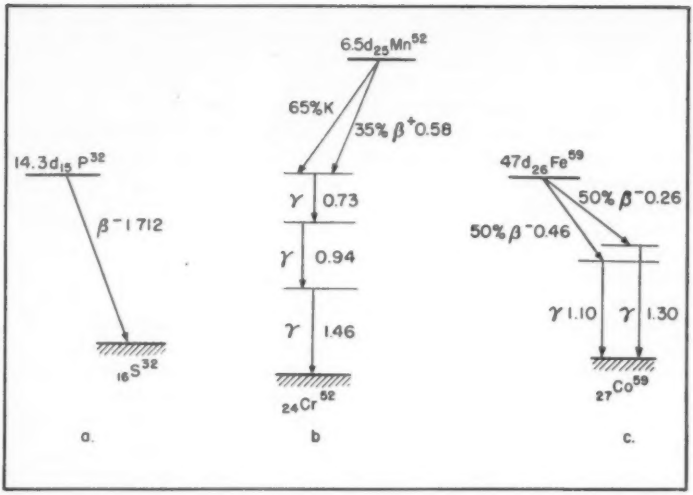

FIG. 2. Disintegration schemes showing the radiations emitted by characteristic isotopes during radioactive transitions. (S^{35}, Osborne, 1947; Mn^{52}, Peacock, *et. al.*, 1946; Fe^{59}, Deutsch, *et. al.*, 1942)

from the nucleus in the form of very rapidly varying electric and magnetic fields transmitted with the velocity of light. They are emitted as single bursts of energy or photons having definite forward momentum. Since the charge on the nucleus does not change, gamma rays result from transitions between different energy states of the same nucleus. The general energy range of interest is 0.1 to 5 Mev.

Internal conversion electrons result when the energy normally emitted by means of a gamma ray is coupled to one of the electrons surrounding the nucleus. Although not accurate, it is justified to think of the gamma ray as striking one of the electrons surrounding the nucleus and knocking it out of its orbit, with an accompanying transfer of energy to the electron. This electron emerges with an energy equal to the energy of the gamma ray minus the energy with which it was originally bound to the nucleus.

Electron capture (or "*K*-capture") is a process equivalent to positive electron emission, wherein a proton is converted into a neutron. Instead of taking place by the emission of a positive electron, the charge is neutralized by the absorption into the nucleus of one of the electrons surrounding the nucleus.

Isomers are identical nuclei in different energy states. An isomeric transition (I.T.) is thus the change from the higher to the lower energy state. It takes place either by the emission of a gamma ray or a conversion electron. In contrast to normal gamma-ray emission the excited level exists for a finite time, *i.e.*, it is in a metastable state.

Methods of Disintegration of Isotopes

In order to show how certain isotopes disintegrate, a group of typical energy level diagrams is shown in Fig. 2. The atomic number of the isotope changes on a horizontal scale with an increasing number to the right, and decreasing to

the left. The vertical distance between the lines is proportional to the magnitude of the radiation energy involved.* The crosshatched line represents ground level states of the product nuclei.

We see again that *K*-capture and positive beta-particle emission, are competing processes. Both may be present in the same isotope, *e.g.*, Mn^{52} in Fig. 2*b*. In fact, different beta-ray energies may be competing processes as shown in Fig. 2*c*. This can occur for beta plus as well as for beta minus.

An example of conversion electrons is not shown in Fig. 2. However, as a competing process to gamma-ray emission, it will be present to a small extent in all the gamma rays listed. Its occurrence is much more probable the lower the gamma-ray energy and the higher the atomic number of the nucleus.

A conversion electron, as well as *K*-capture, results in an atom with a hole or vacancy in one of the electron shells. In the subsequent refilling of the empty space in the electron shell, the characteristic X-rays of the element are emitted. Since the electrons in the *K*-electron shell have the highest probability of being nearest to the nucleus, these electrons are usually the ones absorbed. Hence, the name *K*-capture, even though an electron in the *L* and *M* shells may actually be involved. For *K*-capture, the radiation is always characteristic of the element next lowest in atomic number $(Z - 1)$ to that of the radioactive isotope (Z) under consideration. For internal-conversion electrons, the radiations are representative of the excited nucleus from which they are emitted. These radiations can be typical of the element $Z - 2$ (alpha emission), $Z - 1$ (beta plus or *K*), Z (I.T.), or $Z + 1$ (beta minus). By observing this distinctive radiation, one can assign the conversion electron to the proper element. Isomeric transitions were first demonstrated to be definitely present by this method.

General Energy Considerations

Except for their ultimate fate, the reactions of high-energy positive and negative electrons can be considered identical when they pass through matter. This might be surprising because the forces acting on them due to electric and magnetic fields are oppositely directed. Since positive electrons are created in or near the nucleus, they generally receive energy from the repulsive force due to the positive charge on the nucleus. In opposition to this, the negative electrons created under similar circumstances lose energy to this electric field. Considered in pairs they will have slightly different energy distributions.

The fact that the positron does not exist in nature in a stable form gives rise to an important reaction which occurs with the annihilation of the positron. When the positive electron has lost most of its velocity by the interaction with the surrounding material, it will finally combine with a nearby electron. This annihilation results in a neutralization of the charge, and a complete disappearance of the mass. This is a striking example of the equivalence of mass and energy, as the mass is converted into two photons or X-rays. These two photons are emitted in opposite directions and each has an energy corresponding to the mass of one of the electrons—providing the positron is exactly at rest, which is usually almost true. In this circumstance, each photon has an energy of 0.51 Mev.† If

* In the case of beta rays, the vertical distance between the lines is proportional to the *maximum* energy.

† The energy equivalence of a mass *m*, at rest, is given as mc^2, in ergs. One atomic mass unit is equivalent to 931 Mev, and hence the rest mass of the electron is approximately 0.51 Mev.

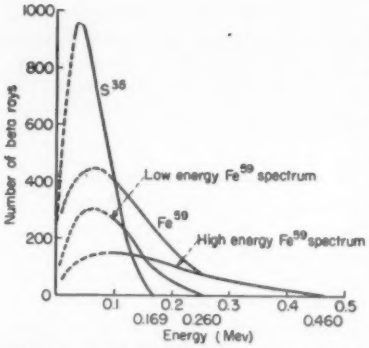

FIG. 3. The beta-ray spectra of S^{35} and Fe^{59} showing beta rays with all energies from some minimum value (probably zero for negative beta particles) up to a definite maximum. The sulfur isotope spectrum is simple, and that of iron multiple, consisting of two simple spectra of identical relative abundance. Both are typical of the spectra of other isotopes, but other spectra consist of more than one simple spectrum

annihilation takes place when the positron still has kinetic energy, the energy will be divided and added to the two photons, which will have sufficient forward direction to preserve the momentum of the positron.

Figure 3 is a plot for two isotopes (S^{35} and Fe^{59}) of the number of beta particles within a small energy interval against the energy of the particles. This would be called a number energy plot of the beta-ray spectrum. This graph shows that beta particles from any one radioactive element are found to be emitted with a wide spread of energy values. *The maximum energy of the beta ray is usually the value quoted when the beta-ray energy is given in tables and references.* The average energy of the particles emitted by a certain isotope is roughly ⅓ of the maximum energy. Better individual values have been determined from a graphical integration of known experimental data by Marinelli (*1*). E_{av} has values from 0.25 to 0.45 of E_{max}. Whenever the isotope has two maximum energies, as does Fe^{59}, the spectrum is a superposition of two simple spectra, as shown in Fig. 3. Single vertical lines would represent conversion electron energies, each of which would have a discrete energy value as compared to the continuous energy distribution of the beta particles.

A difference of minor applied importance is concerned with the number of beta particles emitted as beta plus and beta minus rays with zero energy. In Fig. 3 it will be noticed that the curve has been drawn to give zero particles at zero energy. For beta plus particles this would appear physically impossible, because any positive particle which came out of the nucleus would be given repulsion energy by the charge on the nucleus. It would therefore be expected that the distribution of beta plus particles would cross the axis at a finite value. The experimental details of this end of the spectrum are not at all well known, and do not appear important to the applied problem at hand.

When the wavelength of the radiation is small compared to the dimensions of an atom, the radiation will react separately with the individual particles composing the atom (*i.e.*, electrons, nucleus). When the wavelength of the radiation is comparable with atomic dimensions, the radiation will react with the total atom. This second type of interaction will become increasingly important as the energy of the radiation decreases, since the wavelength of the radiation is inversely proportional to the energy of the radiation.

From the standpoint of collisions, when the wavelength of the radiation is small, the matter which is being penetrated is predominantly empty space. The principal mass of an atom is found within the nucleus, which has a radius of about 10^{-12} cm. The total atom has a radius of about 10^{-8} cm. A high energy electron, a

gamma ray, or an alpha particle having dimensions on the order of 10^{-10} to 10^{-12} cm, will, in general, penetrate and pass right through any atom found in its path. The nucleus, due to its small size and strong localization of charge, will be very difficult to hit.

However, the volume occupied by the atoms is important in this sense: an electric field, which binds electrons to the nucleus, is present in each atom. This electric field will have important effects upon the penetrating particles (scattering and pair production).

For high-energy radiations, the energy with which the electrons in the material being penetrated are bound to the nucleus can be neglected, except for the innermost electrons of heavy atoms. The binding energy of the electrons will vary from 10 ev to 10,000 ev.

Since the most numerous interactions will be with electrons rather than nuclei, the main result, from the observer's standpoint, will be the ionization of the matter being penetrated. The penetrating radiations are moving with a very high energy through a practically empty space made up of weakly bound electrons and an occasional nucleus. The principal means of energy dissipation for these radiations will be by the ejection of electrons from the atoms through which they pass. The ejected secondary electron will frequently have sufficient energy to pass through the material, removing tertiary electrons from other atoms encountered. This separation of charges from the atoms creates ions. The ionization of the material being penetrated is the principal means used for detecting the radiations.

Alpha Particles

Alpha particles are characterized by very dense columnar ionization and a rapid attenuation by matter. They are stopped by 2 to 8 cm of air and by 20 to 40 microns (10^{-4} cm) of tissue or equivalent material. They create an amount of ionization in air varying from 2,000 to 3,000 ion pairs per mm of path length as they leave their source, to a peak of 6,600, to zero at the end of their range. Evidence of high concentration of ionization is shown by the scintillations or light flashes created when alpha particles impinge upon a zinc sulfide screen.*

Alpha rays find useful application as localized sources of intense ionization. An example is found in industrial plants where fire and explosion hazards are great. The alpha-ray sources are placed in strategic spots, where the ionization they create removes frictional charges and prevents electrostatic sparking. Alpha rays have also been used as a source of energy for luminous paints; as a salve for ionization treatment of skin disorders; and as an ion source to stabilize and hasten the onset of discharge in gaseous discharge tubes.

Table 1 (*2*) lists the main alpha-ray lines from the naturally radioactive alpha-ray emitters, the energy of the emergent particles, and the associated half-lives. Since the number of disintegrations is inversely proportional to the half-life, fairly large amounts of the long-lived materials may be required to obtain a certain desired number of alpha particles per unit time.

Figure 4 is a plot, for a certain alpha particle, of the ionization per mm of path length in air as a function of the distance from the *end* of the path. The range is measured from a point on the horizontal axis at the right where the particles are emitted.

The experimentally observed ionization curve for a number of alpha particles will have a statistical spread in ionization. This is represented by the

* Sulfide screens have been widely used as a means of detection of alpha rays. As each particle strikes the screen, its energy is transformed by the zinc sulfide crystals into energy of fluorescent radiation, which is visible on the screen as a bright scintillation.

TABLE 1

Natural Alpha Emitters

Disintegrating Nucleus	*Isotopic Classification*	*Energy of Emitted Alpha Particle*	*Half-life*
U I	$_{92}U^{238}$	4.21	4.56×10^9 y
U II	$_{92}U^{234}$	4.79	2.7×10^5 y
Io	$_{90}Th^{230}$	4.76	8.3×10^4 y
Ra	$_{88}Ra^{226}$	4.88	1590 y
Rn	$_{86}Rn^{222}$	5.59	3.825 d
RaA	$_{84}Po^{218}$	6.11	3.05 m
RaC	$_{83}Bi^{214}$	5.61*	19.7 m
RaC′	$_{84}Po^{214}$	7.83	1.5×10^{-4} s
Po	$_{84}Po^{210}$	5.40	140 d
Th	$_{90}Th^{232}$	4.28	1.39×10^{10} y
RdTh	$_{90}Th^{228}$	5.52	1.9 y
ThX	$_{88}Th^{224}$	5.79	3.64 d
Tn	$_{86}Rn^{220}$	6.40	54.5 s
ThA	$_{84}Po^{216}$	6.90	0.14 s
ThC	$_{83}Bi^{212}$	6.20†	60.5 m
ThC′	$_{84}Po^{212}$	8.95	3×10^{-7} s
AcU	$_{92}U^{235}$	4.59	7.13×10^8 y
Pa	$_{91}Pa^{231}$	5.14	3.2×10^4 y
Ac	$_{89}Ac^{227}$	5.10‡	13.5 y
RdAc	$_{90}Th^{227}$	6.16	18.9 d
AcX	$_{88}Ra^{223}$	5.82	11.4 d
An	$_{86}Rn^{219}$	6.95	3.92 s
AcA	$_{84}Po^{215}$	7.51	2.10×10^{-3} s
AcC	$_{83}Bi^{211}$	6.74§	2.16 m
AcC′	$_{84}Po^{211}$	7.58	5×10^{-3} s
Sm	$_{62}Sm^{149}$	2.4	1.3×10^{11} y

*0.04 % ‡1 %
†35 % §99.68 %

dotted curve (Bragg curve) which tails off at the end of the path. This tailing off is due to the statistical nature of the stopping process and is called "straggling." It has been over-emphasized in the curve to demonstrate its effect. The heavy line, which drops off to zero at the origin of the horizontal axis, represents a particle having the most probable path length or mean range. This curve is the most useful, since the shape of the straggling will usually depend upon the experimental set-up. For an ideal experiment, the range distribution should show a symmetrical, normal-law distribution about the mean range, with a standard deviation of about one percent. Thus about a third of the alpha rays will have a path length in air which differs from the mean range by more than one percent.

The relation between the energy and the mean range of the alpha ray for air at 15° C and 760 mm pressure is shown in Fig. 5. The curve can be represented fairly well by

$$R = kE^{1.5}$$

where R is the mean range, k a constant of proportionality, and E the alpha particle energy.

In materials other than air, the range L is given to a good approximation ($\pm 15\%$) by the Bragg-Kleeman Rule:

$$L = 0.0003 \frac{R}{\rho} (A)^{1/2}$$

where A is the atomic weight (mean value for mixed materials), and ρ is the density of the material in question. R can be obtained for air from Fig. 5.

Alpha particle ranges can be measured quite precisely. The straggling mentioned above occurs principally in the first few centimeters of the path length, and the form of the ionization curve will be independent of the initial energy of the particle when viewed from the end of the mean range towards the source. Due to experimental effects, the ideal straggling distribution will be smeared out and possibly distorted. Such an experimental effect will be produced by instrument resolution and finite source thickness, causing some of the particles to lose energy by the time they leave the source. However, by the use of known alpha-ray sources, a straggling parameter can be determined (*3*), and once the calibration has been performed, the instrument can be used for other particles, such as the identification of other alpha activities by means of a range determination.

A satisfactory theory for the slowing down of heavy-charged single particles,

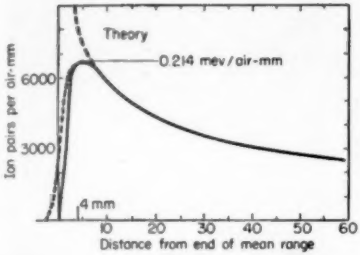

FIG. 4. Specific ionization in air due to mean-range alpha particles, where the dotted curve is a Bragg curve. The tailing-off is due to straggling, and the effect has been exaggerated

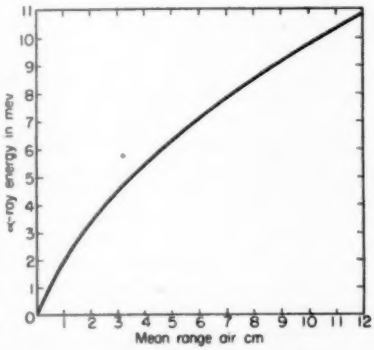

FIG. 5. Alpha-ray energy versus its mean range in air

which is valid for high energies, has been developed by Bethe and Bloch (*4*). However, Fig. 4 shows that the theory breaks down as the particle energy approaches zero. Roughly, it predicts that the amount of ionization I for a given material per unit path length will be given by:

$$I = k\left(\frac{z}{V}\right)^2 (NZ)$$

where k is a known proportionality constant, z the number of charges on the particle, V its velocity, N the number of atoms per unit volume, and Z the mean atomic number. The residual range from the point where I is measured (at the velocity V) is given by:

$$R_{res} = k' M/z^2V^2(NZ)$$

where k' is also a known constant, and M the mass of the particle. Thus, I and R_{res} can be measured, and, with a knowledge of one of the three quantities (z, V, or M), the other two can be determined. These relations are useful in many ways for the investigation of fundamental charged particles.

The large amount of ionization within a few centimeters simplifies the measurement of the relative number of alpha particles, for reasonably sized ionization chambers will contain most of the ionization. The ionization pulses from alpha particles are larger than those from other types of radioactive radiations; therefore, they can even be counted with high backgrounds of other radiations. When it is desired to suppress the alpha particles in a given application, very thin absorbers will suffice.

When solid samples are being measured, care must be exercised to account for the rapid absorption of these particles. In ionization measurements, this absorption will be even more critical than it is when the particles are being counted.

Very occasionally an alpha particle will come close enough to a nucleus in an absorbing material and will be deflected or scattered through large angles. Such scattering is consistent with the picture of the atom as a heavy charged nucleus with light surrounding electrons. In this manner, Rutherford and co-workers first demonstrated the particle concept of the atom. Also, the even rarer event of the penetration of the nucleus was the first observation leading to the discovery of nuclear disintegration.

High Energy Electrons

Single or homogeneous electrons. Per unit path length in air an electron

with high energy will create about $\frac{1}{1000}$ of the amount of ionization created by an alpha particle under the same circumstances. The attenuation of a beam of electrons will thus be less for the same amount of material, since the loss per unit path length is smaller. However, interactions of high-energy electrons are much more complex than those of alpha particles. This is due to the large difference in mass. Thus, the alpha particle, being much heavier than the atomic electrons, will move through the material in a fairly straight line, whereas the electron will be deflected both by the electron and magnetic fields of the atom. Since the high-energy electron is scattered many times, its path will not be straight.

Ionization will result by the same mechanism as for alpha particles, but additional effects will be important. The electron interactions are usually divided into two classes: (*a*) inelastic scattering (ionization and X-ray production), (*b*) elastic scattering (deflection by the electron and nuclear fields without loss of energy). Ionization, however, is the most important interaction for electrons as well as for alpha rays. Within the limits of experimental measurements, the ionization created by high energy electrons and by alpha particles can be described by the same theory, if relativity effects are taken into account. Since the velocity remains near the velocity of light, the electronic ionization per unit path length in any one material will be constant and independent of energy as long as the energy remains high. For air at 20° C and atmospheric pressure, the ionization is fairly accurately described by the equation:

$$I = 45/\beta^2,$$

where I is the ionization per cm of path length, and β is the ratio of the velocity of the electron to the velocity of light.

The number of ions per centimeter of path will depend upon the number of

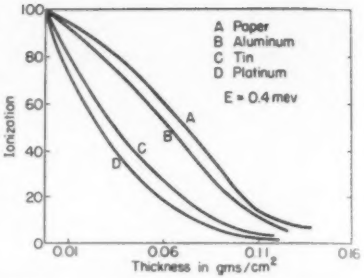

FIG. 6. Absorption curves for homogenous electrons. Curves are only representative

electrons per cubic cm. The velocity will still be constant over most of the path even though the path varies in length according to the rate of energy loss or ionization. Then the energy lost per small element of path length dr is proportional to the number of atoms per cubic centimeter multiplied by the number of electrons in each atom (Z). The number of atoms per cubic cm is given by the ratio of density (ρ in grams per cubic cm) to atomic weight A multiplied by Avagadro's number η. Expressed mathematically:

$$dE_{loss\ (ion)} = \text{const.}\ (\rho\eta Z/A)dr$$

Z/A is about constant for all elements except hydrogen, and changes gradually from 0.5 for ordinary materials to 0.4 for Pb. Thus the *ionization* will depend upon the product ρdr, and is proportional to *the number of grams per square centimeter of material.*

The high velocity electron, being light, can be deflected by the electric fields associated with the particles of the atom. For the electronic scattering, the probability of deflection will increase about linearly with Z, and for nuclear scattering it will increase about as Z^2. In hydrogen the two effects are about equal. In practice the effect of the nuclei will predominate; hence when we speak of scattered electrons, we mean nuclear scattering.

The amount of scattering diminishes rapidly with increasing energy, but cannot be neglected, as its probability is reasonably high for the thickness of materials generally used. Also, the angular deflections are frequently increased by multiple scattering events. Thus, in traversing a given material, the path length is 1.5 to 4 times the actual straight line distance. The transition from single to multiple scattering for electrons of approximately 1 Mev takes place in usual materials at thicknesses of 0.1 to 1 milligram per sq cm, the thickness increasing with decreasing Z.

Figure 6 shows the ionization from electrons penetrating various materials as a function of the thickness. These curves are for initially homogeneous electrons of 0.4 Mev (*5*). From previous theory one expects this to be a straight line, and the variations can be attributed to scattering, since it has been demonstrated that individual curves can be made convex or concave by variations in the experimental set-up.

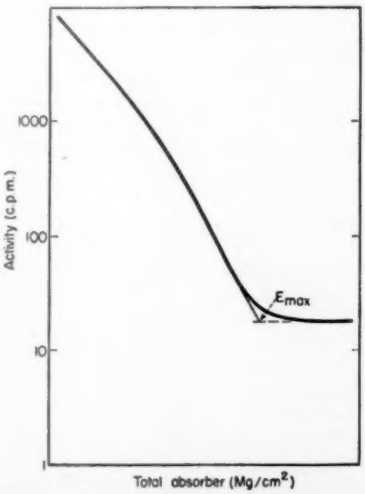

FIG. 7. Beta-ray absorption curve, typical of absorption of the number of particles penetrating aluminum when counted by an end-window, bell-type counter

In addition to the nuclear scattering just mentioned, electrons may radiate electromagnetic energy or X-rays when they are sharply deflected by the nucleus. This type of secondary radiation is known as "Bremsstrahlung" and is the source of the continuous X-ray spectrum from ordinary X-ray tubes.

Since the interaction involves the conversion of kinetic energy into electromagnetic photon energy, the normal energy conservation present in simple mechanical collisions is not observed. In cloud chamber pictures, ionization following nuclear scattering is unaltered after the deflection, hence the energy is conserved (the mass of the nucleus is great enough so that the energy it receives can be disregarded). This deflecting collision, where the mechanical or kinetic energy is conserved, is called "elastic scattering." In contrast electronic radiation is inelastic, and in the cloud chamber the ionization is markedly decreased after deflection. The photon ionization is not seen in these studies. Therefore from the cloud chamber picture, it would appear that energy was not conserved.

The loss in the electron's energy due to radiation is directly proportional to the product of the energy and Z^2 for the absorber. For energies above 1.5 Mev, the ratio of the radiation loss to the ionization loss is given by:

$$\frac{dE_{loss\ (rad.)}}{dE_{loss\ (ion)}} = \frac{kZ^2E}{Z} = \frac{ZE}{820}$$

For 10 Mev electrons traversing lead, the two effects, therefore, are found to be equal. The loss of energy for each is 1.6 Mev per millimeter of lead.

In ordinary X-ray tubes (electronic energies on the order of 0.15 Mev) the conversion is very inefficient, but for cosmic rays it is an important factor.

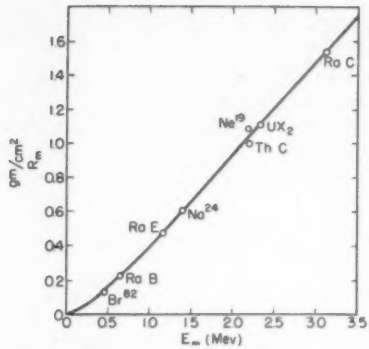

FIG. 8. Maximum range versus maximum energy of beta rays

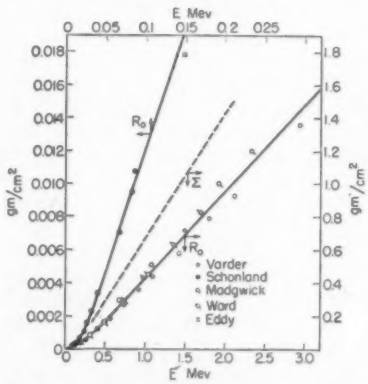

FIG. 9. Maximum range versus energy of homogenous electrons

Beta particles. Beta particles are the most frequently measured particle in the widespread tracer application of radioactive isotopes. The reasons for this are their ease of measurement and sensitivity, and their presence or availability in many of the elements from low to high Z. Also efficiency of particle detection approaches 100% per particle.

Figure 7 is typical of the type of absorption curve obtained when a flat sample is placed in front of a flat window, bell-type Geiger counter. It is to be noted that the curve is cpm (counts per minute) versus absorber thickness and not ionization or radiation intensity. Recent literature is sometimes confusing as to how the measurements have been made. With reasonable accuracy this curve can be represented by:

$$N/N_0 = e^{-\mu g}$$

where N_0 is the counting rate without absorber, N is the counting rate with g grams per sq cm of absorber, and μ is the mass absorption coefficient.

The mass absorption coefficient μ is nearly *independent of the atomic weight of the absorber*. It rises only slightly with increasing atomic number. This is due to the sole dependence of ionization or energy loss upon the grams per sq cm of material (to the degree previously discussed), to the statistical distribution in energy that the different beta particles have when emitted, and to the increased scattering at low energies. The relation between μ and the maximum beta-ray energy is given roughly ($E_{max} > 0.5$ Mev) by:

$$\mu = 22/E_{max}^{1.5}$$

It is to be emphasized that the shape of the absorption curve is dependent upon numerous factors, some of which have not been completely evaluated. Different detectors will not respond in the same way. For example, in a Geiger-Müller counter, the response is proportional to the number of particles entering the sensitive volume, and is independent of particle energy if at least one ion is created per particle. But in an ionization chamber the response is proportional to the average ionization per particle. For beta rays, this will change with the amount of absorption, which will depend upon the shape of the number-energy distribution. The number-energy distribution is only reasonably constant and not well known below 0.05 Mev.

Much better experimental evidence is

available on the maximum range of beta rays. Figure 8 is a plot for beta rays of maximum range versus maximum energy (*6*). Figure 9 is a similar plot for homogeneous electrons. A comparison of these two graphs indicates that beta particles and homogeneous electrons have similar maximum ranges. (Homogeneous electrons are observed to have slightly higher values in the linear portion of the curve, but it is to be expected that this is due to experimental differences.) Therefore, to obtain maximum ranges of low-energy, beta-ray spectra, the curve for homogeneous electrons may be used (*7*).

Comparative measurements on beta-ray activities can be made with facility. Precautions must be taken to compare the samples under sufficiently identical conditions. The various parameters that must be considered are: geometry, absorption between the sample and detector (include any window in the detector), backscattering of the sample holder (*8*), and self-absorption within the sample. The desired experimental accuracy will determine the emphasis to be placed on each of these variable factors.

Geometry is increasingly important as the sample is moved closer to the detector. A few millimeters change in this distance may well account for several percentages of difference in the activity detected. Sample uniformity must be considered here as well as for self absorption.

Absorption limitations can be roughly estimated by the equations and curves just presented. The care required will increase with lower energy spectra; many detectors will not measure the activity desired without a fair loss of activity. One cm of air at atmospheric pressure can be considered equivalent to one milligram per sq cm of material.

Table 2 is given to show the relative importance of backscattering (*8*). The absolute activities have been

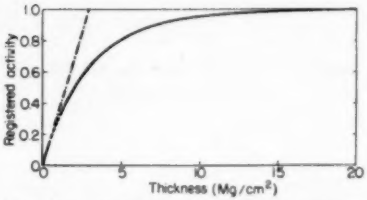

FIG. 10. Relative activity for various amounts of material in sample assuming an infinite thickness as 1. The activity per gm of material is held constant

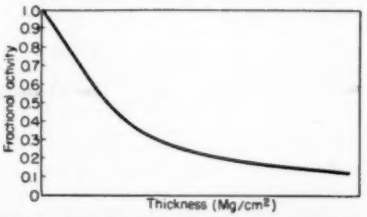

FIG. 11. Fractional activity measured versus amount of material in sample

determined by beta and gamma coincidence methods, and the table is only intended to be representative.

Where it is desired to compare measurements on samples with different amounts of material, self-absorption corrections can be made (*9*). By one method a large amount of material of the type on which the measurements are to be made is prepared with a constant amount of specific activity, *i.e.*, the same amount of activity per gram of sample. Then varied amounts of the material are measured and a plot of the type shown in Fig. 10 is made of the data. Without loss of beta rays in the sample itself, the activity should rise linearly with the initial slope indicated by the straight line. The ratio between the curves gives the fractional amount of the sample being measured. This is replotted in Fig. 11 to give a correction curve for the amount of material in the sample.

A second method gives this information directly. The samples are made

TABLE 2

Beta-ray Counter Efficiencies for Different Backing Materials

Backing Material	Co^{60} (5.3*y*) (0.31 *Mev*)	I^{131} (8.0*d*) (0.595 *Mev*)	Cu^{64} (12.8*h*) (0.60 *Mev*)	Na^{24} (14.8*h*) (1.38 *Mev*)
Paper*	0.10	0.13	0.12	0.28
Copper	0.19	0.22	0.24	0.37
Silver	0.22	0.23	0.26	0.43
Lead	0.26	0.29	0.28	0.47

* Backing material is paper, with the solution containing the material soaked into the filter paper; this corresponds to a thick source.

up containing a constant amount of activity and varying amounts of sample carrier material. Thus the plot gives the effect of the self absorption directly. This method is, of course, limited by the amount of material for a given amount of activity to start with, which puts some question upon the determination of activity with zero self-absorption. In the former method it is certain that the activity should go to zero. However, the inaccuracies of working with small amounts of material are inherent in both methods.

Both methods should be used, as each should give the same curve for Fig. 10, and will yield different information about the experimental procedure. Thus, the first method breaks down when the small sample to large sample geometry changes, or backscattering differences are large, and the assumed straight line relation is no longer valid. The second method takes these factors into account automatically. On the other hand, the first tells directly when a sample has an infinite thickness and the latter will not.

A first approximation to self-absorption is given by the equation:

$$f = \frac{1}{\mu g_0}(1 - e^{-\mu g_0})$$

where f is the fraction of the total activity in the sample, and g_0 the sample thickness (gm/cm²). Refined calculations are available in Reid's paper (*9*).

Although the determination of absolute activities is extremely important as a basis for different laboratory comparisons, we will not discuss them here. It is seen from the discussion that in other methods numerous corrections will be required in order to make absolute determinations by particle counting methods. Comparison should be made with other methods before confidence can be put into the values obtained. According to a private communication, unpublished work of this type has been done and the correlation is excellent.

BIBLIOGRAPHY

1. L. D. Marinelli, R. F. Brinckerhoff, G. J. Hine, *Revs. Modern Phys.* **19,** 25 (1947)
2. J. Mattauch, "Nuclear Physics Tables," (Interscience Publishers, Inc., New York, 1946)
3. M. G. Holloway, M. S. Livingston, *Phys. Rev.* **54,** 18–37 (1938)
4. H. Bethe, *Z. Physik* **76,** 293 (1932); Bloch, *Ann. Physik* **16,** 285 (1933); *Z. Physik* **81,** 363 (1933); Mano, *Ann. Physik* **1,** 407 (1934)
5. E. Rutherford, J. Chadwick, C. D. Ellis, "Radiations from Radioactive Substances," (The Macmillan Co., New York, 1930)
6. R. D. Evans, "The Science and Engineering of Nuclear Power," Chap. 1, (Addison-Wesley Press, Inc., Cambridge, Mass., 1947)
7. L. E. Glendenin, NUCLEONICS **2,** No. 1, 12 (1948)
8. W. C. Peacock, Thesis, MIT (1944)
9. A. F. Reid, "Preparation and Measurement of Isotopic Tracers," p. 83, (J. W. Edwards, Ann Arbor, Mich., 1946)

MANHATTAN DISTRICT DOCUMENTS

ADDITIONAL TITLES of Manhattan District Declassified Documents recently made available to NUCLEONICS appear below and supplement the seven lists previously published therein.

Listed with the name of the paper are its author(s) and MDDC (Manhattan District Declassification Code) number.

Requests for further information concerning the documents may be directed to the Atomic Energy Commission, Technical Information Division, Oak Ridge Directed Operations, Oak Ridge, Tenn. The Technical Information Division will advise requestors where the information contained in the document has been published or otherwise made available, or will provide copies of documents for purchase if the information in them cannot be obtained otherwise.

The Role of the Johns Hopkins University in the Development of the Atomic Bomb. W. B. Burford, III. MDDC 70

Photographs and Feature Article. Chicago Tribune. MDDC 71

Characteristics of Mixing and the Dilution of Waste Stack Gases in the Atmosphere. P. Church, E. Gosline, Jr. MDDC 73

Beneficial Isotopes Available from Atom Bomb Project. G. Robinson, J. McKee, P. Aebersold. MDDC 79

A General Account of the Theoretical Physics Section in the Plutonium Project. E. P. Wigner. MDDC 83

Magnetic Fields Due to Dee Structures in a Synchrotron. A. Clark. MDDC 147

Synchrotron Radio Frequency System. A. C. Helmholtz, J. V. Franck, J. M. Peterson. MDDC 151

Absorption in a High Molecular Weight Non-Aqueous System—Uranium Hexafluoride in Heavy Oil. R. Landau, D. E. Birchenall, G. G. Joris, J. C. Elgin. MDDC 152

Continuous Fluorine Disposal Plant. R. Landau. MDDC 153

Preparation of Fluorine. K. E. Long, C. F. Swinehart, G. C. Whitaker. MDDC 156

Measurement of Electric Field Strength in a Cavity Resonant at 200 Mc. W. K. H. Panofsky. MDDC 173

A Colorimetric Method for the Determination of Uranyl Ion. F. H. Priest, G. L. Priest. MDDC 175

Measurement of Density of Liquid UF_6. H. F. Priest. MDDC 176

Preparation of Uranium Pentafluoride. H. F. Priest. MDDC 177

The Thermal Conductivity of Liquid UF_6. H. F. Priest. MDDC 179

The Vapor Pressure of Uranium Hexafluoride In Equilibrium with Uranium Pentafluoride. H. F. Priest. MDDC 181

The Reaction of Fluorine Oxide with Sodium Hydroxide. E. Simons, T. P. Wilson, S. C. Schuman. MDDC 186

Precautions to be Observed in Handling, Shipping and Storage of Fluorine. District Safety Branch. MDDC 208

The Preparation of Chlorofluorocarbons. R. C. Downing. MDDC 209

Neutron Spectroscopy. J. R. Dunning. MDDC 210

Blood Chemistry Study in Dogs Exposed to Chronic X-Radiation. K. Fink. MDDC 211

Callicrein and Radiation. K. Fink. MDDC 212

The Vapor Pressures and Critical Constants of C_6F_{12}, C_7F_{12}, C_7F_{14} and C_8F_{16}. R. D. Fowler, *et al.* MDDC 213

Synthesis of Fluorocarbons by the CoF_3 Process. J. M. Hamilton, Jr. MDDC 214

The Effects of Acute and Chronic Doses of Roentgen Rays on Monkey Finger Ridge Detail. R. A. Harvey. MDDC 215

The Effect of Short Wavelength Radiations on Human Finger Ridge Detail. R. A. Harvey. MDDC 216

The Rate of Utilization of Cross-Circulated Platelets in the Thrombopenic Cat. J. S. Lawrence, W. N. Valentine. MDDC 217

Semi-Popular Motion-Picture Record of the Trinity Explosion. J. E. Mack. MDDC 221

Nomographic Charts for Nuclear Reactions. J. L. McKibben. MDDC 223

Capture Cross Sections of I^{127}, In^{115}, Ag^{109}, Au^{197}, Ag^{107} for Neutrons of Various Energies. E. Segre, *et al.* MDDC 228

Lithium, Proton Neutron Reaction. R. F. Taschek. MDDC 229

Luting for Pipe Threads in Fluorine Lines. C. F. Weber, W. B. Byrford, III, B. W. Lewis, S. B. Bitterlich. MDDC 230

Metabolism of Inhaled Fission Product Aerosols. R. Abrams, H. Seibert, A. Potts, W. Lohr, S. Postel. MDDC 248

The Pathological Anatomy of Uranium Poisoning. T. B. Barnett, R. G. Metcalf, MDDC 249

Studies on the Effects of Massive Doses of Roentgen Radiation on Mortality in Laboratory Animals. R. D. Boche, F. W. Bishop. MDDC 250

Tracer Studies with Inhaled Eight-Day Iodine. M. Dailey, I. Wender, R. Abrams. MDDC 251

Catalasuria as a Sensitive Test for Uranium Poisoning. A. L. Dounce, E. Roberts, J. H. Wills. MDDC 252

The Mechanism of Action of Uranium Compounds in the Animal Body. A. L. Dounce. MDDC 253

Tolerance to Uranium Compounds. F. Haven. MDDC 257

Toxicity Following the Parenteral Administration of Certain Soluble Uranium Compounds. F. Haven, H. Hodge. MDDC 258

The Effect of Total Body X-Irradiation on a Pre-Existing Induced Anemia in Rabbits, Part I—The Response of Animals with a Phenylhydrazine-Induced Anemia. L. O. Jacobson, E. K. Marks, E. L. Simmons. MDDC 261

Studies of the Toxicity of Various Uranium Compounds when Fed to Experimental Animals. E. A. Maynard, H. C. Hodge. MDDC 263

The Distribution and Excretion of Uranium. W. F. Neuman. MDDC 264

The Toxicology of Compounds of Uranium Following Application to the Eye. J. A. Orcutt. MDDC 265

The Toxicology of Compounds of Uranium Following Application to the Skin. J. A. Orcutt. MDDC 266

The Preparation of Morphologically Intact Leucocytes from Peripheral Blood (Part I). S. Schwartz, L. DeGrazia, K. Cheney, M. G. Hasenfus, S. Cohen. MDDC 267

The Administration of Radioactive Materials to Animals by Tracheal Intubation. H. C. Seibert. MDDC 268

The Preparation of Morphologically Intact Leucocytes from Peripheral Blood (Part II). T. P. Singer, S. Schwartz, I. Silverbach. MDDC 269

An Apparatus for Maintaining a Slow and Constant Rate of Injection. R. H. Synder, B. Lawrence, R. D. Finkle. MDDC 270

Characteristics of Uranium Poisoning. J. Henry Wills. MDDC 271

The Absorption of Slow Neutrons by Indium. B. D. McDaniel. MDDC 272

The Interaction of Nuclear Radiations with Matter. R. L. Platzman. MDDC 273

Project Handbook. Chapter I—Part 1–6. Constants and Conversion Factors. R. Platzman. MDDC 274

Acute Toxicity of Inhaled 275-day Ce^{144}. H. C. Seibert, R. Abrams. MDDC 329

Delayed Effects of Single Exposures to Beta Rays. J. R. Raper, P. S. Henshaw, R. S. Snider. MDDC 578

New Observations on Two-Dimensional Condensation Phenomena. Sydney Ross, G. E. Boyd. MDDC 864

An Integration Radiation Meter for Beta and Gamma Rays, Sigmion, Mark 10, Model 70. Argonne National Laboratory. MDDC 884

Ryerson Pocket Meter. Argonne National Laboratory. MDDC 886

Fluorocarbons. Robert D. Fowler, William B. Burford, III. MDDC 898

Description of and Instructions for Operation and Maintenance of a New Model Gamma Ray Pocket Survey Meter. O. G. Landsverk. MDDC 952

Heat Transfer in Sphere Beds. F. Johnson, R. Bentley, R. Maurer. MDDC 990

Analysis of Thorium-Chromium Mixtures. Richard E. Ewing, Charles V. Banks. MDDC 1031

Laboratory Production of Enriched BF_3 from CaF_2-BF_3. R. E. Zedler, R. I. Luman. MDDC 1155

Synthesis of Phenanthrene-9-C^{14}. Clair J. Collins, Weldon G. Brown. MDDC 1159

C^{14} Tracer Studies of the Rearrangements of Unsymmetrical Alpha-Diketones: Phenylgloxal to Mandelic Acid. O. Kenton Neville, Weldon G. Brown. MDDC 1168

Preliminary Studies in the Toxicology of Beryllium. The Effect of Intratracheal Injection of Beryllium in Experimental Animals. Charles W. LaBelle, Martha Reid Cucci. MDDC 1232

Determination of Trace Amounts of Elements by Radioactivation Analysis. Herbert M. Clark, Ralph T. Overman. MDDC 1329

The Halides of Neptunium. L. Brewer, L. Bromley, P. Gilles, N. Lofgren. MDDC 1417

The Ionic Absorption Spectra of the Uranium Halides in a Polar, Non-aqueous Solvent. C. C. Sterett, V. P. Valkins. MDDC 1473

The Dry Box. Los Alamos Laboratory. MDDC 1507

Investigations on the Absorption Spectra Induced in Single Crystals of Magnesium Oxide by Exposure to Various Types of Radiation. Charles A. Boyd, Dow Rich, Eugene Avery. MDDC 1508

The Synthesis of Phenathrene-9-C^{14}. Clair J. Collins, Weldon G. Brown. MDDC 1509

Note on the Stability of Pu(IV) in Alkaline Solution. R. E. Connick, W. H. McVey, G. E. Sheline. MDDC 1510

Note on the Stability of Pu(VI) in Alkaline Solution. R. E. Connick, W. H. McVey, G. E. Sheline. MDDC 1511

The Quantitative Spectrographic Analysis of the Rare Earth Elements. V. A. Fassel, H. A. Wilheim. MDDC 1512

The Preparation of Technetium Metal. S. Fried. MDDC 1513

Calculation of Internal Conversion Coefficients. G. Goertzel, M. E. Rose. MDDC 1514

Techniques for the Preparation of Thin Films of Radioactive Material. D. L. Hufford, B. F. Scott. MDDC 1515

The Reaction $He^3(n,p)H^3$ and the Neutrino Mass. D. Hughes, C. Eggler. MDDC 1516

An Ionization Chamber for Alpha-Ray Measurements. R. Livingston. MDDC 1517

Use of Code Words. Los Alamos Declassification Group. MDDC 1518

Waterproofing and Shockmounting Portable Meters. E. W. Molloy. MDDC 1519

On Gaseous Self-Diffusion in Long Capillary Tubes. W. G. Pollard, R. D. Present. MDDC 1521

Triphosphatase and Other Phosphatases on the Surface of Living Yeast Cells. A. Rothstein, R. Meier. MDDC 1522

High Resistance Bridge (Range 10^8 to 10^{12} Ohms). R. J. Smith. MDDC 1523

A Study of Variations Accompanying Low Current Ionization Chamber Measurements. R. K. Swank, H. Palevsky. MDDC 1524

Artificial Radioactive Isotopes of Polonium, Bismuth, and Lead. Chapter III—Light Isotopes Produced by High Energy Particles. D. H. Templeton. MDDC 1525

The Conversion of UF_4 to U_3O_8. A. D. Trevebaugh, W. D. Cline, J. C. Warf. MDDC 1526

Laboratory Handling of Radioactive Material: Protection of Personnel and Equipment. P. C. Tompkins. MDDC 1527

Excitation Function of the Reaction $C^{13}(n,2n)C^{11}$ at High Energies. W. Heckrotte, Peter Wolff. MDDC 1532

Techniques for Irradiating Microorganisms with Artificially Radioactive Materials, Part I—Radioactive Material in Suspension. G. E. Stapleton, E. Loftus, I. Armstrong. MDDC 1535

Determination of Oxygen in Tank Nitrogen by Its Conversion to Water and the Measurement of the Dewpoint Temperature. H. A. Bernhardt, *et al.* MDDC 1542

Study of Sources of Contamination in the Analysis of Radioactive Materials. R. J. Gettens. MDDC 1544

Mass Spectrographic Mass Assignment of Radioactive Isotopes. Richard J. Hayden. MDDC 1546

Further Measurements of Polarized Neutrons. D. J. Hughes. MDDC 1548

Induction of Mutations in Paramecium Aurelia by Beta Radiation. R. F. Kimball. MDDC 1550

Rotary Leaf Filter. Myron Kratzer. MDDC 1552

Determination of Plutonium in Human Urine. W. H. Langham. MDDC 1555

Diffraction Effects in Neutron Attenuation Measurements. E. M. McMillan, D. C. Sewell. MDDC 1558

Crystal Radii of the Heavy Elements. W. H. Zachariasen. MDDC 1572

The UCl_3-Type of Crystal Structure. W. H. Zachariasen. MDDC 1573

Radiocarbon of High Specific Activity. Arthur H. Snell, L. D. Norris. MDDC 1584

Phosphorus Turnover and Photosynthesis. Sam Aronoff, Melvin Calvin. MDDC 1589

The Assessment of Gamma Radiation Dosage by Means of Radioisotopes in Mockups. J. G. Hoffman. MDDC 1590

Writing of Reports and Memoranda. D. R. Inglis. MDDC 1591

Ultrasonic Velocity in Some Liquid Fluorocarbons. R. T. Lagemann, W. E. Woolf, J. S. Evans, N. Underwood. MDDC 1592

Ionization Chamber Studies of Energy Transfer from 100 Mev Neutrons to Light Nuclei. R. Loevinger. MDDC 1593

Stars in Photographic Emulsions, Part I. Experimental. E. Gardner, V. Peterson. MDDC 1594

The Relative Energies of the Gamma Radiations from Co^{60} and Zn^{65}. E. N. Jensen, L. J. Laslett, W. W. Pratt. MDDC 1595

The Comparative Metabolism and Distribution of Carrier-Free Radioarsenic (As^{74}). H. Lanz, Jr., J. G. Hamilton. MDDC 1596

Progress Report to August 1947, Medical and Health Physics Section, Part A—Cobalt Distribution. P. P. Weymouth, L. R. Wasserman, N. Berlin, R. Rosenthal. MDDC 1597

Oscilloscope Camera Self-Supporting (consisting of 9 drawings). Los Alamos Laboratory. MDDC 1598

The Velocity Distribution of the Neutrons Emitted from a Slow Neutron Source. C. P. Baker, B. D. McDaniel, R. F. Bacher. MDDC 1599

The Preparation of Carrier-Free I^{131}. D. S. Ballantine, W. E. Cohn. MDDC 1600

Heats of Reaction of the Aqueous Uranium Oxidation-Reduction Couples. B. J. Montana. MDDC 1603

The Evaporation of Gallium. S. K. Haynes. MDDC 1604

Dosage Determination with Radioactive Isotopes—II*

BIOLOGICAL CONSIDERATIONS AND PRACTICAL APPLICATIONS

When radioactive isotopes are employed either as tracers or in therapy, it is important to be able to determine the radiation dosage. This cannot, in general, be measured, but when the half-life, radiation energy, and biological uptake and excretion are known, it can be calculated.

The first part of this paper was devoted to the development of formulas for dosage rates and total dosages for beta- and gamma-ray emitting isotopes, together with some subsidiary expressions. Since the basic information regarding radiation disintegration schemes and energies is scattered through many journals, it has been considered desirable to collect the pertinent data. Two extensive tables were presented for beta and gamma rays, respectively, giving half-life, radiation, average energy, fraction disintegrating per day, and specific dosage data, including safe tracer concentration, for some 38 isotopes of more than 30 elements.

In the second part, practical applications of the formulas are illustrated. The importance of such biological considerations as relative tissue concentrations and excretion rates is brought out. Particularly considered is the determination of safe tracer doses.

IN DISCUSSING the applications of the beta- and gamma-ray dosage formulas developed in Part I† of this paper, it is convenient first to summarize the main results. The numerical values of the different constants for some 38 isotopes are given in Tables 1 and 2 in Part I and will be used here.

Beta-ray Emitters

When a radioisotope emits only beta rays, the dose is essentially confined to the regions containing the material because the range of the beta particles in tissue is only a few mm.‡ The *total dose D_β in equivalent roentgens*, due to the complete disintegration of a radioelement biologically stable and present in a uniform concentration of C microcuries per gram of tissue, is

$$D_\beta = K_\beta C \text{ e.r. per } C \ \mu\text{cd per gram of tissue} \quad (4)$$

where

$$K_\beta = 88\bar{E}_\beta T \text{ e.r. per } \mu\text{cd per gram of tissue} \quad (4a)$$

T is the half-life of the isotope in days and $\bar{E}_\beta$ the *average* energy per disintegration of the beta rays in Mev.

Gamma-ray Emitters

When an isotope emits gamma rays, the dosage problem is more complicated. Gamma rays released in a gram of tissue produce only a small amount of ionization therein; most of their energy is expended elsewhere along their paths.

The *total dose* D_γ due to gamma rays emitted by the complete disintegration

* This paper is based in part on work done under contract N6-ORI-99 with the Office of Naval Research.

† NUCLEONICS **2**, No. 4, 56 (1948).

‡ Many organs in small animals used in experiments dealing with isotopes emitting high energy beta rays are not small in comparison to the range of the beta particles. Proper estimate of the dose in these instances is, in general, very complicated, and must be left to the future.

of a radioelement biologically stable and present in a uniform concentration of C microcuries per gm of tissue is given by

$$D_\gamma = K_\gamma C g \text{ roentgens per } C \text{ } \mu\text{cd per gram of tissue} \quad (16)$$

where

$$K_\gamma = 1.44 t I_\gamma \times 10^{-3} \text{ roentgens per } \mu\text{cd at 1 cm in air} \quad (16a)$$

K_γ expresses the number of roentgens at 1 cm distance in air due to the *complete disintegration* of an unfiltered point source of one microcurie. $1.44 \times t$ is the average life in hours. I_γ is the dose rate in roentgens per hour at 1 cm in air from an unfiltered point source of one millicurie. The quantity g in equation 16 is a *geometrical factor* depending on the size and shape of the tissue mass under consideration and on the absorption of the gamma rays; g can be calculated for only one point at a time and it is a function of the coordinates of this point.

For *radon* filtered by 0.5 mm Pt, I_γ corresponds to the well-known figure of 8.4 r per mc-hr at 1 cm distance in air, and $K_\gamma = 133 \times 8.4 \times 10^{-3} = 1.1$ r per μcd of radon at 1 cm in air. ¶

No general statement can be made regarding the relative contributions of the beta and gamma rays to the total radiation dosage. The relative amounts of energy emitted as beta and gamma rays are characteristic of but different for each isotope. Also the geometrical factor g, which is a function of both penetration of the gamma radiation and size of the organ, is likely to vary tremendously with the problem. As an illustration, the beta- and gamma-ray doses of Na^{24} for the center of the human body will be calculated in a later section.

Distribution of the Radiation in Tissue

The physical data presented in Part I enable the experimenter to calculate the actual dose delivered to a tissue or individual whenever the isotope concentration C is known as a function of time. This depends on amount of isotope administered, species and metabolic state of the test animal, mode of administration, chemical form in which the radioelement is given, etc.

Physiological information of this nature is of great importance; the literature shows that a good deal of animal work has been done on the relative uptake of various isotopes by different tissues at different times. As an example, Fig. 5 presents the relative radiation doses delivered in different tissues in mice (*1*) injected intraperitoneally with a single dose of P^{32} in the form of Na_2HPO_4. The animals were sacrificed at various times after the administration of the material, and the concentration of P^{32} was determined for the various tissues and organs. With this information it was possible to calculate the dose of radiation received by each tissue as a function of time. Similar calculations were made for the whole body, assuming uniform distribution. The "theoretical" whole-animal dose** after complete disintegration of the isotope, was taken as 100 percent, and all other tissue doses referred to this value. Thus, at the end of three weeks, 64 percent of the theoretical complete dose had been delivered; but all tissues

§ Biophysics Laboratory, Sloan-Kettering Institute for Cancer Research, New York.

‖ Dept. of Radiology, College of Physicians and Surgeons, Columbia University, New York.

¶ Numerical values for the different gamma-ray lines of Ra, RaB and RaC are given by R. D. Evans, NUCLEONICS 1, No. 2, 39 (1947).

** By "theoretical" whole-animal dose is meant the dose Dg which would have been obtained in the animal after complete disintegration of the isotope on the assumption of uniform concentration in the animal and of total lack of biological elimination.

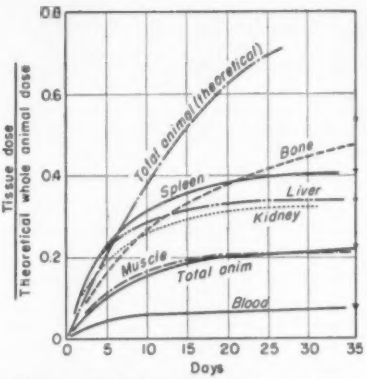

FIG. 5. Radiation dosage due to beta-ray activity of P^{32} in different tissues in mice as a function of time. Points on right margin are actual tissue doses obtained by extrapolation to infinite time. Theoretical whole animal dose equals K_β times number of microcuries administered divided by total weight of the animal

tested, except the bone, had already received practically all their radiation because, by this time, most of the P^{32} had disappeared. The liver, for example, had received about 33 percent of the theoretical uniform dose. At that time, the bone had received 39 percent; but in the bone, the dosage increased to 48 percent at the end of 36 days.

No tissue actually attained the theoretical dose or would have attained it after longer periods of time because of biological elimination. From the curves, the actual tissue dosage per μc of P^{32} thus administered in a mouse of 25 grams can now be calculated. The total animal concentration would be 0.04 μc per gram and the "theoretical" total animal dose $D_\beta = K_\beta \times 0.04 = 885 \times 0.04 = 35.4$ e.r. (K_β from Table 1). The liver, then, at the end of three weeks, would have received 33 percent of this value or 12 r; similarly the bone at 36 days would have had $0.48 \times 35.4 = 17$ r.

It is recognized that, with the use of P^{32} in mice, these determinations are not as accurate as one would wish because the linear dimensions of most organs are smaller than the range of a considerable portion of the beta particles emitted by P^{32}. Similar information in larger animals would yield more reliable figures. Conversely, this type of calculation would be fairly accurate even in a small animal, if soft beta-ray emitters (H^3, C^{14}, S^{35}, etc.) were used.

When working with humans, it is not possible, in general, to study concentrations throughout the body and their variations with time by *in vivo* measurements; the extreme concentration of iodine in the thyroid is an exception. For most isotopes, information must be obtained from biopsy and autopsy measurements; hence data are meager.

Differential Absorption Ratio

To take into account the differences in uptake which lead to differences in dose for the various tissues, it is convenient to express the concentration in terms of a "differential absorption ratio" (D.A.R.). For any tissue, this is the ratio of concentration of an isotope in that tissue to the average concentration in the body (neglecting excretion). Thus, if a particular tissue has a D.A.R. of 1, it should receive the same dose of radiation as the average of the whole body; if it has a D.A.R. of 10, it should receive ten times as much radiation (*vide infra*).

In calculating the *safe doses for tracers*, it is highly desirable to have some idea of the range of the D.A.R.'s. The safe dose is assumed to be 0.1 r per day for the entire body; if a certain tissue has a D.A.R. of 10, it may receive 1 r while the rest of the body receives 0.1 r. This may lead to undesirable irradiation of certain tissues or organs from a dose believed safe otherwise.

The procedure outlined above needs clarification. In general, single tissues and the whole body have different rates and modes of elimination, hence the tissue D.A.R. will vary with time. The

question then arises as to the time at which D.A.R.'s have significance in determination of tissue dosage. Evidently the D.A.R. will be too low when taken too soon after the isotope administration because the concentrations have not yet stabilized. Likewise adoption of the D.A.R. after several half-lives will have little or no significance because most of the isotope has already disintegrated. One useful index, whenever the isotope reaches the body tissues through the circulatory system, could be the stabilization of the plasma concentration. No general rule, however, can be given and good judgment is of paramount importance, since it must be realized that exact information on total tissue dose requires knowledge of the isotope concentration in that tissue throughout several half-lives.

Effective Half-life

Elimination of a radioisotope from a given tissue obviously affects the dose delivered since a fraction of atoms initially present in the tissue will not disintegrate therein. In the case of a *constant rate of elimination*, in so far as total dose is concerned, the fundamental formulas, 4 and 16, still apply, provided that by the half-life is meant the effective half-life, T_{eff}:

$$T_{eff} = \frac{T \times T_b}{T + T_b}$$

of the isotope in the tissue as affected by both disintegration and elimination.

$T = 0.693/\lambda$, λ = physical decay constant

$T_b = 0.693/\lambda_b$, λ_b = rate of elimination constant

In instances of extreme concentrations, as in the case of *radioiodine* I^{131} administered to humans, the effective half-life can be obtained directly from repeated *in vivo* measurements. Within 24 hours after administration of a dose of radioiodine, almost all of it is either concentrated in the thyroid gland or

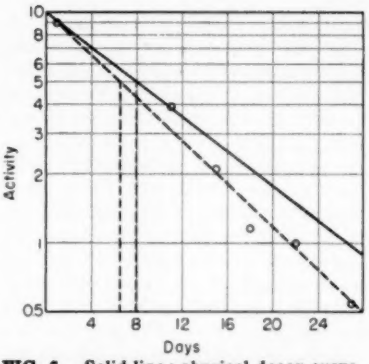

FIG. 6. Solid line: physical decay curve of I^{131} half-life, 8 days. Broken line: actual decay curve of I^{131} in a hyperthyroid patient; effective half-life, 6.5 days

eliminated from the body. The activity in the thyroid can be determined with a Geiger counter in a fixed position over the thyroid gland. If there were no excretion of the material from the gland, these counts should decrease exactly in accordance with the physical decay curve for the iodine (Fig. 6, heavy line: $T = 8$ days). The actual series of counts in a patient treated with I^{131} for hyperthyroidism is shown in Fig. 6 (broken line); the effective half-life in this case is 6.5 days. It is evident that the use of this number instead of 8 in equation 4 results in a decrease of 20 percent in the administered dose, an amount which is probably clinically significant in therapeutic work.

It would now be possible to calculate from formula 4 the beta-ray dose delivered under normal conditions if the initial concentration C were known. This can be determined either by actual biopsy or "guessed" by estimate of the gland weight and measurements of the radioactive content of the gland by proper *in vivo* observations.

Tracer Isotopes—Examples

In order to illustrate the use of the material presented in this paper, dose

calculations will be given for two radioisotopes frequently used in tracer experiments and in therapy. Further examples will be found in the clinical part of a paper on this subject by the same authors (*2*).

Radioactive phosphorus, P^{32} (beta particles only). If the P^{32} isotope were evenly distributed throughout the body and no elimination took place, the values of Table 1 (Part I) would be directly applicable. Thus, if 2.4 μc per kg of tissue weight gives a dose of 0.1 e.r., an initial radiation dose of d e.r. per day will require a concentration x μc/kg such that $2.4 : 0.1 = x : d$; namely,

$$x = \frac{2.4 \times d}{0.1}$$

$= 24 \times d$ μc per kg of tissue weight

If a total radiation dose D_β (e.r.) is to be given to a tissue, the concentration in that tissue should be such that

$$D_\beta = K_\beta C$$

or $C = \frac{D_\beta}{885}$ μc of P^{32} per gram of tissue weight.

As discussed earlier, the most exhaustive information on the distribution of this isotope in mice (*1*) shows that the highest radiation dose is given to bone, followed in order by spleen, liver, kidney, muscle and blood. In general, the limited information on adult humans, obtained for the major part from autopsies of leukemic patients (*3–8*), does not contradict the results in mice, provided that only non-infiltrated tissue obtained from patients given single doses of P^{32} be taken into consideration. Limited data on non-irradiated surgical material are also available (*9*). The most reliable D.A.R.'s on *bone* are of the order of unity, though wide variations are quoted not only among individuals but also among portions of the same bone (*4, 9*). The absolute values of the D.A.R.'s for human bone—as in the case of mice—seem to bear no detectable relation to the time elapsed between administration and assay; this indicates a slow "net" elimination of P^{32} from bone.

The highest D.A.R. reported (*6, 9*) on *human marrow devoid of leukemic infiltration* can also be taken as of the order of unity for the first few days following P^{32} administration. Data on sternal aspiration (*6*), however, are decidedly lower, being much closer to those of blood. The latter, in humans, receives "apparent" doses of the order of 20 percent of the theoretical whole body dose (*10*). It seems therefore that doses of the order of 2.4 μc per kg of body weight can be safely administered, though they may produce wholly transitory but definite biological effects. Such reactions have been reported by Low-Beer and Treadwell (*11*) for concentration of 6–9 μc per kg of body weight.

If P^{32} is administered intravenously in *insoluble form* (*12*) the deposition in the liver and spleen is likely to be very marked. These authors report 80–89 percent in the liver (dog and mouse); if this were to obtain in humans the D.A.R. would be:

$$\text{D.A.R.} = \frac{\mu\text{c in liver/liver weight}}{\mu\text{c administered/body weight}} = \frac{0.89 \times 70}{1.7} = 36.7$$

where 1.7 kg is the weight of the average human liver (*13*). In this case, the maximum permissible concentration would be $2.4/36.7 = 0.066$ μc per kg of body weight or a total tracer dose of $0.066 \times 70 = 4.6$ μc for a 70 kg man.

Radioactive sodium, Na^{24} (beta and gamma radiation). This sodium isotope, administered orally or intravenously, is eliminated in very small amounts during times comparable to its half-life of 14.7 hours. Since it is distributed rather uniformly throughout the body (*14, 15*), computation of beta-ray dosage can be made on the basis of D.A.R. = 1. The factor S_β of

Table 1 can be applied directly in the case of small animals where the beta rays account for most of the radiation dose, the factor g in the gamma-ray formula being very small. For larger animals and humans, however, the gamma-ray contribution cannot be neglected. In this case, dosage calculations become more involved.

As pointed out above, the contribution of gamma rays to the daily tissue dose is

$$d_\gamma = K_\gamma C g f_d \text{ roentgens,}$$

where K_γ = roentgens per μcd at 1 cm in air

C = concentration in μc per gram of tissue weight

f_d = fraction of atoms destroyed in one day

g = geometrical factor which is a function of size and shape of tissue volume and penetration of radiation

For purposes of calculation, one may assume that the human trunk is a cylinder of radius $R = 20$ cm and height $2Z = 60$ cm, and that C is constant throughout. Then the highest dose is delivered at the midpoint of the axis and g can be expressed with sufficient approximation* as

$$g_j = 314 - 4140\mu_j$$

where μ_j is the absorption coefficient of the gamma rays in tissue. For the gamma rays from sodium (see Table 2 and Fig. 2), the values of μ_j are 0.0296 and 0.0233 per cm, respectively. An average $\mu_j = 0.025$ may be assumed for the present calculation and hence $g = 210.5$. Substituting for K_γ and f_d the values from Table 2, one obtains: $d_\gamma = 0.40 \times 0.68 \times 210.5\ C = 58.0\ C$ roentgens per day at the trunk's center. Similarly (Table 1):

$$d_\beta = 29 \times 0.68 \times C$$
$$= 19.7C \text{ e.r. per day}$$

Hence the *total dose for the first day*

$$d_{\beta+\gamma} = 77.7C$$

Since 68 percent of the atoms disintegrate during the first day, $77.7C$ is 68 percent of the *total dose* $D_{\beta+\gamma}$:

$$D_{\beta+\gamma} = 100/68 \times 77.7 = 114C \text{ e.r.}$$

For the tolerance dose of 0.1 r for the first day

$S_{\beta+\gamma} = 0.1/77.7 = 0.0013$ μc per gram, or

$= 1.3$ μc per kg of body weight.

When tracer studies are to be carried out once or a few times on an individual, for diagnostic purposes, the physician may legitimately employ doses considerably in excess of those giving only the radiation permitted for continuous exposure. The diagnostic radiologist does not hesitate to give local exposures of several roentgens, and to repeat these at need. In human studies with radioactive isotopes, consideration must be given to all the factors involved in the individual case—the D.A.R.'s, the volume and radiosensitivity of the tissues receiving the greatest dose, the number of times the test is to be repeated, the possibility of the patient receiving radiation from any other source, and any other pertinent data.

* Nucleonics **2**, No. 4, 63 (1948).

BIBLIOGRAPHY

1. L. D. Marinelli, J. M. Kenney, *Radiology* **37**, 691 (1941)
2. L. D. Marinelli, E. H. Quimby, G. J. Hine, *Am. J. Roentgenol. Radium Therapy* **59**, 260 (1948)
3. L. A. Erf, *Am. J. Med. Sci.* **203**, 529 (1942)
4. L. A. Erf, *Proc. Soc. Exptl. Biol. Med.* **47** 287 (1941)
5. A. Forssberg, *Acta Radiol.* **27**, 88 (1946)
6. J. M. Kenney, *Cancer Research* **2**, 130 (1942)
7. E. Reinhard, C. Moore, O. Bierbaum, S Moore, *J. Lab. Clin. Med.* **31**, 107 (1946)
8. S. Warren, *Cancer Research* **3**, 334 (1943)
9. H. Q. Woodard, J. M. Kenney, *Am. J. Roentgenol. Radium Therapy* **47**, 227 (1942)
10. L. D. Marinelli, *Am. J. Roentgenol. Radium Therapy* **47**, 210 (1942)
11. B. V. A. Low-Beer, A. de G. Treadwell, *J. Lab. Clin. Med.* **27**, 1294 (1942)
12. H. B. Jones, C. W. Wrobell, W. R. Lyons, *J. Clin. Invest.* **23**, 783 (1944)
13. H. Lisco, private communication
14. D. M. Greenberg, W. W. Campbell, M. Murayama, *J. Biol. Chem.* **136**, 35 (1940)
15. L. A. Hahn, G. Ch. Hevesy, O. H. Rebbe, *Biochem. J.* **33**, 1549 (Table VI) (1939)

ELECTRONICS FOR THE NUCLEAR PHYSICIST—IV

Four methods of generating pulses for nuclear experiments and two means of stabilizing power supplies are discussed in this final article in a series of four on fast electronic circuits

By W. C. ELMORE

Swarthmore College, Swarthmore, Pennsylvania

XII. The Generation of Pulses

Pulse generators are often used in nuclear experiments (*1*) to provide regularly spaced signals for timing; (*2*) to initiate one or more sequences of events having a definite time relationship to the initial pulse (multiple trigger generators); (*3*) to calibrate the gain of pulse amplifiers; (*4*) to test the transient response of amplifiers; (*5*) to form part of coincidence circuits. We shall first consider several circuit elements used to generate pulses and then describe a pulse generator for testing and caliprating pulse amplifiers.

1. Thyratron Circuits. In Fig. 47 is shown a circuit element, based on the 2050 thyratron, for generating fast positive and negative trigger pulses which are of very short duration and of uniform shape. The time constant RC determines the rate at which pulses can be initiated, that is, C is (almost) recharged in a time 3RC following the firing of the thyratron.

The thyratron has a delay in firing which is less than 0.1 μsec provided the grid is considerably over-volted by the input trigger. The current through the thyratron can rise to full value in 0.01 μsec.

Sometimes it is convenient to produce pulses at a fairly constant rate by using a thyratron as a relaxation oscillator. For this purpose the circuit element shown in Fig. 48 is useful.

The triode thyratron (884) does not have the steep firing characteristic of the tetrode (2050) and so makes a steadier relaxation oscillator. The shape of the output pulse is determined by R_1 and C_1 and is not influenced by the value of C which, with the resistance R, determines the repetition frequency for given bias voltages. (In both the circuits of Figs. 47 and 48 the plate resistance R must be kept large enough to insure that the thyratron extinguishes.)

The shape of the output pulse derived from a thyratron circuit can be made nearly rectangular by replacing the capacitor whose discharge produces the pulse (C_1 in Fig. 48) by an open-ended delay line. To avoid reflections from the input end of the delay line

EDITOR'S NOTE: The first three articles in this series included discussions of the following: use of Laplace transformations, response of circuit elements to step functions, transient response of voltage amplifiers, signal-to-noise ratio of counter amplifiers, design of pulse amplifiers, transient analysis of a two-stage feedback amplifier, discriminators and scaling circuits, counting-rate meters, random pulse circuits and delay-line pulse shaping.

the resistance across which the pulse is generated (R_1 in Fig. 48) should be made equal to the characteristic impedance of the line. This method is sometimes used in generating rectangular pulses for modulating magnetrons in radar, and occasionally finds use in a laboratory pulse generator.*

2. The Blocking Oscillator. A blocking oscillator is a convenient element for generating fast, narrow pulses, especially for fast coincidence circuits. It may also be used as a free-running relaxation oscillator and as an element in frequencing dividing circuits. A typical circuit element, arranged for external triggering, is shown in Fig. 49. Both tubes *T*-1 and *T*-2 are normally biased off. A fast positive trigger applied to the input produces a negative pulse at the plates *T*-1 and *T*-2 and, by coupling through the special blocking-oscillator transformer, a positive pulse at the grid of *T*-2. Tube *T*-2 then conducts, and by regeneration the grid is temporarily driven positive, perhaps +100 v, and the tube momentarily draws several hundred milliamperes of plate current. Negative charge collected by the grid resides on the capacitor C and prevents (blocks) a second oscillation. Hence a positive pulse may be taken from the

* E. W. Titterton, V. L. Fitch, *Rev. Sci. Instr.* **18**, 639, 1947.

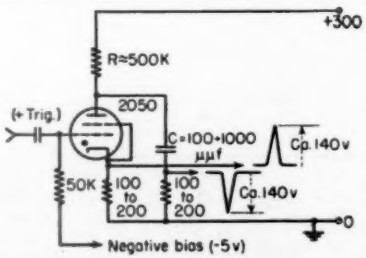

FIG. 47. Method of generating fast pulses with a thyratron

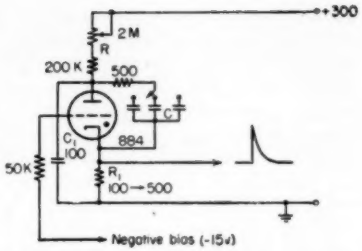

FIG.48. Thyratron relaxation oscillator

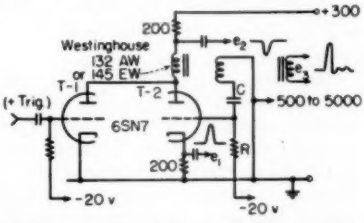

FIG. 49. Blocking oscillator arranged for external triggering

resistance in series with the cathode, a negative pulse from resistance in the plate circuit, or a pulse of either sign, (followed by minor oscillations) from a third winding of the transformer. Ordinarily only one of these methods is employed at one time, depending on the demands of the circuit to which the element is coupled. The time constant, RC, determines the maximum repetition frequency.

There exist several useful types of blocking-oscillator transformers. The 132 AW can be used to generate approximately triangular-shaped pulses perhaps 0.3 μsec wide at the base and the 145 EW perhaps 1 μsec wide. Other available transformers can be used for narrower (0.1 μsec), or for wider pulses. The grid capacitor C should ordinarily be at least 500 μμf in order that the oscillation be sufficiently violent. As low as 200 μμf can be used for very narrow pulses. For high duty ratios and for narrower pulses,

the 6SN7 should be replaced by a tube having greater current capabilities and power dissipation (triode-connected 6AC7, 6AG7, 6V6, 6L6, etc.). Pulses can be made more nearly rectangular-shaped either (*1*) by putting some resistance in series with the grid or (*2*) by replacing C by an unterminated delay line. It is usually necessary to decouple a blocking oscillator from the plate supply to avoid transients on the supply lines. A blocking oscillator is made free-running by returning the resistor R to ground, or better, to +300 v.

The design of circuits incorporating blocking oscillators usually proceeds in a semi-empirical manner guided by previous experience. It is worthwhile to become familiar with the behavior of blocking oscillators using an oscillograph having a fast slave sweep circuit to examine wave forms occurring at various points in the circuit. The maximum frequency at which a blocking oscillator can be conveniently run is of the order of 1 Mc per sec, although the top limit may be as high as 10 Mc per sec. Blocking oscillators are very convenient sources of narrow, standard pulses for fast coincidence circuits. In this application they are triggered by a pulse from an amplitude discriminator.

3. The Univibrator. Long pulses with rise times of several microseconds are best generated using a circuit element termed a *univibrator*. The sort of circuit involved is illustrated in Fig. 50. If a negative bias supply is not available, a common cathode biasing (which is regenerative) can be used for the univibrator. Tube *T*-1, which is normally non-conducting, serves to couple a positive trigger to the univibrator. Tube *T*-3 is normally conducting, with grid current being drawn, and with its plate at about +80 v. Tube *T*-2 is therefore cut off, with its plate resting at +300 v. A positive trigger applied to the grid of *T*-1 lowers the potential of the plates of *T*-1 and *T*-2 and the grid of *T*-3 is driven to cut-off by the capacitive coupling from the plate of *T*-2. Hence the plate of *T*-3 rises

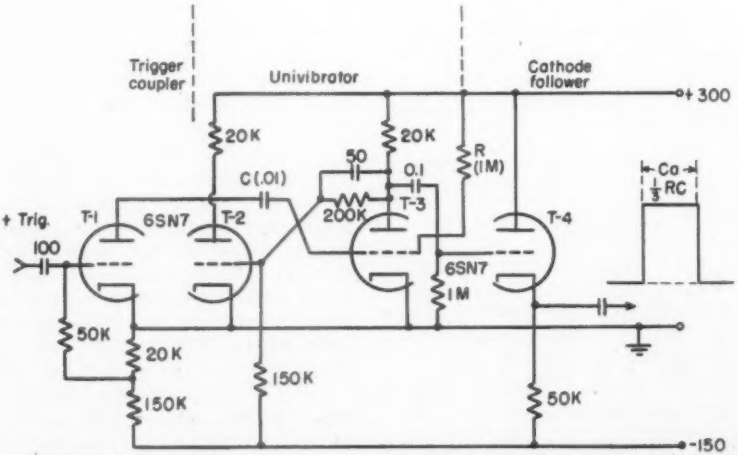

FIG. 50. Univibrator with input coupling and cathode-follower output stage

nearly to +300 v, bringing T-2 into the conducting region (T-2 actually draws some grid current), and so the new regime is preserved until enough charge flows through R to discharge C, causing T-3 to conduct again, at which time the circuit flips back to its original state. A positive pulse (gate) can be taken from the plate of T-3 (as shown) or a negative gate from the plate of T-2. The duration of the gate is about (RC/3). The shortest practicable gate is in the range 3–5 μsec. A circuit of this type is often used as the basis for a trigger delay circuit, *i.e.*, one can obtain fairly narrow trigger pulses by differentiating the rectangular gate. There are various methods available for controlling the duration of the delay, indeed, to make the delay depend linearly on the setting of a potentiometer. It should be noted that the front of the negative gate at the plate of T-2 can be made to have a fast rise time (0.1 μsec) if tube T-1 is supplied a very fast trigger pulse. This behavior is often made use of in applications of the circuit element.

4. The Generation of Step Waves of Known Amplitude. For testing and calibrating amplifiers used in nuclear physics it is convenient to have a pulse generator producing pulses of the form shown in Fig. 51. The following characteristics of these pulses should be noted:

1. The rise is several times faster than that of customary amplifiers.

2. The duration of the *flat* top is much longer than the short time constant in the amplifier used for shaping pulses.

3. The pulses have a gradual decay which is necessary to avoid a large output pulse from the amplifier and is the opposite sign from the usual pulse (positive). (Such a pulse is produced by "differentiation" by the pulse-shaping network of the amplifier.) If such a pulse were to occur, the amplifier would

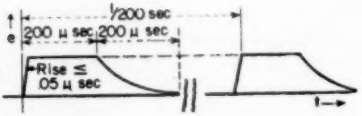

FIG. 51. Pulses for calibrating pulse amplifiers

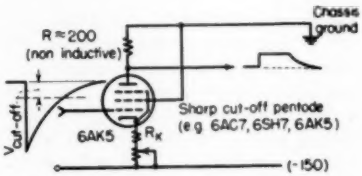

FIG. 52. Portion of pulse generator

be overloaded, since the output stages are usually asymmetrically biased.

The best method of producing a step signal appears to be the sudden cutting off of a current through a resistor whose value, taken in conjunction with the stray capacitance shunting it, gives a sufficiently short rise time. If the voltage across the resistor (before the current is cut) is accurately known, then a voltage step of known amplitude is generated. A method for cutting the current suddenly is shown in Fig. 52. If a signal of the form shown is applied to the grid, a *positive* pulse of the desired form for calibration is produced at the plate. The screen of the pentode serves to prevent distortion of the pulse by capacitively feeding through to the plate the fast pulse applied to the grid. If the same method is used to produce a *negative* pulse at the cathode, capacitive feed-through of the grid signal usually causes an undesired overshoot at the leading edge of the negative output pulse. Hence, if negative steps are required, it is best to generate positive steps and to invert them by a wide-band amplifier having a negative gain of unity (stabilized by feedback). Pulses are best generated at a level of 0.1 to 1

volt, (by varying R, or by varying the current through the pentode) and low-level pulses secured by a capacitance-compensated resistance attenuator located preferably at the end of the cable connecting the pulse generator to the amplifier input.

The rate at which pulses are generated is best kept low (say 200 cps) (*1*) to insure that all voltages in the circuit recover to their normal values between successive pulses; (*2*) to give a rate convenient for driving the usual scaling circuit; (*3*) to permit the pulse amplitude to be measured (with only a small percentage correction) by measuring the average plate current of the pentode. It is desirable, however, to have the rate high enough to examine the output of the amplifier with a cathode-ray oscilloscope without recourse to subdued lighting.

The generation of the pulses supplied to the grid of the pentode in Fig. 52 can be accomplished by the circuit arrangement shown in Fig. 53, which is part of a pulse generator designed by Sands (*10*, part 3). The thyratron relaxation oscillator based on tube *T*-1 runs at about 200 cps and furnishes sharp positive trigger pulses through a delay line to the grid of *T*-2, which is normally cut off since its cathode is held at about 10 volts above its grid. Each delayed pulse at its grid produces a fast negative pulse at its plate. This pulse is coupled to the capacitor C through a diode *T*-3 which is so biased that the first portion of the pulse (which is not very fast) is not used. The voltage across C thus has the form indicated, with a recovery time constant RC = 100 μsec. The diode evidently disconnects the capacitor C from the plate of *T*-2 once the pulse is formed. A positive pulse is coupled from the cathode of *T*-1 through a cathode follower (not shown) to serve as a trigger for the sweep of an oscillograph. The output signal base line is about 25 v above the −150 line in order that the cathode resistance R_K in Fig. 53 can be reasonably large. A fairly large value for R_K helps to stabilize the steady current through the signal-generating tube (by cathode current feedback).

The amplifier of gain −1 used to invert the output pulses can be similar to the 3-tube feedback loop described in Sec. V. The negative pulses are then taken from the plate circuit of the third tube of the loop.

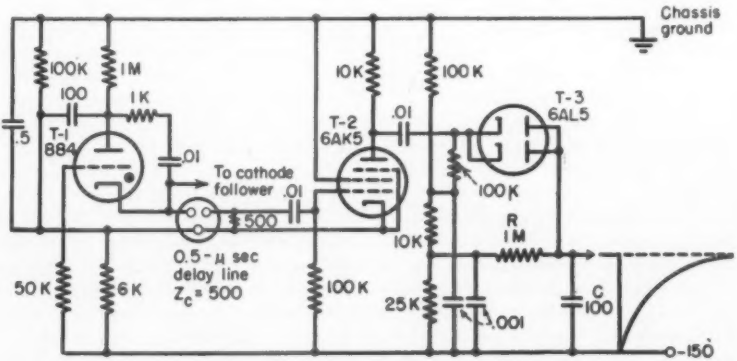

FIG. 53. Portion of pulse generator

A power supply for plate and bias voltages is stabilized (*1*) to reduce to a negligible point fluctuations in d-c voltage resulting from a-c line fluctuations; (*2*) to afford a low source impedance, thus minimizing interactions between portions of a circuit connected to the supply; (*3*) to reduce ripple voltages.

1. VR-Tube Stabilized Supplies. The simplest sort of stabilized supply, useful for low current drains, is one based on a glow tube, or voltage regulator (VR) tube, such as the VR-75, VR-90, VR-105 and VR-150. An equivalent circuit for such a supply is shown in Fig. 54 where E_1 is the equivalent source voltage of the transformer-rectifier-filter arrangement used, R_1 is its equivalent source impedance and R_2 is a series dropping resistor whose value is chosen to make the current through the VR tube have a suitable value, *e.g.*, 22.5 ma.

To understand the factors influencing the design of such a supply we shall first define several quantities and then derive formulas for R and E to take into account a prescribed variation in load current and in supply-mains voltage. Let

I_{min} = smallest load current expected

I_{max} = greatest load current expected

$$I_L = \frac{I_{min} + I_{max}}{2} = I_L$$

= mean load current

$\Delta I_L = I_{max} - I_{min}$

= variation in load current

V = voltage across VR tube

Since it is permissible to allow a variation in current from 5 to 40 ma through modern VR tubes, the current through the VR tube should be made $(5 + 40)/2 = 22.5$ ma for the current I_L and for the line voltage at its average value. We shall allow for a variation of $\pm 100\ r$ percent in the line voltage, for instance of ± 10 percent ($r = 0.10$). Evidently the current through the VR tube will vary from one limit where the voltage E is $100\ r$ percent low and the load current is I_{max} to the opposite limit where E is $100\ r$ percent high and the load current is I_{min}.

By Ohm's law,

$$\frac{E - V}{R} = .0225 + I_L, \qquad (86)$$

where E is the source voltage of the transformer-rectifier-filter circuit with the supply-mains voltage at its middle value. In addition, the change in current through the VR tube due to the two causes just mentioned is

$$\frac{\Delta E}{R} + \Delta I_L \leq 0.040 - 0.005$$

$$= 0.035 \text{ amp}, \qquad (87)$$

where $\Delta E = 2rE$ for the worst possible case.

On eliminating E between Eqs. (86) and (87) and placing $r = 0.10$, we find that

$$R \geq \frac{V}{0.1525 - 5\Delta I_L - I_L}. \qquad (88)$$

For example, suppose the load current can vary from 5 to 25 ma making $I_L = 0.015$ amp, and $\Delta I_L = .020$ amp. If $V = 150$ v, then Eq. (88) gives $R \geq 4.0$K and Eq. (86) indicates that $E_1 = 300$ v. Part of the resistance R is furnished by the source impedance of the transformer-rectifier-filter arrangement; the remainder must be furnished by the series dropping resistor. If the values of R and therefore of E are less

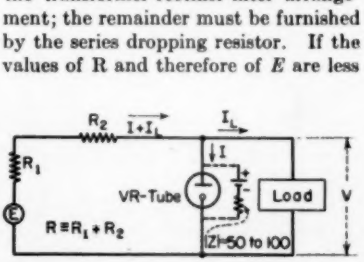

FIG. 54. Equivalent circuit of a VR-tube stabilized power supply

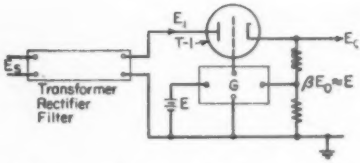

FIG. 55. Basic circuit of a power supply of the degenerative type

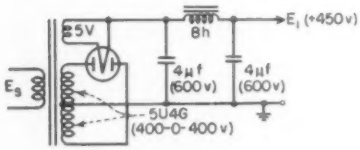

FIG. 56

those computed, then the VR-tube current may fall outside its proper range of values under adverse conditions of load-current and line-voltage variations.

2. Electronically Stabilized Power Supplies. Power supplies stabilized by one or more VR tubes in series are inadequate when large currents are to be stabilized, or when it is important to achieve a high degree of stabilization. In such cases electronic regulation is used, with a VR tube or a battery furnishing a steady reference voltage. It is found that stabilized supplies of a simple degenerative type are the most generally satisfactory, and only this type will be discussed here.

The basic circuit of a power supply of the degenerative type incorporating a series regulating tube is shown in Fig. 55.

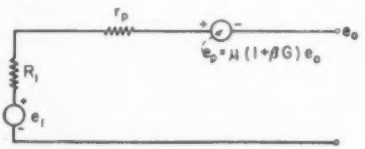

FIG. 57. Equivalent circuit of stabilized supply

The supply-mains voltage E_s (115 v ± 10 v) is converted into a d-c voltage E_1 by the transformer-rectifier-filter portion of the circuit, which may take the simple form shown in Fig. 56. Good filtering is not essential since ripple is removed by the stabilizing circuit. A fraction β of the output voltage is compared with a reference voltage E, and the difference amplified by a *difference* amplifier, which is direct-coupled to the grid of the series triode T-1. If E_0 tends to increase above its equilibrium value, a negative signal is applied to the grid of T-1, thus tending to restore E_0 to its equilibrium value. To evaluate the performance of such a supply it is convenient to define the *stabilization factor*

$$S = (E_0/E_s)(dE_s/dE_0), \qquad (89)$$

the *internal impedance*

$$R = -dE_0/dI_0 = -e_0/i_0 \qquad (90)$$

and the *smoothing factor*,

$$\alpha = dE_0/dE_1 = e_0/e_1. \qquad (91)$$

Evidently S is the factor by which line voltage variations are reduced, R is the effective internal resistance of the supply and α is the fraction by which ripple is reduced between the input and output voltages of the stabilizing circuit. Let us now compute approximate formulas for these quantities for the circuit of Fig. 55.

An equivalent circuit for the supply is indicated in Fig. 57, where R_1 is the impedance looking back into the filter, r_p and μ are the plate resistance and amplification factor, respectively, of T-1 and $(1 + \beta G)e_0$ is the signal applied between the grid and cathode of T-1. The voltages e_1 and e_0 represent changes in E_1 and E_0, respectively.

Using elementary circuit analysis we find that

$$S = \frac{E_0}{E_1}\mu\beta G \qquad (92)$$

$$R = \frac{R_1 + r_p}{\mu\beta G} \qquad (93)$$

and

$$\alpha = \frac{1}{\mu\beta G} \qquad (94)$$

where it is assumed that $\beta G \gg 1$. These relations will be used to predict the approximate performance of two practical circuits which will now be described.

Let us first consider the well-known stabilizing circuit employing a pentode difference amplifier, Fig. 58. The following points of design should be noted for this circuit.

1. The plate load resistance R of the pentode is returned to +450 (not +300), so *T*-2 is working well as an amplifier when the grid of *T*-1 approaches the potential of its cathode.

2. The screen voltage for *T*-2 is secured from the bleeder furnishing current to *T*-3.

3. The capacitor C_1 (and resistance R_1) allows ripple to be fed degeneratively to the grid of *T*-2 without attenuation (by a factor $\beta = \frac{1}{3}$).

4. Current for *T*-3 is secured from the stabilized side of the circuit.

If we assume the following reasonable values, $E_1 = 550$, $E_0 = 300$, $R_1 = 800$, $G = 250$, $\beta = \frac{1}{3}$ (for steady voltages), $\beta = 1$ (for ripple voltages), $\mu = 5$, $r_p = 750$ (triode-connected 6Y6), then

$$S = \frac{300}{550} \times 5 \times \frac{1}{3} \times 250 = 230$$

$$R = \frac{750 + 800}{5 \times \frac{1}{3} \times 250} = 3.7 \text{ ohms}$$

$$\alpha = \frac{1}{5 \times 1 \times 250} = 8 \times 10^{-4}$$

(for ripple)

The measured performance of a supply of this sort is usually found to be somewhat inferior to the predicted performance. The trouble appears to arise from the VR tube whose voltage varies somewhat as the current through it changes (as the result of a current change through the pentode).

A stabilizing circuit giving better performance is shown in Fig. 59. Tube *T*-4 constitutes a difference amplifier which is very stable against variations in grid-cathode, effective

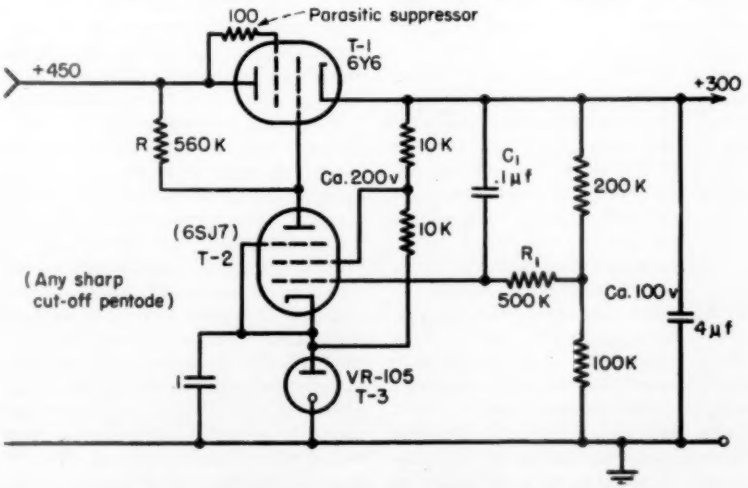

FIG. 58. Stabilizing circuit with a single pentode amplifier

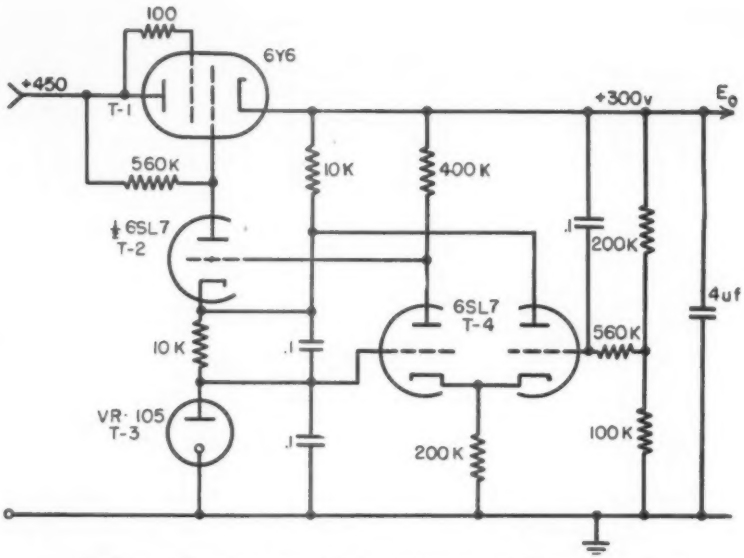

FIG. 59. Stabilizing circuit with a double triode difference amplifier

contact difference in potential (on account of symmetry of voltages and currents and on account of the degeneration afforded by the large cathode resistor to signals occurring equally at both grids). It has a gain of about thirty from right-hand grid to left-hand plate. The left-hand plate is connected to the grid of a second triode stage (*T*-2) having a gain of perhaps 50, so the overall gain is a little over 1500, say 1700. On this basis we find

$S = 1550$

$R = 0.55$ ohms

$\alpha = 1.2 \times 10^{-4}$ (for ripple),

which represents a sevenfold improvement over the simpler supply. For many applications the improvement in performance is not worth the increased number of circuit components.

At high frequencies, or for fast signals, the response of a stabilizing circuit is poor, so it is necessary to shunt the output of the stabilized supply with a capacitance of 4 μf or greater. The supply in Fig. 59 usually oscillates without this capacitance.

To increase the current rating of a supply, any number of triodes can be connected in parallel. It is a wise precaution to place a parasitic suppressor resistance in series with each grid and each screen, for instance, 100 ohms. In addition, it is good practice to place a resistor of perhaps 47 ohms in series with each cathode, in order to insure a reasonably equal division of current among the tubes which are in parallel. One usually allows a maximum of 75 ma for each 6Y6. Where more than one 6Y6 is required, the newer 6AS7, designed especially for stabilizer circuits, is particularly suitable. The 6AS7 requires a greater grid swing to cover a wide range of load variations so the circuit of Fig. 59 may have to be modified before a 6AS7 can be substituted for the 6Y6.

NUCLEONIC EVENTS

KOWARSKI SPEAKS ON FRANCE'S PLACE IN INTERNATIONAL PICTURE OF ATOMIC ENERGY DEVELOPMENT

The following is the text of a talk given by Dr. Lew Kowarski, Directeur Technique, Commissariat à L'Énergie Atomique, at Brookhaven National Laboratory on February 6:

"The scope of the French atomic effort, compared to that of Britain and the United States, can be summarized in a simple formula: France stands in about the same ratio to Britain as Britain to the United States. The numerical value of this ratio is, roughly, of the order of 10, if such criteria are considered as the annual budget (France: several million dollars; United States: several hundreds of millions) or the total manpower employed (France: hundreds; United States: tens of thousands).

"What results can we hope to achieve with this one percent of the American effort? It is obvious, to begin with, that it would be folly to divert any fraction of these limited resources toward military applications; in fact, no such intention has ever been harbored and there are on record several authorized declarations that the aims of the French atomic effort are exclusively peaceful. Our attention is focused on that not-too-remote future (perhaps in a generation or so) when atomic energy will be of considerable economic importance. When this time comes, every country which intends to go on playing a not-too-insignificant role on the world stage should have their own specialists in the atomic field.

"The time to start the training of this national 'layer' of atomic scientists and technicians is *now* and, as the very first step, the nuclear chain reaction has to be produced on the national soil so as to quit the realm of Sunday supplements and to become a concrete reality. We are building our first reactor, with this aim in view and not as a first step toward a French Hanford.

Center Planned for Pure Research

"Even on this modest scale, our first plans proved to be overoptimistic. We started with planning on the lines of the Argonne heavy-water pile. The choice of moderator was suggested by its availability from the Norwegian plant; besides, it reduced the necessary amount of the other essential ingredient. We soon found, however, that we had not yet mastered the technique of the large scale manufacture of pure metal and, on the other hand, that the design of our very first reactor should be kept as free as possible from technical complications, especially in regard to the heavy-water circuit which calls for corrosion-proof pumps and plumbing. Accordingly, we decided on a heavy-water and oxide uncooled reactor, capable of reaching perhaps a few kilowatts, instead of a few hundred kilowatts, as a steady level of operation.

"In addition to the reactor, we want to encourage pure physics research with what *we* might call modern techniques. We are building a 'bigger-than-usual' cyclotron which in America would be called a small conventional one (62 inches). We want to build a few pieces of equipment which would enable us to do precision nuclear work—above all a modern Van de Graaff and, possibly,

a cavity accelerator of a not-too-ambitious type. We want to create a research center around these instruments, on a scale comparable to Clinton or Argonne, but this will take time. We decided to build our first reactor in a provisional center near Paris which I shall describe presently.

Factors against Rapid Development

"With one cent to show against every American dollar, with one higher-class scientist working in a field belabored by a hundred American colleagues, can we hope to rival one percent of the American achievement? The two situations are not comparable on a simple quantitative basis. Let me mention first the adverse factors. A dollar, even reckoned in devaluated francs, cannot buy as much in France, in the particular branches of production required, as it can buy in this country. I have just heard that private industrial firms will supply Brookhaven with a cyclotron and a Van de Graaff. This sort of getting immediately usable value for your dollar is utterly unthinkable in France. The state of our industry imposes on us the necessity of making almost everything in our own workshops with our own manpower. For example, we have to prepare compressed uranium oxide for our first reactor. Hydrogen furnaces required for this preparation cannot be ordered from outside industrial firms; we have to make them ourselves. We make, of course, all our amplifiers, scalers, surveying instruments, and beta and gamma Geiger counters. We make most of the measuring instruments needed for making our electronic equipment. If we need pure chemicals, we have to purify them ourselves; we have to test their purity ourselves; we have to work out analytical procedures for these tests and build all the specialized chemical apparatus ourselves. A considerable proportion of our manpower thus goes into tasks which, in America, would not be part of the project at all.

"The same limitation does not hold for the budget because the enforced buying of raw materials instead of ready-made products probably enables us to get a better return for our dollar. Another advantage is a greater degree of control of delivery times. It cannot be denied, however, that this enforced diversity of our technical activities is, on the whole, a nuisance and when some among you (I hope there will be many) come to visit our Chatillon Laboratory near Paris and see that this reputedly 'atomic research' center consists mainly of workshops making very ordinary things, you will no doubt subscribe to this judgment.

"A further difficulty is that our people are rather badly paid and have a much harder life than you have. As a result, the working output per man is lower. We try to compensate for this with enthusiasm, and it is here that we begin to find some favorable factors in our situation.

Young Graduates Eager to Participate

"The publicity value of atomic energy should be mentioned first. Whether it is the scare thrown by the bomb, or some expectation of a new era in technology, those on whom we depend for our budget and allocations, give us practically everything the country can afford, and those who give us their skill and will to succeed give *them* freely. There is a considerable enthusiasm among the younger generation, especially the young graduates just out of the universities and technical schools. They want to work on this glamorous job and we get the best pick of them. Their individual quality is quite high, even when their knowledge of atomic physics, or of the technique of physical research, is insufficient. It often is, because the atmosphere in the universities and in the other research

laboratories is not as lively as in this country. Fortunately our young people are eager to learn and we have something to teach them.

"An amusing consequence of the awed enthusiasm with which atomic activities are surrounded is our present ability to get supplies through channels which would be harder to tap under more ordinary circumstances. For example we are rather well off, relatively, in radio components because we were able to make good use of the vast resources of the Military Surplus Camps. We were also lucky with our machine tools. A few energetic henchmen were dispatched at a suitable moment to Germany, or to the same Surplus Camps; they used their atomic prestige and, as a result, our Chatillon workshops are rather well equipped. The postwar confusion can sometimes be turned to good account and we try to use our intuition.

"A favorable factor specific to France, and rather unique on the European continent (Britain, of course, has to be excluded), is the presence of a few scientists who have participated in the Allied atomic development practically from its inception. I am one of them myself, and there are a few others —perhaps less than half a dozen in all— who came in at different stages to work in France, Britain, and Canada. One of them was on the Manhattan project itself. Somewhat unwillingly and unwittingly, and to a limited extent, France found itself inside *the* curtain. Chatillon has its guards, as you in Brookhaven have yours; we are responsible for some of the secrets and our people are bound by certain, not-very-explicit-but-very-binding secrecy rules. Time is nearing—we are not there yet—when we shall start to get original results and a situation will then arise which may require a more explicit consideration. As I have already stated, the position of France is, in this respect, unique on the European continent, with one individual exception—and, as far as I know, there is little or no atomic development in Denmark.

"Such is the balance of favorable and adverse factors which, so far, enabled us to establish a cluster of designing offices, workshops and testing laboratories in the disused Fort de Chatillon near Paris. (By choosing an actually fortified piece of ground we went, as you see, one step farther than you!) When I saw it last, just over a week ago, the first concrete was being poured on the site of the reactor. We like to believe that the chain-reacting condition will be reached sometime in 1948, not before Christmas, of course. Its flux, not much below that of the first Chicago pile or of the British 'Gleep,' will enable us to make tracers on a significant scale. With its two other functions—that of a research and training instrument, and that of a testing ground for the materials and equipment which will go into bigger and better piles—we feel that this first reactor will repay our efforts.

Plans Include Graphite Reactor

"As a next stage we contemplate the building of a graphite reactor, perhaps not as ambitious as the one which is now being built at Brookhaven, but big enough to carry us beyond the purely laboratory stage. So far, even with our guidance, French industry was able to prepare only the sort of graphite suitable for use in reflectors—and in the reflector of our first reactor, French-made graphite will be used. We are trying to do better, and at the same time we are developing physical testing methods similar to those used in your atomic laboratories. During the last year, using our own equipment and people of technical schools, we went as far as to measure the diffusion length of our commercially supplied graphite. From the start we got results as accu-

rate, or better, than what we could obtain by chemical analytical methods. Later on we shall have to put some uranium lumps into the graphite structure and see for ourselves what happens in such a lattice. We are not there yet, but we are getting nearer.

"Other kinds of neutron research, for instance, the study of resonance capture, will be necessary to enable us to proceed with the design of our future reactors. We have an extensive program of chemical research planned because the preparation of pure graphite and pure uranium, and even the current checking of the purity of heavy water, call for analytical techniques which, so far, have never been applied or studied in France. In fact, it seems to be the result of my experience in different countries that, when a country starts from scratch on an atomic project, the worst bottleneck is analytical chemistry. It is there that qualified people, able to apply methods they have never used before, are needed almost by the score. The situation is quite different in electronics, for instance, where we have no lack of qualified people, at least on the scale required for the construction of a reactor. In mechanical and general engineering, highly qualified specialists are none too plentiful in France, but there are enough of them for our needs. In countries like Sweden and Switzerland, the situation is, in this respect, even more favorable.

Activity in Other European Countries

"This brings me to the more general subject of what is happening in other European countries. There are definite ideas about atomic projects in Sweden, Norway, and Holland and somewhat less definite projects in Belgium and Switzerland. A striking feature is the tendency to think along strictly national lines. For instance, Norway thinks of building its own heavy-water pile, but since Norwegian population is somewhat smaller than one-tenth of the French population, this means that we have again to move ten decibels down the scale. It is my opinion, which I have often expressed in the course of my travels, that there seems to exist a critical size of the effort which a country has to spend in order to produce a sustained chain reaction. France may just be able to supply such an effort, but I doubt whether Holland, or Sweden, or Norway can do it if each of these countries is taken separately. A common Western European effort would very considerably increase our chance of success, but nothing seems to have started yet on these lines.

"Going back to France, I would like to mention that our Atomic Energy Commission is essentially civilian. Theoretically it is headed by the Prime Minister, but in these busy and shifting times, the powers of the Prime Minister are, in fact, delegated to the High Commissioner and to the Administrator-General. The High Commissioner, whose responsibilities can be compared, in our parallel and proportionate picture, to those of Lilienthal, is Professor Joliot, to whose devotion and organizing ability we owe, in my opinion, not only such partial successes as we can boast of, but also the very existence of our organization as a live and functioning body. The remainder of the Commission is composed of distinguished French scientists such as Professors Irene Joliot-Curie, Pierre Auger and Francis Perrin, a Secretary-General, and a military gentleman. There exists a liaison with the Navy, the Office of Aeronautical Research, and so on.

"Apart from our main offices in Paris and at Fort de Chatillon, work is also done at various Paris laboratories and much more significant outposts, such as the chemical factory at Le Bouchet (30 miles out of Paris) where uranium compounds are refined on a

modest industrial scale, and the Saclay site (10 miles out of Paris) on which our permanent research center will be built. Our total staff is about 500, not including the miners employed in the extraction of low-grade ores in metropolitan France and elsewhere, notably in the colony of Madagascar. At Chatillon proper, the staff is about 250, including all necessary help such as cleaners and drivers; out of this number about 50 or so are graduates, mostly in chemistry and electronics."

(A lively discussion followed; excerpts from Dr. Kowarski's statements at that time follow).

Exchange of Information with Eastern Europe: "Eastern European scientists have an easy access to all published material, but there are no visits or interchange of people, and when Eastern scientists come to see people in Western Europe, they never ask questions, possibly because this might reveal the degree of their knowledge or ignorance. The reality of the iron curtain, in this one field of human activity about which I feel myself entitled to judge, cannot be denied and it is a highly dense variety of iron indeed. It is significant that, when Joliot attended the Russian Academy celebrations in 1945, several months before Hiroshima, he could not even visit the Radium Institute of Leningrad."

Atomic Research in Western Europe: "The *British* establishment at Harwell is of size comparable to Argonne or Brookhaven. Its director, Sir John Cockcroft, was the head of the Canadian project during its decisive years. The 'Gleep' which has been working since August 15, 1947, is, as far as we know, the first reactor built outside the Western Hemisphere. There is also a production plant somewhere in Northern England; not being in the Sacred Trust I know nothing about it. The British have plenty of high-quality scientists; they are very much alive and, considering the rather extreme economic plight of their country, they are doing pretty well.

"The *Swedes* seem to have developed a little curtain of their own. They have high hopes based on their highly developed mechanical industry, as the evidence General Groves gave in the U. S. Senate a few years ago will corroborate.

"The *Norwegians* have the enormous asset of their heavy-water production, and once you have enough heavy water it is difficult not to make a reactor. That is why we have so eagerly embraced the heavy-water technique and, incidentally, secured what is probably nearly the whole Norwegian output for about two years.

"The *Dutch* have a fine physical research center, headed by Dr. Casimir, at the Philips plant in Eindhoven. In some items, such as the commercialized high-voltage (about 1 Mev) generator of the Cockcroft-Walton type, they are ahead of everybody else. They are now developing a pressurized Cockcroft-Walton, possibly for several Mev, which is an entirely new departure. The frequency-modulated cyclotron which the Amsterdam physicists are now assembling in collaboration with Philips, while not as large as the one at Berkeley, will probably provide valuable opportunities for fundamental physical research. Later on, they may have to convert it to the classical mode of operation and use it for making tracers. I do not think that the Dutch have any immediate plans for pile development.

"The *Belgians* have, or ought to have, some uranium and that is probably their main asset.

"The *Swiss* have many highly qualified physicists, both experimental and theoretical. Their mechanical industry is, in some respects, ahead of this country but, again, they are a small nation and, if they stay by themselves,

I do not think they will get very far. I have no knowledge of any reactor for Switzerland.

"It can be said then, that as far as pile-building goes, there are very definite results in Britain, a few hopeful people in France and a few even more desperately hopeful people in Sweden. This just about sums up the situation in Western Europe."

Public Opinion on the Atomic Question in France: "The state of public opinion has a very definite bearing on our chances of success because the attitude of the nation as a whole conditions the whole attitude of that lively and enthusiastic section of the French youth from which we draw most of our staff. We cannot get anywhere without a nucleus of highly qualified, devoted, and generous workers. In the present difficult conditions, one has to be very unselfish, a kind of a sucker, in order to get enthusiastically absorbed in long-range work that is not immediately profitable. Fortunately, suckers of this sort are born every minute in France and there is a realization that atomic development is a very important task.

"We have to give the taxpayer the impression that he *gets* something for his money; this is being done through the usual channels, mainly lecture and press. At first the French press was somewhat apathetic, or perhaps they assumed wrongly that they were dealing with a delicate subject about which the least said, soonest mended. Gradually they started asking for interviews and publishing them, although at first it was very difficult to restrain them from stating, as a sort of monotonously fresh novelty, that Professor This or That knows how to make an atomic bomb. A statement of this kind, ascribed to Joliot, created some stir a year ago in this country; what Joliot substantially said was that one had to have two or more subcritical fragments and had to bring them together so as to achieve a supercritical total mass. A periodical published in the United States printed this revelation in heavy black type and for weeks wires were buzzing. In July, 1947, Joliot held a press conference and after that things straightened out. Since then French papers have from time to time published pictures of Chatillon—the big block of graphite used in diffusion experiments being taken apart or put together, an assistant, preferably a girl, handling a scaler, and that sort of thing. On the whole the French people do realize that something is happening. As for appropriations they are decided as a part of the budget of the Prime Minister's department and the Parliament usually approves them in a deferential hurry. So far we have had little difficulty with this aspect, but times might change.

"Reactions from the neighboring populations form an interesting chapter in the story of our public relations. When the Saclay site began to be envisaged, the Government had to appropriate the land, and immediately there was a rabid opposition. It was pointed out that it was unwise to erect a choice military target only eight miles away from the historical buildings of Versailles. Our firm reply was that nothing of military importance was contemplated or was likely ever to be contemplated at Saclay. The British, with similar intentions, did not hesitate to build the Harwell establishment at a comparable distance from Oxford and, after all, Oxford is not devoid of historical interest either. Then Joliot addressed a mass meeting of the neighboring farmers and somehow managed to convince them; there were no local petitions after that. At Chatillon there was no land appropriation to be pushed through; we just moved into territory already held by the Government and accordingly there was no definite opposition. From time to time

we have to deal with informal inquiries as to whether the reactor is a source of great danger to the vicinity and so far we have been able to allay all such unreasonable apprehensions.

"We feel that our refusal to envisage military applications would probably meet with the approval of the majority of the French people. Even if such applications were immediately feasible (which they certainly are not for a certain time to come), the people would say that they do not want to be a target and that France should be left out of the atomic race. This sort of passive isolationism is easy to understand if one has seen what these people have been through these past years."

EUROPEAN SCIENTISTS COOPERATING WITH EDITORIAL BOARD

In recognition of the combined wealth of scientific achievement which their individual accomplishments represent, NUCLEONICS is proud to present brief sketches of the six distinguished European leaders of nuclear research who have this month joined in cooperation with its Editorial Board:

Eduardo Amaldi
(*Italy*)

Dr. Amaldi, born in 1908, obtained his doctorate in physics at the University of Rome, the same university at which he now has a professorship. His extensive contributions to our present knowledge of nuclear forces were founded in his early activities in experimental spectroscopy.

Working with E. Fermi until 1938, he played an outstanding part in the studies which led to the discovery of slow neutrons. During the German occupation, he cooperated actively with the Italian Committee of National Liberation. His work, which he continued at the same time, was then devoted to determining the interaction between protons and neutrons and the scattering of medium velocity neutrons by light nuclei. He has lectured extensively in this country.

Cornelis Jan Bakker
(*The Netherlands*)

Dr. Bakker, editor of the *Netherlands Review of Physics*, was born in Amsterdam in 1904. He received his doctorate "cum laudè" in mathematics and physics from Amsterdam University and in 1931 completed his now well-known thesis on "The Zeeman Effect in the Noble Gas Spectra."

After some time in London working under Fowler, he returned to the Netherlands for research with Zeeman whose famous experiments and scientific inheritance went into establishment of the Zeeman Laboratory in Amsterdam, now under Dr. Bakker's supervision.

From 1933 to 1945, he engaged in significant electronics and nucleonics development work at the Philips Incandescent Lamp Works in Eindhoven, and in 1946 became Professor of Experimental Physics at Amsterdam University. Subsequently he accepted the appointment as managing director of the Instituut voor Kernphysisch Onderzoek (Institute for Nuclear Physics Research) and, as such, supervises the work of the Philips cyclotron there.

John Douglas Cockcroft
(*Great Britain*)

Dr. Cockcroft, knighted in 1948 for his many accomplishments in nuclear science, was born in 1897 and attended the University of Manchester and St. John's College. He holds four academic degrees, including two doctorates from British and Canadian universities.

He went to Cambridge after having worked as an engineer with Metropoli-

tan-Vickers, thus starting his university training later than most students. At the Cavendish Laboratory, he conducted research under Rutherford and, in 1932, with Walton, became the first to accomplish nuclear disintegration by artificial means. A member of the British team working on the atom bomb project, he spent much time during the war in Canada.

Sir John Cockcroft is the Jacksonian Professor of Natural Philosophy at the University of Cambridge, Fellow of St. John's College, and Director of the British Atomic Energy Research Establishment at Harwell.

George Hevesy
(Denmark and Sweden)

Dr. Hevesy, one of the world's pioneers in nuclear research, was born in Hungary in 1885. His investigations, which have embraced the physical, chemical, and biological fields, brought him the Nobel Prize in Chemistry in 1943.

In Switzerland he assisted Haber and Rossignol with the synthesis of ammonium, and in England he began his study of radioactive matter and participated with Rutherford and Moseley in research on rare earths. With Coster, he is credited with discovering and isolating the element hafnium.

A check into the separation of the isotopes of radium D and lead decided his career. With Paneth in 1913, he made the first application of isotopic tracers. In 1934, he prepared radiophosphorus and used it for the first time in biological research. Since then, he has used this radioelement brilliantly to probe the absorption, circulation, and elimination functions of both plants and animals.

Dr. Hevesy is presently conducting research with isotopes at the Institute of Theoretical Physics in Copenhagen, Denmark, and also at Stockholm, Sweden.

Frederic Joliot-Curie
(France)

Dr. Joliot-Curie, born in Paris in 1900, received an engineering degree from the Ecole de Physique et Chimie in 1923. After a short career in industry, he began his study of the properties of radioelements at the Institut du Radium and, in 1930, received his Docteur-ès-science.

A former associate of Marie Curie, Dr. Joliot-Curie is married to her daughter, Irene. Their marriage has also been a scientific partnership in chemistry, for together they won the Nobel Prize in 1935 for their research in artificial radioactivity.

In addition to a professorship at the Collège de France which he accepted in 1937, Dr. Joliot-Curie has held many distinguished scientific posts.

He was mobilized as a captain in the artillery during the war and given supervision of all French work in atomic research. Before Paris fell, he was influential in securing on loan all of Norway's stock of heavy water, previously kept from the Germans. A leader in the resistance movement during German occupation, Dr. Joliot-Curie made safety of the precious heavy water certain by sending it to England with two of his assistants.

Since the liberation of Paris he has been named Director of the Centre National de la Recherche Scientifique and High Commissioner of the French Atomic Energy Commission.

Paul Scherrer
(Switzerland)

Dr. Scherrer, President of the Swiss Atomic Energy Commission, was born in St. Gallen, Switzerland, in 1890. He began his work in physics at the Eidg. Technischen Hochschule (E.T.H.) in Zurich and pursued his studies at the Universities of Koenigsberg and Göttingen in Germany. In 1916 he received

his Ph.D. for the study of dispersion of optical rotation of hydrogen.

His early work, a method for determining crystal structure by X-rays, using crystalline powders instead of large crystals (Debye-Scherrer method), had a great impact on the development of our knowledge of matter. Among his numerous investigations that followed were those on magnetic and piezoelectric properties of matter and the specific heat of crystals. His work also includes research on cosmic rays carried out at the Jungfraujoch Scientific Station in Switzerland, which he helped to organize.

A brilliant lecturer, Dr. Scherrer has been Professor of Physics and Director of the Physics Institute at the E.T.H. since 1920.

CONCRETE BUILDING CONSTRUCTED FOR 2,000,000-VOLT X-RAY UNIT

A building, specially designed to house the two million volt X-ray machine recently installed by the Babcock and Wilcox Company to examine the welds in high-pressure, high-temperature boiler drums manufactured at the Barberton (Ohio) Works, has been completed.

The 70 by 30 foot building in which the machine is housed was designed to provide complete protection against X-rays and at the same time to give full freedom of movement in examining pressure vessels up to 13 feet in diameter and 70 feet in length.

The walls are of concrete with a maximum thickness of 40 inches, decreasing to 9 inch thickness toward the top of the 32 foot room. Access to the control room, which is an extension on one side of the building, is through a concrete maze with walls 40 in. thick.

With the new machine, which has been in operation for several months, production of large pressure vessels is said to have been speeded up considerably because of the much shorter exposure time now required in X-raying pressure vessels 4½ to 6½ inches thick.

FAIRCHILD NEPA PROJECT HOLDS SEMINAR AT OAK RIDGE

A classified seminar in nuclear physics was conducted by the NEPA (Nuclear Energy for Propulsion of Aircraft) division of Fairchild Engine and Airplane Corporation at Oak Ridge last month. A group of about 100 prominent nuclear physicists, engineers, and experts from the aircraft industry, educational institutions, and the armed services met to discuss advanced problems in the long-range program of research on the application of nuclear energy to the propulsion of aircraft.

Lecturers at the seminar included: A. C. G. Mitchell, Indiana University; Martin Deutsch, MIT; Morris Kolodney, City College of New York; Alexander Hollaender, Oak Ridge National Laboratory; John W. Irvine, Jr., MIT; Bernard Feld, MIT; Clark Goodman, MIT; and Harry Soodak, MIT. In addition, members of the NEPA staff delivered lectures.

EFFECT OF RADIOACTIVITY ON PLANTS TO BE STUDIED

A study of the influence of radioactive materials on growth of crop plants is being undertaken jointly by the Atomic Energy Commission and Department of Agriculture. The research will be financed by a grant from AEC to the Bureau of Plant Industry, Soils, and Agricultural Engineering. It will be conducted by a number of agricultural experiment stations cooperating with the bureau. Radioactive materials will be used in both greenhouse and field experiments on a variety of crops grown on different soil types.

Part of the special materials required will be provided by the AEC.

Three-fold objective of the research

is: (1) to measure the effect of additions of radioactive materials to soil and fertilizer on the growth, maturity, yield, and composition of various representative crops; (2) to determine the influence of low activities of alpha, beta, and gamma radiation on the germination of seed and the growth and vigor of seedlings; and (3) to ascertain the influence of the radioactive materials on the number and activity of the bacteria and other soil micro-organisms.

Many experiments have been conducted in Europe and America to study the result of radioactivity on plant growth. The results have been conflicting and inconclusive, showing apparently beneficial effects in some cases, no influence whatever in others, and apparently harmful effects in still others. Reports of exceptionally good crops near Nagasaki have stimulated interest in the problem. Investigations by qualified American and Japanese scientists, however, fail to reveal any basis for the claim that radiation from the atomic bomb helped the crops.

BERKELEY GROUP ANNOUNCES RESULTS ON PHOTOSYNTHESIS

A group of University of California scientists, working on a project for the AEC, have announced new results of their investigations into the problem of photosynthesis. They reportedly have obtained for the first time a complete picture of all the intermediate compounds which are formed when plants, using chlorophyll and sunlight, break down carbon dioxide and water to form sugars, starches, carbohydrates and other energy compounds.

The new intermediate products are phosphoglyceric acid, which is the next to the last stop on the way to sugars; and triose phosphate, the last intermediate in the process before a true sugar is formed. Triose phosphate is itself a simple kind of sugar.

This research, done by Melvin Calvin and Andrew Benson of the Radiation Laboratory at Berkeley, was reported by Dr. Calvin at a recent meeting in Cleveland.

ONR-REPORTED RESEARCH

The following information on recent research was reported by the Office of Naval Research:

New High-intensity, Gamma-ray Source. Kolstad, Schultz, and Montgomery at Yale University are now developing a microwave resonant cavity operating on 50 megacycles which is expected to serve as a new type of high-intensity, gamma-ray source. The cavity is of the coaxial re-entrant type. Protons from a high-current ion source, located within the inner conductor, are to be accelerated across a 1-inch gap by radiofrequency voltages of about 1.5 Mev. Upon striking a lithium coating on the opposite wall, the protons yield 17 Mev gamma rays through the $Li(p,\gamma)$ reaction. This instrument was described at the recent New York meeting of the American Physical Society. The belief has been expressed that a gamma yield of about 10^8 or 10^9 photons per second could be obtained. [*This work is not ONR-supported. The electron microwave accelerator at Yale is on an ONR contract.*]

G-M Counter Design for Short Delays. Mandeville and Sherb at the Bartol Research Foundation have recently reported [*Phys. Rev.* **73,** 90 (1948)] measurements on the delay times in a small beta counter of their design. They passed beta particles through two counters side by side and recorded the coincident counts with a fast circuit. No loss in the coincidence rate was found as the resolving time of the circuit was decreased to 0.08 microseconds. Since that report, the circuit has been improved and the resolving time dropped to 0.035 microseconds, still without change in the coincidence counting rate. This indicates

that for these counters the delay times are a small fraction of a tenth of a microsecond.

The counters had a sensitive volume of 5 cm in length and 1.5 cm in diameter. They were filled to a pressure of 7 cm Hg with an argon-ether mixture whose ratio of partial pressures was 17:3.

Electro-disintegration of Nuclei. Laughlin, Skaggs, Hanson and Orlin of the University of Illinois reported at a recent meeting of the American Physical Society on a relatively new type of nuclear reaction. Very rarely in the past has anyone caused disintegrations by electron bombardment of nuclei. The cross section for such reactions is expected to be very small. The Illinois group has now succeeded in bringing the electron beam out of the doughnut of their 22-Mev betatron so that it may be used for bombarding various targets. The current is about 10^{-8} amperes. This new intense beam has permitted the detection of the rare reaction $(e;n,e')$ by which a neutron is ejected from either a copper or a silver target.

In such a reaction, the high-speed electron passes so close to the target nucleus and so fast as to cause excitation due to the electromagnetic field of the moving electron. The electron is thus not captured but merely proceeds onward with reduced energy. The cross sections measured so far have been in the neighborhood of 10^{-28} cm^2, or about 400 times smaller than the gamma-disintegration cross sections for the same nuclei.

BUREAU OF STANDARDS ISSUES TABLES OF BESSEL FUNCTIONS

Of interest to nuclear technologists, as well as other design engineers and physicists, is the recent publication of extensive tables of the Bessel functions $Y_0(x)$, $Y_1(x)$, $K_0(x)$, and $K_1(x)$ in the region between 0 and 1. These tables (Applied Mathematics Series 1), prepared by the National Bureau of Standards, are now available as a 71-page booklet, constituting the first in the new Applied Mathematics Series, which will include mathematical tables, manuals, and studies by the National Applied Mathematics Laboratories of the bureau. They may be obtained only from the Superintendent of Documents, Government Printing Office, Washington 25, D. C., at 35 cents each.

RAILROAD FEDERATION JOINS U. OF CHICAGO ATOMIC GROUP

First action by the railroad industry to explore the possibilities of atomic energy has been taken by the Federation for Railway Progress, a non-profit organization, in conjunction with the atomic research program of the University of Chicago, according to an announcement by W. C. MacMillen, president of the federation.

The federation becomes another member of the program established by the University of Chicago. Already set up by the university are the Institute for Nuclear Studies, the Institute of Metals and the Institute of Radiobiology and Biophysics.

AUSTRALIAN BIBLIOGRAPHY ON TRACER ELEMENTS AVAILABLE

Three bibliographies on medical uses of radioisotopes have been prepared by T. H. Oddie, of the X-ray and Radium Laboratory, Council for Scientific and Industrial Research, Melbourne, Australia, and are being distributed by the C.S.I.R. Information Service, St. Kilda Road, Melbourne.

Bibliographies available are:

Use of Radioisotopes for Blood Disorders—Tracer Elements, No. 2; Applications of Radioisotopes to the Thyroid Gland—Tracer Elements, No. 3; and Applications of Radioelements in General Biology, Bacteriology and Parasitology—Tracer Elements, No. 4.

ABSTRACTS

CHEMICAL PUBLICATIONS

Penetration of aluminum by the radioelements 17-hour zirconium, 77-hour tellurium, and 67-hour molybdenum ejected during uranium fission, F. Suzor (Coll. de France, Paris), *J. phys. radium* **8,** 39–44 (1947). Aluminum foil was placed in layers above a copper support containing an electrolytically deposited layer of uranium. The latter was irradiated with slow neutrons, and the foils were analyzed for fission fragments. The minimum and maximum penetrations of the fragments in aluminum are given.

Preliminary experiments for the study of the nuclear reaction by using photographic plates. I. Homogeneity of the range of deuteron beams produced by the cyclotron, R. Sagane, N. Yamamoto, Y. Imai, *Bull. Inst. Phys. Chem. Research (Tokyo)* **22,** 701–706 (1943). A study of the effect on the homogeneity of the deuteron beam from a small cyclotron of different operating conditions.

The diffusion distance in water for thermal neutrons, A. Berthelot, R. Cohen, H. Rul, *Compt. rend.* **225,** 403–408 (1947). The diffusion distance in water was found to be 2.77 ± 0.04 cm with $CdSO_4$ solution as adsorbant and 2.88 ± 0.07 with Pyrex containing B_2O_3 as adsorbent.

Activation of inert gases by neutrons, W. Riezler (Physik Inst., Bonn), *Naturwissenschaften* **33,** 53–54 (1946). Pure Kr and Xe were irradiated with thermal and fast neutrons, and the activity of the products was measured.

X-ray excitation of lutecium, J. Dunworth, B. Pontecorvo (Natl. Research Council, Montreal), *Proc. Cambridge Phil. Soc.* **43,** 429–432 (1947). The X-ray excitation of Lu leads to a β-activity of 3.4 ± 0.1 hr corresponding to a half-life absorption thickness in Al of 70 mg sq cm.

Separation and enrichment of artificial radioactive sodium isotope $_{11}Na^{21}$, U. Drehmann (Forsch. Anstalt Reichspost, Berlin). *Naturwissenschaften* **33,** 24 (1946). Of the Rd-Na formed by irradiating MgO with neutrons, 90% can be removed by boiling with water.

Recovery of radioactive strontium in unweighable quantity, L. Gerhardt (Kaiser Wilhelm Inst. Chem., Berlin), *Naturwissenschaften* **33,** 24–25 (1946). A detailed procedure is given for the preparation of small quantities of the 55-day Sr isotope.

The separation of barium from radium by radiometric adsorption analysis, R. Lindner (Kaiser Wilhelm Inst. Chem., Berlin), *Naturwissenschaften* **33,** 119–121 (1946). The chromatographic method combined with radiometric analysis can be used to separate Ra and Ba. Al_2O_3 was used as the adsorbent.

The formation of isotope 85^{218} B. Karlik, T. Bernert (Inst. Radiumforschung Akad., Wien, Austria), *Naturwissenschaften* **33,** 23 (1946). If 85^{218} is formed by α-disintegration of 87^{222}, then the latter should be detectable; it could not be found, however.

Separation of protoactinium from its entrainers: titanium, zirconium, and tantalum, M. Bachelet, G. Bouissières (Inst. Radium, Paris), *Bull. soc. chim. France* **1947,** 281–283. The important methods of separation are described.

Coincidence device of 10^{-8}–10^{-9} sec resolving power, Z. Bay, G. Papp (Inst. Atomic Physics, Budapest), *Nature* **161,** 59–60 (1948). Electron multiplier tubes have been used in coincidence circuits having resolving powers as high as 5×10^{-9} sec. The resolving times were measured by a direct method whereby an artificial pulse was fed to both input circuits, one of which contained an extra length of lead which introduced a time lag.

Electron multiplier tube of large effective cathode surface area, P. S. Faragó (Tungsram Research Laboratory, Ujpest 4, Rumania) *Nature* **161,** 60 (1948). Electron multiplier tubes of extremely short impulse period have been made. The disadvantage of small cathode surface has been eliminated, so that an effective surface of 100 cm^2 is easily obtained.

Nuclear models, I. N. Sneddon, B. F. Touschek (Univ. of Glasgow), *Nature* **161,** 61 (1948). Wilson's spherical shell model for the nucleus of a heavy atom is brought into better agreement with calculations made by the authors by con-

sidering the neutrons to form a central spherical core which is surrounded by a spherical shell of protons.

Observations on the tracks of slow mesons in photographic emulsions, C. Lattes, G. Occhialini, C. Powell (Univ. of Bristol), *Nature* **160,** 486–492 (1947). The following conclusions were arrived at: *1*) two types of mesons exist, of different mass, called π- and μ-mesons; *2*) some slow mesons (σ-mesons) can enter nuclei to produce disintegrations with the emission of heavy particles; *3*) σ- and possibly π-mesons can be produced in processes connected with explosive disintegration of nuclei.

Progress in nuclear physics, *Nature* **160,** 492–494 (1947). A report on the conference of nuclear physics at Harwell during September 18-19, 1947.

Nuclear explosion recorded by photographic emulsion method, R. Roy (King's College, London), *Nature* **160,** 498 (1947). A nuclear burst caused by cosmic rays at sea level was photographed. Twenty-two particles were ejected in various directions in the form of a star. It is probable that all of the tracks were due to protons.

Gamma-ray yield curves of separated neon isotopes bombarded with protons, K. J. Broström, T. Tuus, J. Koch (Inst. Theoret. Physics, Copenhagen), *Nature* **160,** 498–500 (1947). Neon targets, prepared by bombarding silver discs with beams of the different neon isotopes in a mass spectrometer, were irradiated with protons, and resonance peaks determined from gamma-ray measurements. The characteristic differences between the resonance spectra of the three neon isotopes agree with present knowledge of resonance processes in light nuclei.

Excitation of nuclei by electrons, B. Touschek (Univ. of Glasgow), *Nature* **160,** 500 (1947). The excitation of nuclei by electrons may be explained on the basis of the electromagnetic interaction between the electrons and the protons of the bombarded nucleus. Expressions are given for the cross section for this process, which give the correct order of magnitude.

Scattering of neutrons by lead, R. Latham, J. Cassels (Cavendish Lab., Cambridge), *Nature* **161,** 282–283 (1948). Using a cyclotron and neutron velocity selector, the scattering cross section of lead as a function of the neutron energy was determined for scattering angles between 30 and 150 deg. The upper limit of the residual scattering caused by the presence of several isotopes of lead is 0.6 ± 0.3 barn. The minimum value of the coherent scattering cross section is about 10 barns. Both results fail to agree with previous values.

High energy physics, E. O. Lawrence (Univ. of Calif., Berkeley), *Amer. Scientist* **36,** 41–49 (1948). A review of the recent experiments with the 184-inch synchro-cyclotron.

The absorption of gamma rays from Co^{60}, W. Mayneord, A. Cipriani (Natl. Research Council, Chalk River, Ont.), *Can. J. Research* **25A,** 303–314 (1947). Absorption measurements of the gamma rays of Co^{60} and radium were made in a number of materials. The gamma rays of Co^{60} are almost monochromatic, and are therefore suitable for testing theoretical absorption formulas.

A low-pressure glow-discharge proton source, P. Lorrain (Natl. Research Council, Montreal), *Can. J. Research* **25A,** 338–356 (1947). A cold-cathode proton source operating at about 200 v at a pressure of a few microns is described. The discharge is similar to that of a Philips vacuum gage. Operating characteristics and ionization processes are discussed.

Action of slow neutrons on bromide ions in solution, P. Süe, L. Melander, *Compt. rend.* **225,** 413–415 (1947). Aqueous solutions of phenol and NH_4Br were irradiated with slow neutrons, and the phenol was then extracted with benzene. The activity of the two layers was measured. A small amount of Br^- was found to be combined with the phenol, and possible mechanisms for this are discussed.

Electric method of separation of nuclear isomers, L. Rusinov, A. Karamian (Physico-Tech. Inst., Leningrad), *Compt. rend. acad. sci. U.R.S.S.* **55,** 599–600 (1947). Ethyl bromide was irradiated with slow neutrons, and then electrolyzed using a silver anode and a platinum cathode. The radiometric analysis of the anode showed activities with half-lives of 18 min, 4.2 and 34 hr.

A technique for the study of isotopic exchange reactions, M. Haïssinsky, B. Pullman, *J. phys. radium* **8,** 33–35 (1947). Exchange reaction studies are best carried out using thick layer of radioactive samples to minimize selfabsorption

errors. The thickness of sample beyond which no increase in activity results is independent of the physical or chemical state of the substance.

Isotopic exchange in the systems MnO_2/Mn^{++} and PbO_2/Pb^{++}, B. Pullman, M. Haïssinsky, *J. phys. radium* **8,** 36–38 (1947). The exchange rates were studied for the two systems and were found to be similar. The rates show that the exchange is rapid initially, but becomes diffusion-controlled. The differences in these systems previously reported were probably due to variations in the oxide preparations.

Exchange reactions between ferric and ferrous ions in perchloric acid using a diffusion separation method, L. Van Alten, C. Rice (Purdue Univ., Lafayette, Ind.) *J. Am. Chem. Soc.* **70,** 883–884 (1948). Radioferric ion was used to investigate the electronic exchange between ferric and ferrous ions in 3 M perchloric acid. The ferric and ferrous ions were separated by their diffusion from the exchange mixture across a sintered glass membrane into 3 M perchloric acid (ferric ion diffuses more rapidly). The half-time for exchange at 25° was found to be 18.5 ± 2.5 days.

Exchange reaction between thallium (I) and thallium (III) ions in perchloric acid and nitric acid solutions, R. Prestwood, A. Wahl (Washington Univ., St. Louis, Mo.), *J. Am. Chem. Soc.* **70,** 880–881 (1948). $Tl^{204,206}$ was used to study the exchange reaction, and the rate was found to be slow and measurable. A fast but reproducible exchange was induced at the time of separation of the two ions, but could be corrected for. Typical experiments give the exchange half-time as 67 ± 5 hr with 3.5 f $HClO_4$, and 36 ± 4 hr with 1.5 f $HClO_4$. Using 1.5 f HNO_3 the exchange half-time was found to be 1.6 ± 0.2 hr. All these measurements were taken at 24.8 ± 0.2°.

Long-life zirconium from uranium-235 fission, A. Grosse, E. Booth (Columbia Univ.), *J. Am. Chem. Soc.* **70,** 465–466 (1948). Experimental details are given of the work which led to the positive identification of a 66-day isotope of Zr. The correct mass assignments for the 17-hr and 66-day isotopes are 97 and 95, respectively.

The exchange reaction between the two oxidation states of thallium in perchloric acid solutions, G. Harbottle, R. W. Dodson (Columbia Univ.), *J. Am. Chem. Soc.* **70,** 880 (1948). The exchange reaction was investigated using $Tl^{204,206}$ (half-life about 3 yr). The dependence of the rate on the concentrations of thallous and thallic perchlorates, the acid concentration, and the temperature was studied. The specific rate constant is 2.0 moles^{-1} liter hours^{-1} at 49.5° with 0.4 f perchloric acid, and the activation energy is 12 kcal/mole.

. . . I. W. RUDERMAN

LIFE SCIENCE PUBLICATIONS

Abstracts of papers presented at the 32nd annual meeting of the Federation of American Societies for Experimental Biology, held March 15–19, are to be found in the *Federation Proceedings*, Vol. 7, No. 1. Those abstracts of interest to isotope workers are described here by title and page only:

Hemin synthesis with glycine containing C^{14} in its α-carbon atom; 2.

A Geiger-Müller counter system for tracer studies of gas exchanges in man; 5.

Decrease in the radiosodium and thiocyanate spaces during growth; 32.

Susceptibility of X-rayed animals to histamine and to adenosine; 90.

Influence of temperature on radiosensitivity in the frog; 90.

Rate of penetration of electrolytes into nerve fibers; 105.

Fetal gastric secretion of radioiodine applied precutaneously to pregnant animals; 110.

Effect of phytate and other food ingredients on the absorption of radioactive iron; 112, 298.

The effect of adrenal cortical extract on adrenal response to total body X-irradiation; 121.

On the fate of labeled pyruvic acid in the intact animal; 142.

Tissue incorporation and excretion of radioactive carbon administered as carbonate; 143.

Synthesis of fatty acids in rat liver slices; 146.

Protein and peptide turnover with respect to lysine in guinea pig liver homogenate; 147.

Immunochemical studies with proteins labeled with trace amounts of radioactive iodine; 153.

Oxidation-coupled phosphate exchanges in the acid-insoluble esters of cell-free liver preparations; 155.

Rate of $C^{14}O_2$ excretion following intraperitoneal administration of isotopic bi-

carbonate and acetate; 156.

Application of the isotopic derivative method of analysis to protein hydrolysates; 163.

Quantitative analysis of protein hydrolysates on paper chromatograms by isotopic derivative method; 164.

The arrangement of amino acids in silk; an application of the isotopic derivative technique; 168.

The excretion of labeled calcium by normal and thyroparathyroidectomized rats; 168.

On the origin of stercobilin in humans; 169.

Study of the oxidation of the labile methyl group of dietary methionine traced with C^{14}; 170.

Studies on the nitrogen metabolism of tomato using N^{15}-labeled ammonium sulfate; 170.

Preliminary observations on the renal excretion of radioiodine after administration of tracer doses; 178.

Purification and properties of *E. coli* bacteriophage T_6; 179.

Rate of protein formation in the livers of partially hepatectomized rats; 180.

The *in vitro* synthesis of heme from glycine by nucleated red blood cell; 188.

The metabolism of the α, γ, and β hydrogen atoms of L-leucine; 191.

Influence of the thyroid upon incorporation of deuterium into tissue constituents of the rat; 193.

The role of acetylphosphate in the phosphoclastic and dismutation reactions of pyruvate; 194.

In vitro utilization of glucose by rat diaphragm muscle; 197. Incorporation of C^{14}-labeled glycine into the protein of tissue homogenates; 200.

Total body water by D_2O tracer study in protein depletion; 213.

Statistical problems involved in the use of radioactive tracers in pharmacology; 219.

Elevation of serum protein-bound iodine after large doses of radioactive iodine; 251.

Adenylpyrophosphatases and other phosphatases in the cell surface of living yeast; 252.

Iron absorption in normal subjects and in patients with anemias of varied etiology; 270.

Tumor therapy by the direct infiltration of radioactive colloidal metallic gold; 271.

Preparation of radioactive gold colloids for use in the therapy of malignancies; 279.

The zone of activity of antibodies as determined by the use of radioactive tracers; 308.

Control of hemorrhagic syndrome and reduction in X-irradiation mortality with a flavone, P. Rekers, J. Field (Univ. of Rochester, N. Y.), *Science* **107,** 16–17 (1948). Sub- and mid-lethal doses of total body X-irradiation produce an uncontrollable hemorrhagic diathesis in dogs. Resistance to this internal bleeding is greatly raised by feeding rutin, 50 mg three times a day, beginning one week before irradiation. Some of the treated dogs developed a temporary severe thrombocytopenia and leucopenia.

The utilization of adenine for nucleic acid synthesis and as a precursor of guanine, G. Brown, P. Roll, A. Plentl, L. Cavalieri (Sloan-Kettering Inst. for Cancer Research, New York), *J. Biol. Chem.* **172,** 469–484 (1948). Adenine containing N^{15} in positions 1 and 3 was synthesized and fed to rats, from whom the mixed nucleic acids, and from them, adenine and guanine were isolated. Both purines were found to contain N^{15}, indicating that dietary adenine is utilized for the synthesis of nucleic acids and guanine. Adenosine triphosphate, isolated from muscles, was found to have a lower N^{15} concentration. Of the allantoin excreted, 27% was derived from the ingested adenine. Very little degradation to urea and ammonia and no observable conversion to pyrimidines occurred. The allantoin, isolated by an improved procedure, was found to be labeled uniformly in all four N atoms. The similar results obtained on feeding uric acid, labeled in the 1 and 3 positions, indicate that a symmetrical intermediate is formed in the degradation of uric acid. The finding that dietary guanine is not incorporated into nucleic acids was confirmed.

Are phospholipids obligatory participants in fat transport across the intestinal wall? D. Zilversmit, I. Chaikoff, C. Entenman (Univ. of Calif. Med. School, Berkeley) *J. Biol. Chem.* **172,** 637 (1948). Fasted dogs were injected with radioactive phosphate and 6 hours later sections from their duodenum, jejunum and ileum were removed. From these, the specific activities of the mucosal phospholipid P and acid-soluble P were determined, and the ratios of the two values calculated. The ratios were about the same for each part of any given dog, indicating that the rates of turnover of phospholipid in the three parts are the same. A repetition of this experiment with fat-fed dogs gave similar values for the ratios, suggesting that the passage of

fat across the intestinal wall does not affect the turnover rate for phospholipids. Similar lack of effect was found in other experiments, in some of which the effect of different fats and age were studied. The conclusion drawn is that fat can pass through the small intestine without involving phospholipids as intermediates.

The inhibitory action of iodide upon organic binding of iodine by the normal thyroid gland, J. Wolff, I. Chaikoff, (Univ. of Calif. Med. School, Berkeley) *J. Biol. Chem.* **172,** 855–856 (1948). A series of rats were injected with varying amounts of KI^{131} and at various intervals blood and thyroid glands were removed. The total plasma and glandular organic I contents were calculated from radioactivity determinations. Increasing the I dose decreased greatly the rate of conversion to organically bound I (in the fraction insoluble in trichloracetic acid). When the total plasma I concentration drops below 15–25 γ percent, the inhibition is lifted.

Penetration of radioactive sodium and chloride into cerebrospinal fluid and aqueous humor, Jun-Ch'uan Wang (Univ. of Minnesota, Minneapolis) *J. Gen. Physiol.* **31,** 259–268 (1948). Isotonic salt solutions, containing Na^{24} or Cl^{38}, were injected intravenously into anesthesized dogs. At various intervals samples of blood, cerebrospinal fluid, and aqueous humor were withdrawn and analyzed for radioactivity (the corpuscles were first removed from the blood). It was found that the concentrations of the labeled ions in the anterior chamber and the cisterna magna gradually approach that of the plasma. The times required to reach half the plasma concentrations are, for Cl and Na: 34 and 27 minutes for aqueous humor, 90 and 95 minutes for cerebrospinal fluid. From the radioactivity of the plasma it was calculated that ⅓ of the body water is available for dilution of Na and Cl.

An extension of the isotope dilution method, K. Bloch, H. Anker (Dept. of Biochem., Univ. of Chicago) *Science* **107,** 228–229 (1948). When very small amounts of an isotopic substance are to be isolated and analyzed, it is convenient to add some nonisotopic carrier to ease the isolation. By using 2 separate aliquots, adding different amounts of carrier, and determining the isotope concentrations of the 2 isolated samples, one can calculate amount and isotope concentration of substance originally present.

Chromosome breakage in plants induced by radioactive phosphorous, T. Arnason, E, Cumming, J. Spinks (Univ. of Saskatchewan, Saskatoon) *Science* **107,** 198–199 (1948). Germinating seeds and young seedlings were treated with radioactive Na_2HPO_4 (0.18 and 0.018 microcurie per seed), and wheat plants were grown in soil containing P^{32}. Aberrations observed included chromosome fragments, chains of 3 or 4 chromosomes, rings of 4, unequal pairs, and anaphase and telophase bridges and fragments. The chromosome breakage must have occurred some divisions before formation of pollen mother cells and spikelets.

Chronic myelogenous leukemia, J. Lawrence, R. Dobson, B. Low-Beer, B. Brown (Divs. of Med. Physics, Medicine, and Radiology, Univ. of Calif., Berkeley) *J. Am. Med. Assoc.* **136,** 672–677 (1948). A detailed description of a study made on 129 patients treated with P^{32}, alone or together with X-rays. Comfortable life was prolonged, but P^{32} seems to be little superior to roentgenray treatment, the main advantages being convenience of administration and absence of radiation sickness. Leukemic cells seem to be little or no more susceptible than normal cells to P^{32} radiations, so that dosages must be carefully fixed. No evidence was found that the doses used produced neoplasms.

The use of isotopes in surgical research, F. Moore (Harvard Med. School, Boston) *Surg. Gynecol. Obstet.* **86,** 129–147 (1948). A discussion of the general uses of isotopes with emphasis on practical aspects. A detailed consideration of the determination of fluid volumes with radioactive isotopes is presented, with 72 references.

Autographic localization of radioiodine in stained sections of thyroid gland by coating with photographic emulsion, C. Leblond, W. Percival, J. Gross (Dept. of Anatomy, McGill Univ., Montreal) *Proc. Soc. Exptl. Biol. Med.* **67,** 74–76 (1948). The tissues are fixed, embedded in paraffin, sectioned and stained. The sections are then dehydrated and coated with celloidin. A fluid photographic emulsion, prepared from lantern slide plates, is deposited on the sections, allowed to dry, and left for the proper exposure time, after which it is developed. The histological details can be seen through the silver granules in the emulsion.

Injurious effects of whole body neutron irradiation in animals, T. Leucutia (Harper Hospital, Detroit) *Am. J. Roentgenology* **59,** 133–136 (1948). A review.

Distribution and rate of metabolism of phosphorus compounds in Trypanosoma equiperdum, S. Moraczewski, F. Kelsey (Dept. of Pharmacology, Univ. of Chicago) *J. Infect. Diseases* **82,** 45–51 (1948). Trypanosomes were incubated with radioactive phosphate for varying periods of time and 4 P fractions (acid-soluble, phospholipid, nuclei acid, phosphoprotein) were isolated and analyzed for activity. A similar study was made in which infected rats were injected with radiophosphate and the distribution of activity in the same fractions determined in the trypanosomes and rat heart, liver and plasma. Uptake of P^{32} by the parasite was somewhat greater in the *in vivo* experiments. The specific activity of all but the acid-soluble P was consistently greater in the trypanosomes than in the host, indicating the parasite's ability to assimilate inorganic P from the surroundings.

. . . NORMAN S. RADIN

PHYSICAL PUBLICATIONS

Range of Ra-α-Be neutrons in water, J. Rush (Duke Univ., Durham, N. C.), *Phys. Rev.* **73,** 271–273 (1948). The distribution of neutrons in water surrounding the approximate point source of the radium-beryllium type was measured as a function of the distance from the source. Thin indium foils were used as detectors by irradiating them and then measuring their activations with a counter. The migration area (one-sixth the mean square of the distance from the source to the point where the neutron is captured) is found to be 54.7 cm^2 for all activating neutrons, 45.4 cm^2 for indium resonance neutrons.

Neutrons and gamma-ray yields from deuterons and carbon, C. Bailey, G. Freier, J. Williams (Univ. of Minnesota, Minneapolis), *Phys. Rev.* **73,** 274–278 (1948). Carbon targets were bombarded with deuterons of energy between 0.85 and 3.25 Mev, produced by an electrostatic generator which controlled their energy to 0.2%. Gamma rays and neutrons were produced, the former in a $C^{12}(d,n)N^{13}$ reaction, the latter from the excited state of C^{13} produced by $C^{12}(d,p)C^{13*}$. A "long counter," of detection efficiency approximately independent of energy, counted the neutrons emitted, first at 0°, then at 90° in the laboratory system. The gamma rays emitted were also counted. The resonance widths observed varied from 10 to 100 kev, and the neutron and gamma-ray resonances occurred in different places. Neutrons were emitted with a strongly preferred forward direction, as seen by the much larger number at 0°.

The charge distribution in nuclei and the scattering of high-energy electrons, M. Rose (Clinton National Lab., Oak Ridge, Tenn.), *Phys. Rev.* **73,** 279–284 (1948). Assuming that the forces between charged particles at small distances are of Coulomb nature, the charge distribution and size of nuclei may be determined from the deviations from Mott scattering of electrons of several Mev at large angles. In particular the deuterium wave function might be determined.

Investigation of competing processes show that nuclear excitation and disintegration can be neglected if the electron energy is about 50 Mev and the scattered electrons are observed at an angle which is large but not near 180°. Inelastic collisions with orbital electrons will be unimportant if electrons of about the incident energy are observed at angles near 0° or 180°. Bremsstrahlung can be neglected if only electrons near the incident energy are observed.

Electronic component of cosmic rays in the low atmosphere. I. Theoretical, G. Bernardini, B. Cacciapuoti, R. Querzoli (Univ. of Rome, Italy), *Phys. Rev.* **73,** 328–334 (1948). The problem of equilibrium between mesons and secondary electrons is discussed. Results include: (*1*) number of secondary electrons generated in lead, for various electron energies and lower limits of meson energy; (*2*) number of secondary collision electrons from the atmosphere, of various energies, at sea level and 3,500 meters above. Comparison with knock-on electrons in lead and the meson-electron ratio from Hazen's experiments seems to indicate agreement with this theory.

Radiations from tantalum (182), antimony (122), and indium (116), C. Mandeville, M. Scherb (Bartol Research Foundation, Franklin Inst., Swarthmore, Pa.), *Phys. Rev.* **73,** 340–343 (1948). Radioactive Ta produced by neutron bombardment has a 100-day life-

time, emits β rays of endpoint 0.36 Mev, and the residual nucleus de-excites with emission of two or more rays as indicated by β-γ and γ-γ coincidences. Irradiated Sb shows a 2.8-day activity, giving a maximum β-ray energy of 1.77 Mev (from absorption in Al) and maximum γ-ray energy of 1.19 Mev (from β-γ coincidences). In^{116} has a 54-min activity; β-γ coincidences stop at 0.7 Mev.

Electronic component of cosmic rays in the low atmosphere. II. Experimental, G. Bernardini, B. Cacciapouti, R. Querzoli (Univ. of Rome, Italy), *Phys. Rev.* **73,** 335–339 (1948). Numerical results obtained from the formulas which evaluate the number of secondary cosmic-ray electrons in the low atmosphere are compared with the results of some counter experiments. Results were observed for electrons creating a shower in lead and for mesons producing a secondary electron in it. Side showers were the largest source of error. The results indicate that: (*1*) Even at 3,000 meters the electron component is not in equilibrium with the meson component, whatever the slow meson background. (*2*) At 3,500 meters the electronic component contains some high-energy electrons which are not secondaries of mesons of lifetime 2.3×10^{-6} sec. (*3*) The slow mesons are negligible at sea level and their intensity increases rapidly with height, roughly, as the electron component. (*4*) It is likely that the slow mesons are secondaries of the electron-photon component because this component is also composed of high-energy electrons (*5*) At sea level the penetrating part (above 10 cm Pb) may well consist mainly of mesons whose lifetime-to-mass ratio is 10^{-8} sec/Mev.

The absorption of Na^{24} gamma-radiation in lead, copper, and aluminum, D. Alburger (Yale Univ., New Haven., Conn.), *Phys. Rev.* **73,** 344–346 (1948). The absorption of the two gamma rays of Na^{24}, of energy 2.76 and 1.38 Mev, was investigated for various absorbers, using Geiger counters as detectors. The high sensitivity of the counter makes it suitable for large absorber thicknesses, and the different counting efficiency for the two gamma-rays allows the separation of the two absorption coefficients. The source is placed in a hole in a lead block; the counter is located 60–100 cm from the source. Absorption coefficients agree with Heitler's theoretical curves.

The half-life of carbon-14, L. Norris (Clinton National Lab., Oak Ridge, Tenn.), M. Inghram (Argonne National Lab., Chicago, Ill.), *Phys. Rev.* **73,** 350–360 (1948). The half-life is obtained from the activity (number of disintegrations per second) and the number of C^{14} nuclei in the sample. The CO_2 is roasted from a barium carbonate sample and analyzed in a mass spectrometer in order to determine the relative amount of C^{14}. Another identical sample is introduced into a special counting chamber, containing a windowless tube above the sample. A rotating frame introduces varying absorber thicknesses between sample and counter. The half-life is found to be $5{,}100 \pm 200$ years.

On the polarization of fast neutrons, J. Schwinger (Harvard Univ., Cambridge, Mass.), *Phys. Rev.* **73,** 407–409 (1948). The spin-orbit interaction arising from the motion of the neutron magnetic moment in the nuclear Coulomb field is suggested as a mechanism for producing almost complete polarization of fast neutrons under ideal conditions, with small scattering angles. For 1-Mev neutrons in lead, the scattering angle which gives almost complete polarization is 1.5 deg., but the polarization is still large for angles up to 6 deg. (0.47). Detection is by a second scattering of the polarized neutrons.

Threshold for the proton-neutron reaction in copper, W. Shoupp, B. Jennings, W. Jones (Westinghouse Research Labs., East Pittsburgh, Pa.), *Phys. Rev.* **73,** 421–423 (1948). An electrostatic generator bombards a copper target, and the neutrons from the $C^{65}(p,n)$ reaction are slowed in paraffin and detected in a BF_3 ionization chamber. The threshold is established at 2.164 ± 0.01 Mev by using the $Li^7(p,n)$ reaction, whose threshold was already known, as a voltage standard. The maximum energy of the positron spectrum of Zn^{62} is fixed at 0.335 ± 0.001 Mev.

Development of the frequency modulated cyclotron, J. R. Richardson, B. Wright, E. Lofgren, B. Peters (Radiation Lab., Univ. of California, Berkeley) *Phys. Rev.* **73,** 425–436 (1948). Experimental development of the phase stability principle as applied to a 37-in. cyclotron operated under f-m. Variation is given of the beam current with such factors as the phase stability factor, the modulation frequency, the dee voltage, and the pressure. The kinetic energy of the ions is

plotted as a function of time for ions starting at various times. Problems of probes and deflection of the beam are discussed, as is the actual performance with deuterons and protons.

Note on the Milne problem for a sphere, T. H. Berlin (Johns Hopkins Univ., Baltimore, Md.), *Phys. Rev.* **73,** 437–440 (1948). A solution is obtained which shows the shadow of the sphere and the corresponding discontinuity of the neutron distribution function. A method is given for determining the radius of the sphere and mean free path of the neutrons by experiment.

Angular correlation of scattered annihilation radiation, H. Snyder, S. Pasternack, J. Hornbostel (Brookhaven National Lab., Upton, N. Y.), *Phys. Rev.* **73,** 440–448 (1948). In the annihilation of a positron-electron pair, the pair usually has zero relative angular momentum, so that the two quanta emitted are polarized in mutually perpendicular directions. The radiation scattered into counters arranged for coincidence should then depend on the azimuthal angle between them. Calculations on the basis of the Klein-Nishina formula give the ratio 2.85:1 for the coincidence rate at 82 deg to that at 0. Computations are also made for finite geometry.

Interaction of cosmic-ray primaries with sunlight and starlight, E. Feenberg, H. Primakoff (Washington Univ., St. Louis, Mo.), *Phys. Rev.* **73,** 449–469 (1948). An investigation is made of collision between protons and electrons of very high energy and photons of light, considering electron-positron pair production and recoil photons produced by Compton scattering. In traversals of the solar system or of one galaxy, the number of collisions is insufficient to cause appreciable energy loss in the primary or appreciable production of corresponding secondaries. Electrons (though not protons) may be eliminated in intergalactic distances by Compton collision.

The ionization loss of energy of fast charged particles in gases and condensed bodies, O. Halpern (Univ. of Southern California, Los Angeles), H. Hall (Bu. Aer., Navy Dept., Washington, D. C.), *Phys. Rev.* **73,** 477–486 (1948). This treatment takes into account the polarization properties of the medium, assuming n types of dispersion electrons, and one type of conduction electrons. Curves show the reduction in loss for various momenta of incident particles. Experimental data show good agreement with multifrequency theory.

Natural radioactivity of rhenium, S. Naldrett, W. Libby (Inst. for Nuclear Studies, Univ. of Chicago, Ill.), *Phys. Rev.* **73,** 487–493 (1948). An experiment using OsO_4 mixed with argon as a counter gas, designed to detect K-capture by subsequent emission of Auger electrons, showed no activity of half-life less than 5×10^{11} years. A β activity of Rh^{187}, having half-life of $4 \pm 1 \times 10^{12}$ years and an energy maximum of about 43 kev, has been detected.

Properties of some new types of counters, S. Curran, J. Reid (Univ. of Glasgow, Scotland), *Rev. Sci. Instr.* **19,** 67–75 (1948). Counters of rectangular cross section have been made which show appreciable plateaus; when the wire is not in the center it is more difficult to count particles independently of their path through the counter. Multiple wires asymmetrically placed can be made to operate independently. Offset wires in a counter result in lower working voltages and decreased dead-times. The multiple wire arrangements can be used for coincidence work.

A linear electron accelerator, E. Ginzton, W. Hansen, W. Kennedy (Stanford Univ., Stanford, Cal.), *Rev. Sci. Instr.* **19,** 89–108 (1948). Theory, design problems, and performance of a linear accelerator for electrons are discussed. No difficulty is experienced with orbit instability of electrons if they are injected at ample energy (80 kev experimentally). Phase stability is more difficult, especially for long accelerators which also require multiple-feed points. The best resonator shapes are discussed in terms of the ratio of energy given to the particles to the energy put into the accelerator. It appears that 100 Mev can be attained with 100-foot accelerator length and available power sources; 1 Bev will require either longer lengths or higher power sources.

Measurement of the electron current in a 22-Mev betatron, L. Bess, A. Hanson (Univ. of Illinois, Urbana), *Rev. Sci. Instr.* **19,** 108–110 (1948). The current of the beam is determined by its magnetic field, linking a coil wound around the "donut." The average current is found to be about 0.15 micro-

amperes (the injection frequency multiplied by the circulating charge).

Short time delays in Geiger counters, C. Sherwin (Univ. of Illinois, Urbana), *Rev. Sci. Instr.* **19,** 111–115. (1948) Delays are of two types. The first is due to the time required for the secondary electrons to arrive near the central wire. It can be measured by sending in betas at various distances from the central wire, and is found to have a maximum value of about 10^{-7} sec in a 2.2-cm diameter counter. A second delay, dependent on overvoltage, can be measured as the delay before detection on an amplifier following arrival of the secondary at the center. It may be related to the propagation of the ion sheath.

Neutron cross section of the elements, H. Goldsmith (Brookhaven National Lab., Upton, N. Y.), H. Ibser (Univ. of Wisconsin, Madison, Wis.), B. Feld (M.I.T., Cambridge, Mass.), *Revs. Mod. Phys.* **19,** 259–297 (1948). A review article, containing all the experimental cross sections for fast and slow neutrons that have been declassified. Activation and photo-neutron determinations are omitted. Separate curves are given for low-energy (0.001 ev–1 kev) and high-energy (1 kev–100 Mev) neutrons. A discussion of resonances and their significance is given. Data hitherto unpublished include those of the Argonne and Clinton crystal spectrometer groups, the Argone mechanical velocity selector group, and the Los Alamos and Columbia velocity selector groups.

A study of the nuclear transmutations of light elements by the photographic method, C. Lattes, P. Fowler, P. Cueur (Univ. of Bristol, England), *Proc. Phys. Soc.* **59,** 883–900 (1947). Using Ilford emulsion B1 to detect the tracks of disintegration particles, a study was made of the transmutations of Li, Be, B, and O by 900 kev deuterons. Range-energy relations for protons and alpha particles were determined. The uncertainties in range are not much larger than those due to straggling, so that the method gives high resolving power with respect to the particle energy. Alphas and protons can be distinguished by the appearance of their tracks.

An investigation of the Wilson chamber, J. Milatz, C. Van Heerden (Univ. of Utrecht, Netherlands), *Physica* **13,** 21–32 (1947). The sensitivity of the chamber was calculated from temperature and pressure measurements during and after expansion without vapor in the chamber, and agreed with the observed result with vapor. Sensitivity time is twice as long for expansion to fixed pressure as for expansion to fixed volume.

A new determination of the mean ranges of the α particles from UI and UII, S. Wytzes, G. Van der Maas (Vrije Univ., Amsterdam, Netherlands), *Physica* **13,** 49–61 (1947). With a method based on the fact that the number of secondary ions between a point P on the path of the α particle and the end-point Q is a unique function of the length PQ, detection by an ionization chamber as a detector gave 27.02 mm for UI and 32.58 mm for UII α particles in air at 15° C, 760 mm.

Non-thermal neutron cascade, H. Groenewold, H. Groendijk (Univ. of Groningen, Netherlands), *Physica* **13,** 141–152 (1947). The energy distribution of slow non-thermal (above 1 ev) neutrons cascading in paraffin is found as a function of time. The "tail" which appears after the neutron source is turned on or off, in such instruments as the neutron velocity spectrometer, is considered.

Time lags in Geiger-Müller counters, H. den Hartog, F. Muller, N. Verster (Univ. of Amsterdam, Netherlands), *Physica* **13,** 251–264 (1947). A method is given for experimentally determining the electron-drift velocities which fix transit times of secondary electrons in counters. These are of the order of 2 microseconds (maximum) for a counter of 7-cm diameter filled with 90 mm of argon and 10 mm of alcohol. The factors governing electron mobilities in gas-vapor mixtures are discussed.

On the natural precision of linear ionization chamber amplifiers, K. Keller (Univ. of Utrecht, Netherlands), *Physica* **13,** 326–336 (1947). The influence of multifrequency noise on the accuracy of ionization measurements is discussed and the natural limit on precision deduced.

The stopping power of a metal for alpha particles, H. Kramers (Kamerlingh Onnes Lab., Leiden), *Physica* **13,** 401–412 (1947). A formula for the energy loss per cm of path length is deduced by taking into account the polarization of the conduction electrons in the metal. Modifications by quantum mechanics are discussed.

The production of secondary electrons by collision of mesons in the air and in iron, J. Clay (Univ. of Amsterdam, Netherlands), *Physica* **13,** 433–446 (1947). Coincidence experiments indicate electrons of energy greater than 2 Mev accompany mesons in the atmosphere to the extent of 9–18%. The cross section for secondary electron production in iron is given as 35×10^{-27} cm², and their numbers amount to about 9% of the mesons penetrating the iron.

Coincidence-spectrometry for disintegration problems, K. Siegbahn, A. Johansson, *Arkiv Mat., Astron. Fysik,* **34A,** No. 10, 1–19 (1947). Methods of application of coincidence measurements to complex beta-ray spectra are discussed. A beta-gamma coincidence apparatus is described, consisting of an improved three-stage coincidence amplifier of the Bradt-Scherrer type with resolving time of 3×10^{-7} sec, a magnetic-lens-type beta spectrograph, and a gold cathode gamma-ray counter. The coincidence plateau was determined and the spectrograph was checked by reproducing the spectrum of P^{32}. Various complex spectra were analyzed. In the spectrum of Th(B + C + C″) the upper energy limit of ThC″ was determined as 1.72 Mev. Measurements of Mn^{56} indicated general agreement with the term scheme proposed by Elliot and Deutsch. The coincidence spectrum of K^{42} was determined. The upper limit of the soft beta component is given as 1.92 Mev. This value, determined by Fermi analysis, agrees quite well with 2.04 Mev, a value obtained by other methods. The beta spectrum of Na^{24} was determined as simple on the basis of the experimentally found coincidence spectrum. The upper limit is given as 1.39 Mev.

Nuclear levels in ThC and ThD as studied by means of their γ-rays, A. Johansson, *Arkiv Mat. Astron. Fysik,* **34A,** No. 9, 1–8 (1947). The gamma radiation from Th(C + C + C″) was studied by investigation of the energies of the Compton electrons from copper. The energy distribution was studied in a magnetic lens spectrograph and experimental curves were reproduced. The data indicates the existence of gamma rays of 1.03 and 0.84 Mev. A line at 3.2 Mev reported by several workers was not observed. The intensities of the gamma-ray lines were calculated from the Compton distribution. The intensity ratio of the 0.58 and 0.51 Mev lines was estimated as two to one. This result was checked as far as possible by finding the energy distribution of photo-electrons in lead. A new term scheme for ThC is proposed and the diagram is reproduced.

The magnetic exchange moments for H^3 and He^3, F. Villars, *Helv. Phys. Acta,* **XX,** 476–490 (1947). It is shown that charge exchange connected with the interaction of nucleons gives rise to a magnetic moment for a three-body system in the ground state. A calculation has been carried through using the symmetric pseudoscalar meson theory, according to which the H^3 and He^3 ground states are doublet states (with regard to both spin and isotopic spin) and symmetrical with regard to space coordinates. The magnetic exchange moment is found to be approximately 0.3 nuclear magnetons. The sign is positive for H^3 and negative for He^3. This result agrees with experimental results for H^3 and predicts a magnetic moment for He^3 of approximately −2.1 nuclear magnetons.

. . . HAROLD BROWN

BOOKS

THE PRINCIPLES OF QUANTUM MECHANICS, P. A. M. Dirac, Oxford University Press, New York, 1947, 3rd Ed., $9.00. *Reviewed by Irving Kaplan, Brookhaven National Laboratory, Upton, N. Y.*

Since the appearance of the first edition in 1930, Dirac's book has been the standard work on the fundamental principles of quantum mechanics, and now ranks as one of the classics in the field of physics. The rapid and extensive development of quantum mechanics and the success of its applications to atomic and nuclear phenomena make it certain that Dirac's book will have an important part in the training of future specialists in nuclear physics. It is not

a book for the beginner in quantum mechanics, but is rather for the advanced student and research worker who already has a familiarity with the subject obtained from treatments of a more descriptive nature. For such a person Dirac's book provides a logical, axiomatic development in which wave mechanics and matrix mechanics appear as the "Schrödinger and Heisenberg representations," respectively, of a more general theory. The more abstract and concise treatment of Dirac requires of the reader a greater investment in terms of careful and thorough study than the usual textbook. However, this investment will be amply repaid by a deeper insight into the physical problems of modern atomic theory and the theoretical means for their solution.

The many admirable qualities of Dirac's book serve to emphasize the need which still exists for a textbook which will apply Dirac's methods to those more detailed problems which cannot be treated in a discussion of fundamental principles. It is to be hoped that such a book will appear soon.

Dirac begins with a brief discussion, based on simple conceptual experiments, of the need for a quantum theory. This leads immediately to the introduction of the principle of the superposition of the states of an atomic system, and the indeterminacy principle. The mathematical formulation of these principles is then undertaken in terms of eigenvectors, observables, linear operators and various other mathematical entities. Here, Dirac's use of the "bracket" notation involving his "bra" and "ket" vectors makes for a more closely-knit formalism than that of the second edition. The development of this formalism, which constitutes the framework of quantum mechanics, takes up the first four chapters of the book. Chapters five through eight treat such problems as the equations of motion of a dynamical system with applications to the harmonic oscillator and hydrogen atom, perturbation theory and collision problems. Chapters nine through twelve deal with more advanced topics: the many-body problem, radiation theory (and second quantization), relativistic electron theory and quantum electrodynamics. The discussion of systems with similar particles is based on Fock's treatment of the theory of an assembly of bosons (particles obeying the Bose-Einstein statistics) and is simpler and more elegant than that given in earlier editions of the book. The treatment of quantum electrodynamics is more extensive than that of the second edition and includes the theory of the Wentzel field and the λ-limiting process introduced in order to remove the infinite self-energy of a point electron. In this connection the uncertain state of the theory of the interaction of an electron with the electromagnetic field is pointed out and some possible future directions are indicated.

The style and format of the book are in the fine tradition of the Oxford International Series of Monographs on Physics. The reviewer sincerely hopes that the book will be available in this country in quantities in accord with its excellence.